# Dating of Colluvium from Natural Hillside Catchments on Lantau Island and Eastern New Territories

**GEO Report No. 357**

**R.J. Sewell**

**Geotechnical Engineering Office**
**Civil Engineering and Development Department**
**The Government of the Hong Kong**
**Special Administrative Region**

[Blank Page]

# Dating of Colluvium from Natural Hillside Catchments on Lantau Island and Eastern New Territories

**GEO Report No. 357**

**R.J. Sewell**

**This report was originally produced in April 2020 as GEO Geological Report No. GR 1/2020**

First published, March 2022

Prepared by:

Geotechnical Engineering Office,
Civil Engineering and Development Department,
Civil Engineering and Development Building,
101 Princess Margaret Road,
Homantin, Kowloon,
Hong Kong.

## Preface

In keeping with our policy of releasing information which may be of general interest to the geotechnical profession and the public, we make available selected internal reports in a series of publications termed the GEO Report series. The GEO Reports can be downloaded from the website of the Civil Engineering and Development Department (http://www.cedd.gov.hk) on the Internet.

Raymond WM Cheung
Head, Geotechnical Engineering Office
March 2022

# Foreword

This report presents the results of an age-dating investigation of colluvia in natural hillside catchments on Lantau Island and Eastern New Territories. Samples were collected from six study areas utilising ground investigations carried out under the Landslip Prevention and Mitigation Programme (LPMitP).

The report includes brief geomorphological assessments for each study area, which are based on comprehensive Natural Terrain Hazard Studies (NTHS) carried out by LPMitP consultants and their subconsultants. The investigation adds thirty-one new ages to the natural terrain landslide age dataset for Hong Kong. The new data provide a wider basis of studying the historical landslide activities in the territory.

This report was written by Dr R.J. Sewell. Mr J.R. Hart (GeoRisk Solutions Ltd.), who was an LPMitP subconsultant responsible for overseeing many of the NTHS, provided technical support and comments on the draft. His contributions are acknowledged.

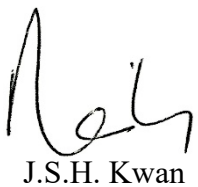

J.S.H. Kwan
Chief Geotechnical Engineer/Planning

## Abstract

Understanding the responses of landscape to past climate changes, particularly in terms of landslide magnitude-frequency relations, is helpful for assessing the potential impact of future extreme weather events. Previous dating studies of relict landslides in Hong Kong focused mainly on large deep-seated failures and coastal debris complexes on Lantau (Sewell & Campbell, 2005; Sewell et al, 2006, 2015; Sewell & Tang, 2015). To expand the current landslide age dataset, six new sites (four in eastern New Territories and two on Lantau) under the Landslip Prevention and Mitigation Programme have been investigated and sampled for dating.

Thirty-one new ages of landslide debris have been obtained using radiocarbon and optically stimulated luminescence (OSL) techniques. The latest data are largely consistent with earlier dating results, suggesting that the relict colluvium is 1,000s (with some 10,000s) rather than 100s of years old. Clusters of large, deep-seated landslides occurred between 65,000-45,000 years and at approximately 32,000 years ago. The more frequent pulses of landslide activities during the early to mid-Holocene is considered related probably to climatic amelioration and rising sea levels. The growing landslide age dataset can improve the interpretation of landslide return periods, thereby facilitating the assessment of potential natural terrain landslide hazards under the changing environmental conditions.

# Contents

# List of Tables

# List of Figures

## 1 Introduction

Past dating studies of relict natural terrain landslides in Hong Kong have been focused principally on 1/ large deep-seated landslides associated with faults in central New Territories and Lantau Island (Sewell & Campbell, 2005; Sewell et al, 2006; Sewell & Tang, 2015), and 2/ debris flows associated with coastal fan complexes in western Lantau Island and their potential relationship to climate change (Sewell et al, 2015). The data obtained from these studies have contributed to a growing landslide age dataset in Hong Kong.

Under the Landslip Prevention and Mitigation Programme (LPMitP), launched in 2010 to systematically deal with the landslide risk associated with both man-made slopes and natural hillside, an important objective was to explore opportunities to develop a quantitative framework for improvements to the design event approach commonly adopted in Natural Terrain Hazard Study (NTHS) for hazard mitigation works. Assessment and mitigation of natural terrain hazards involve interpretation of historical landslide data and consideration of the possible return periods of natural terrain landslides. The estimation of landslide magnitude-frequency relationships based on historical landslide data assumes some constancy in the environmental controls of the landslides. However, the recent IPCC projections on warming of the global climate system (IPCC, 2013) have emphasised the likelihood of increased frequency of extreme weather events, including typhoons and unprecedented rainfall events. Understanding how the landscape has responded to past periods of climate change is therefore helpful for assessing the potential impact of these future extreme weather events on design events adopted in NTHS. There is potential that the landslide age dataset in Hong Kong can improve interpretation of return periods of natural terrain landslides under forecast changing environmental conditions.

## 2 Study Approach

Previous dating studies carried out on relict natural terrain landslides in Hong Kong (Sewell & Campbell, 2005; Sewell et al, 2006; Tang et al, 2009, 2010; Wong & Ding 2010; Wong et al, 2010, Sewell et al, 2015; Sewell & Tang, 2015), have generally targeted geomorphological features, such as relict landslide scarps, landslide debris lobes and/or fans, or very large boulders resulting from rock fall. However, under the LPMitP, dating of single geomorphological features was not always possible as natural hillside catchments were selected for study based on overall risk posed to development rather than specific landslide features. Accordingly, the locations of trial pits and boreholes were constrained by ground investigation works planned for hazard mitigation. In most cases, samples were collected from one or more layers of colluvium exposed in trial pits excavated within hillside catchments. Thick layers (> 0.5 m) of colluvium were assumed to represent the products of relict landslide events, although their source areas remained undefined. A few boreholes were also available for sampling deeper levels of colluvial lobes in the lower parts of some catchments.

## 3 Study Areas, Geology and Physiography

Hillside catchments in six areas were the subjects of the dating investigation. Two study areas were located at Keung Shan and Mui Wo on Lantau Island (Figure 3.1a), while four were located at Tai Wan Tau Road, Sheung Yeung, Razor Hill and Tai Mong Tsai in eastern

New Territories (Figure 3.1b). Detailed geomorphological assessments carried out by a number of independent studies (Keung Shan, AFJV (2012); Mui Wo, Fugro (2015); Tai Wan Tau Road, Fugro, (2012a); Sheung Yeung, Fugro, (2012b); Razor Hill east, OAP (2014); Razor Hill north, Fugro, (2014); Tai Mong Tsai Road, Jacobs, (2014)) were used as a basis for brief summaries of geology, physiography, geomorphology and superficial deposits in each of the study areas.

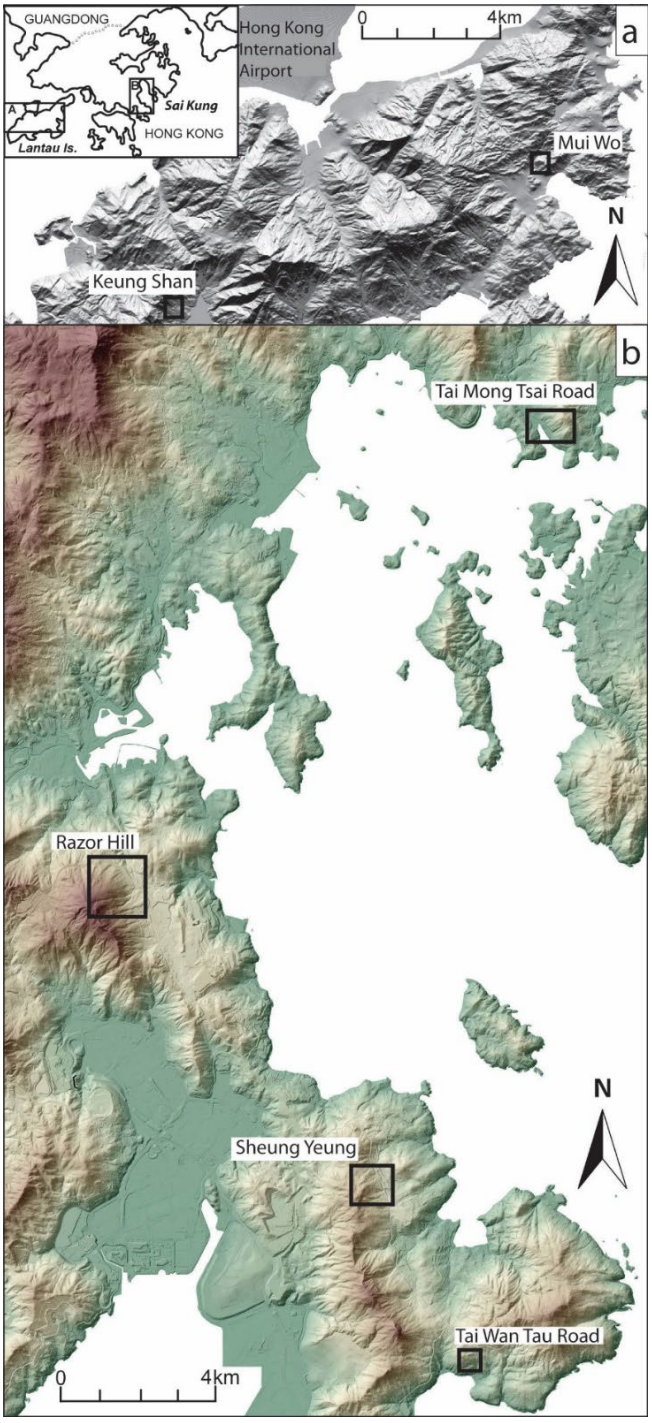


**Figure 3.1 Location Map of Hillside Catchment Study Areas, (a) Lantau Island, (b) Eastern New Territories**

## 3.1 Lantau Island

The Keung Shan study area (Figure 3.2a) comprises moderately steep (20° – 30°), east-facing slopes between 140 mPD and 360 mPD dissected by several well-developed drainage lines occupied by superficial deposits. The lower slopes (< 300 mPD) are underlain principally by rhyolitic lavas and tuffs belonging to the Lantau Volcanic Group (undifferentiated) (GEO, 2000), whereas the upper slopes (> 300 mPD) are underlain by SE-dipping tuffs, tuffites and siltstones belonging to the Pak Kok Member of the Lantau Formation (GEO, 1992) (renamed Lantau Volcanic Group, Sewell et al, 2000). These form steep rock cliffs at the crest of the study area. Superficial deposits comprise dominantly colluvium and taluvium.

The Mui Wo study area (Figure 3.2b) encompasses steep (25° – 35°), west-facing slopes between 20 mPD and 140 mPD overlooking the village of Wang Tong and dissected by several well-developed ephemeral drainage lines in valley depressions infilled with superficial deposits (Figure 3.1a). The underlying geology consists of medium-grained and fine-grained granite, intruded by ENE-trending feldsparphyric rhyolite dykes. The superficial deposits comprise mainly fine-grained colluvium and bouldery colluvium/taluvium within valley depressions. Debris fan deposits are developed near the slope toe of the valley depressions.

## 3.2 Eastern New Territories

The Tai Wan Tau Road study area features steep (25° – 40°), southeast-facing slopes between 56 mPD and 132 mPD overlooking Tai Wan Tau Road and is dissected by a prominent drainage line. The underlying geology comprises dominantly crystal-bearing fine ash tuff of the High Island Formation (Kau Sai Chau Volcanic Group, Sewell et al, 2000). The superficial deposits consist of coarse, relict colluvium draped across the middle slopes, and thick colluvial deposits in the single prominent drainage line.

The Sheung Yeung study area includes steep (30° – 60°), east-northeast-facing slopes between 110 mPD and 350 mPD overlooking the village of Sheung Yeung along Clear Water Bay Road. The slopes are dissected by four hillside catchments which are infilled by superficial deposits and form overlapping debris fans near the slope toe. The underlying geology consists dominantly of trachydacite lava and fine ash tuff of the Pan Long Wan Formation (Repulse Bay Volcanic Group) (Sewell et al, 2000). The superficial deposits consist of bouldery colluvium and taluvium infilling the major drainage lines which dissect older colluvial deposits forming debris fans at the slope toe.

The Razor Hill study area is divided into two subareas: 1/ a steep (25° – 45°) north-facing hillside between 165 mPD and 240 mPD covered in superficial deposits and dissected by prominent drainage lines overlooking Clear Water Bay Road (northeast sub-area), and 2/ a series of steep (25° – 55°), east-facing hillside between about 130 mPD and 430 mPD dissected by several prominent drainage lines filled with superficial deposits and overlooking the Clear Water Bay Road and HKUST staff quarters (east sub-area). The underlying geology of both areas consists of crystal-bearing fine ash vitric tuff of the Che Kwu Shan Formation (Repulse Bay Volcanic Group) (Sewell et al, 2000) whereas the superficial deposits comprise dominantly taluvium in the middle and upper portions of the slopes, and colluvium in the lower portions of the slopes.

The Tai Mong Tsai Road study area includes a steep (25° – 35°), southwest-facing hillside between 20 mPD and 152 mPD overlooking Tai Mong Tsai Road and featuring two prominent hillside catchments infilled with superficial deposits. The underlying geology is composed of tuffaceous siltstone with minor crystal-bearing fine ash vitric tuff of the Mang Kung Uk Formation (Repulse Bay Volcanic Group, Sewell et al, 2000). The superficial deposits infilling the hillside catchments comprise dominantly colluvium, with minor taluvium.

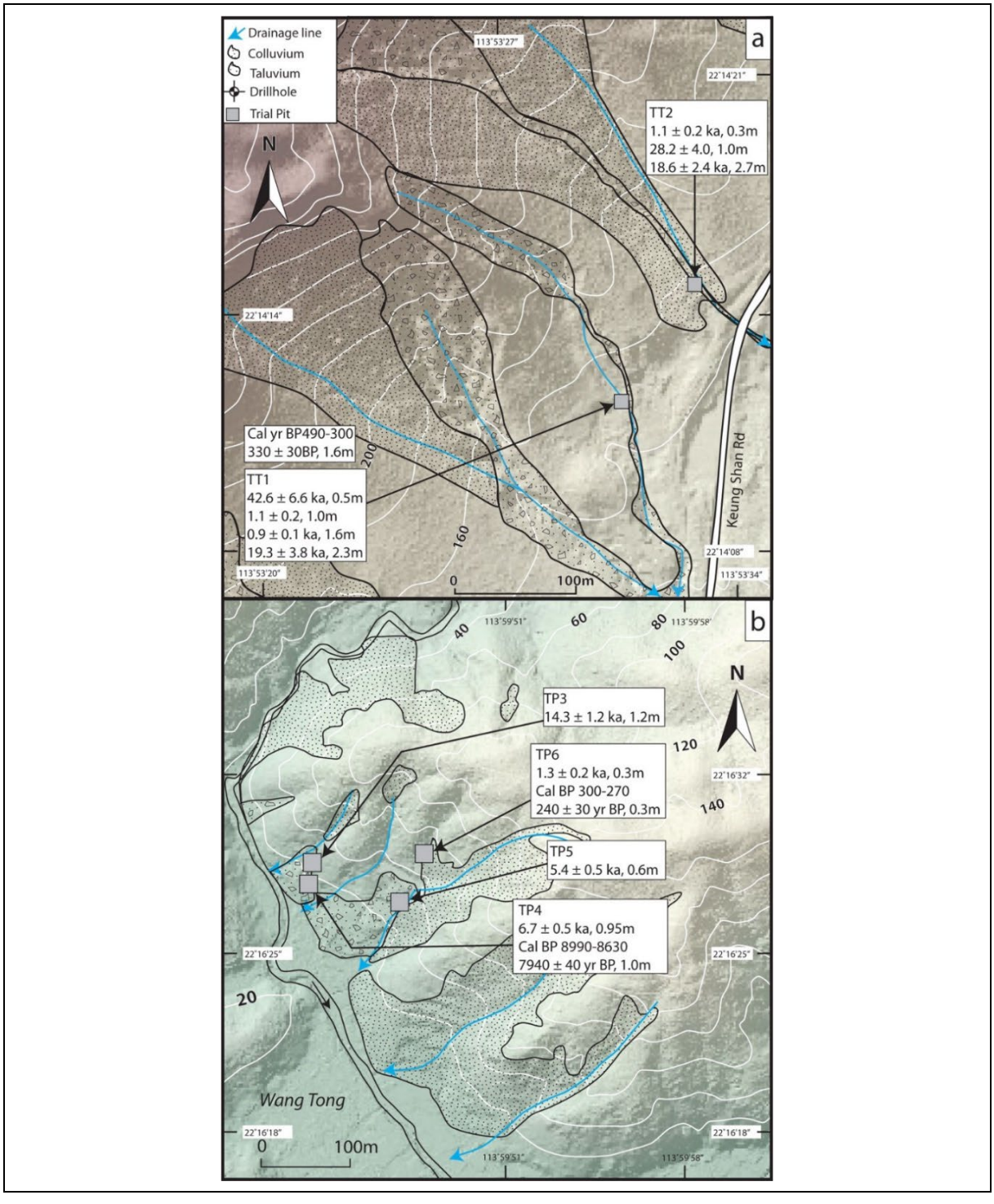


**Figure 3.2 Dated Hillside Catchments at (a) Keung Shan, and (b) Mui Wo, Lantau Island**

## 4 Dating Methodology

Direct dating of relict natural terrain landslides in Hong Kong has been successfully demonstrated using a combination of $^{14}C$, OSL, and terrestrial cosmogenic nuclides (TCN) (Sewell & Campbell, 2005). As no suitable deep-seated rock scarps or boulder debris were identified in the hillside catchment study areas, the dating methods applied were limited to $^{14}C$ and OSL, with the later technique yielding the bulk of the ages. All samples for OSL dating were analysed at the Luminescence Dating Laboratory, Victoria University of Wellington, New Zealand, while the few $^{14}C$ ages were obtained from Beta Analytic, Florida, USA. Full details of the dating techniques are given in Sewell et al (2015). Location details of analysed samples are given in Table 4.1. Descriptions of the analysed samples are given in Table 4.2, and $^{14}C$ and OSL age data are reported in Table 4.3.

**Table 4.1 Location Details of the Analysed Samples (Sheet 1 of 2)**

| Sample No. | Latitude | Longitude | Altitude (mPD) | DBS[1] (m) | Field Code | Sample Type |
|---|---|---|---|---|---|---|
| *Keung Shan* | | | | | | |
| HK13463 | 22.14127805 | 113.5331088 | 145.9 | 0.5 | TT1 | U-100 Sample, horizontal |
| HK13464 | 22.14127805 | 113.5331088 | 145.9 | 1.2 | TT1 | U-100 Sample, horizontal |
| HK13465 | 22.14127805 | 113.5331088 | 145.9 | 2.3 | TT1 | U-100 Sample, horizontal |
| HK13466 | 22.14127805 | 113.5331088 | 145.9 | 1.6 | TT1 | U-100 Sample, horizontal |
| HK13467 | 22.14160365 | 113.5333388 | 153.4 | 2.7 | TT2 | U-100 Sample, horizontal |
| HK13468 | 22.14160365 | 113.5333388 | 153.4 | 0.3 | TT2 | U-100 Sample, horizontal |
| HK13469 | 22.14160365 | 113.5333388 | 153.4 | 1.7 | TT2 | U-100 Sample, horizontal |
| | | | | | | |
| *Mui Wo* | | | | | | |
| HK13824 | 22.16291279 | 113.5944000 | 24.5 | 0.6 | TP3 | U-100 Sample, horizontal |
| HK13825 | 22.16285543 | 113.5944155 | 17.6 | 1 | TP4 | U-100 Sample, horizontal |
| HK13826 | 22.16277297 | 113.5947309 | 27.5 | 0.6 | TP5 | U-100 Sample, horizontal |
| HK13827 | 22.16293334 | 113.5948411 | 48.4 | 0.3 | TP6 | U-100 Sample, horizontal |
| | | | | | | |
| *Sheung Yeung* | | | | | | |
| HK13728 | 22.18312573 | 114.1656357 | 208.0 | 1 | TP4 | U-100 Sample, horizontal |
| HK13729 | 22.18362922 | 114.1702685 | 131.1 | 0.8 | TP8 | U-100 Sample, horizontal |
| HK13730 | 22.18332678 | 114.1704185 | 117.1 | 1.2 | TP11 | U-100 Sample, horizontal |
| HK13731 | 22.18401297 | 114.1700696 | 137.7 | 0.1 | TP15 | U-100 Sample, horizontal |
| HK13732 | 22.18401297 | 114.1000126 | 137.7 | 1.1 | TP15 | U-100 Sample, horizontal |

**Table 4.1 Location Details of the Analysed Samples (Sheet 2 of 2)**

| Sample No. | Latitude | Longitude | Altitude (mPD) | DBS[1] (m) | Field Code | Sample Type |
|---|---|---|---|---|---|---|
| *Tai Wan Tau Rd* | | | | | | |
| HK13855 | 22.17343363 | 114.1736629 | 116.6 | 0.5 | TP3 | U-100 Sample, horizontal |
| HK13856 | 22.17329062 | 114.1738829 | 85.5 | 0.6 | TP6 | U-100 Sample, horizontal |
| HK13857 | 22.17319277 | 114.1738793 | 66.4 | 1.1 | TP10 | U-100 Sample, horizontal |
| | | | | | | |
| *Razor Hill* | | | | | | |
| HK13354 | 22.20230784 | 114.1526909 | 141.3 | 2.4 | BDH2 | Vertical, Mezier |
| HK13355 | 22.20267219 | 114.1521913 | 167.1 | 2.5 | BDH4 | Vertical, Mezier |
| HK13873 | 22.20334247 | 114.1510105 | 228.9 | 1.5 | TP6 | U-100 Sample, horizontal |
| HK13874 | 22.20334247 | 114.1510105 | 228.9 | 2.5 | TP6 | U-100 Sample, horizontal |
| HK13875 | 22.20349179 | 114.1514823 | 177.6 | 1.2 | TP8 | U-100 Sample, horizontal |
| HK13876 | 22.20349179 | 114.1514823 | 177.6 | 2.5 | TP8 | U-100 Sample, horizontal |
| HK13877 | 22.20314737 | 114.1510907 | 255.6 | 1.8 | TP11 | U-100 Sample, horizontal |
| | | | | | | |
| *Tai Mong Tsai Rd* | | | | | | |
| HK13868 | 22.23196918 | 114.1809012 | 31.6 | 3.5 | BH1 | Vertical, Mezier |
| HK13869 | 22.23196918 | 114.1809012 | 31.6 | 6.1 | BH1 | Vertical, Mezier |
| HK13870 | 22.23196918 | 114.1809012 | 31.6 | 6.7 | BH1 | Vertical, Mezier |
| HK13871 | 22.23205438 | 114.1809639 | 42.5 | 0.8 | TP1 | U-100 Sample, horizontal |
| HK13872 | 22.23205438 | 114.1809639 | 42.5 | 0.7 | TP1 | U-100 Sample, horizontal |

Note: 1 DBS = Depth Below Surface.

## Table 4.2 Description of the Analysed Samples

| Sample No. | Sample Description | Field Code | Thickness (m) | Type of Deposit |
|---|---|---|---|---|
| *Keung Shan* | | | | |
| HK13463 | Matrix-supported, firm to soft, blackish grey, sandy silt with much angular to subangular coarse gravel and cobble and occasional boulders | TT1 | 0.8 | Debris flow |
| HK13464 | Matrix-supported, firm to soft, blackish grey, sandy silt with much angular to subangular fine to medium gravel and cobble and occasional boulders | TT1 | 0.7 | Debris flow |
| HK13465 | Clast-supported, firm to soft, blackish grey, sandy silt with much angular to subangular coarse gravel and cobble and occasional boulders | TT1 | 0.6 | Debris flood |
| HK13466 | Matrix-supported, firm, black to blackish grey, slightly clayey silt with some angular to subangular fine to medium gravel, some organic remains and subangular cobbles | TT1 | 0.5 | Buried Soil |
| HK13467 | Matrix-supported, stiff, reddish brown to yellowish brown, sandy silt with much angular to subangular cobbles and boulders | TT2 | 2.1 | Debris flow |
| HK13468 | Matrix-supported, firm to stiff, yellowish brown, slightly clayey sandy silt with much angular to subangular cobbles | TT2 | 0.8 | Debris flow |
| HK13469 | Matrix-supported, stiff, reddish brown to yellowish brown, sandy silt with much angular to subangular cobbles and boulders | TT2 | 1.5 | Debris flow |
| | | | | |
| *Mui Wo* | | | | |
| HK13824 | Matrix-supported, stiff, reddish brown, sandy clayey silt with occasional angular to subangular fine to coarse gravel | TP3 | 2.4 | Debris flow |
| HK13825 | Matrix-supported, stiff, reddish brown, sandy clayey silt with occasional angular to subangular fine to coarse gravel, cobbles and boulders | TP4 | 1.1 | Debris flow |
| HK13826 | Matrix-supported, firm to stiff, yellowish brown and reddish brown, sandy clayey silt with some angular to subangular fine to coarse gravel, cobbles and boulders | TP5 | 2.2 min. | Debris flow |
| HK13827 | Matrix-supported, firm, yellowish brown, sandy clayey silt with occasional angular to rounded fine to coarse gravel, cobbles and boulders | TP6 | 3.0 min. | Debris flow |
| | | | | |
| *Sheung Yeung* | | | | |
| HK13728 | Matrix-supported, firm to stiff, pinkish brown, slightly sandy clayey silt with occasional angular to subangular fine to coarse gravel, cobbles and boulders | TP4 | 0.9 | Debris flow |
| HK13729 | Matrix supported, firm, orangish brown, slightly sandy clayey silt with some angular to subangular fine to coarse gravel and cobbles and occasional boulders | TP8 | 0.6 | Debris flow |
| HK13730 | Matrix-supported, firm to stiff, pinkish brown, slightly sandy clayey silt with much angular to subangular fine to coarse gravel, cobbles and bouders | TP11 | 0.8 | Debris flow |
| HK13731 | Matrix-supported, firm, pinkish brown, slightly sandy clayey silt with some angular to subangular fine to coarse gravel and cobbles and occasional boulders | TP15 | 0.3 | Debris flow |
| HK13732 | Matrix-supported, firm to stiff, pinkish brown, slightly sandy clayey silt with some angular to subangular fine to coarse gravel, cobbles and occasional boulders | TP15 | 2.3 min. | Debris flow |
| | | | | |
| *Tai Wan Tau Rd* | | | | |
| HK13855 | Matrix-supported, firm to stiff, yellowish brown, slightly sandy clayey silt with some angular to subangular fine to coarse gravel, cobbles and occasional boulders | TP3 | 0.8 | Debris flow |
| HK13856 | Matrix-supported, firm to stiff, brown, sandy clayey silt with some angular to subangular fine to coarse gravel, cobbles and boulders | TP6 | 0.8 | Debris flow |
| HK13857 | Matrix-supported, firm, brown, sandy clayey silt with much angular to subangular fine to coarse gravel and cobbles | TP10 | 0.9 | Debris flow |
| | | | | |
| *Razor Hill* | | | | |
| HK13354 | Matrix-supported, firm, yellowish brown, slightly sandy clayey silt with occasional angular to subangular fine to medium gravel | DBH2 | 1.1 min. | Debris flow |
| HK13355 | Matrix-supported, firm, yellowish brown, sandy clayey silt with some fine to coarse angular gravel | DBH4 | 5.6 | Debris flow |
| HK13873 | Matrix-supported, firm, light brown, slightly sandy silt with some subangular fine to coarse gravel | TP6 | 1.2 | Debris flow |
| HK13874 | Matrix-supported, firm to stiff, moist, light brown, slightly sandy clayey silt with some subangular to subrounded fine to coarse gravel | TP6 | 1.1 min. | Debris flow |
| HK13875 | Matrix-supported, firm, moist, brown, slightly clayey sandy silt with some subrounded fine to coarse gravel | TP8 | 1 | Debris flow |
| HK13876 | Matrix-supported, firm, moist, brown, slightly clayey sandy silt with some subangular fine to coarse gravel | TP8 | 1.2 | Debris flow |
| HK13877 | Matrix-supported, firm, moist, light brown, very clayey silt with some subangular to subrounded fine to coarse gravel | TP11 | 0.6 | Debris flow |
| | | | | |
| *Tai Mong Tsai Rd* | | | | |
| HK13868 | Clast-supported, firm to stiff, yellowish brown, sandy clayey silt with much angular to subangular fine to coarse gravel | BH1 | 3.6 | Debris flow |
| HK13869 | Clast-supported, firm to stiff, brownish yellow, sandy clayey silt with some angular to subangular fine to coarse gravel | BH1 | 3.7 | Debris flow |
| HK13870 | Clast-supported, firm to stiff, yellowish brown, sandy clayey silt with some angular to subangular fine to coarse gravel and occasional cobbles | BH1 | 0.9 | Debris flow |
| HK13871 | Matrix-supported, stiff, brown, clayey sandy silt with much subangular fine to coarse gravel | TP1 | 0.7 | Debris flow |
| HK13872 | Matrix-supported, stiff, brown, clayey sandy silt with much subangular fine to coarse gravel | TP1 | 0.7 | Debris flow |

## Table 4.3 Radiocarbon[1] and Optically Stimulated Luminescence Data for the Analysed Samples (Sheet 1 of 2)

| Sample No. | Lab. Code[2] | U (μg g$^{-1}$)[3] | U (μg g$^{-1}$)[4] | U (μg g$^{-1}$)[5] | Th (μg g$^{-1}$)[6] | K% | d$D_e$/dt (Gy ka$^{-1}$) | Water % | *a*-value | $D_e$ (Gy) | d$D$/dt (Gy ka$^{-1}$) | OSL age (ka) |
|---|---|---|---|---|---|---|---|---|---|---|---|---|
| *Keung Shan* | | | | | | | | | | | | |
| HK13463 | WLL953 | 4.80 ± 0.56 | 4.54 ± 0.32 | 4.76 ± 0.43 | 38.76 ± 0.42 | 2.88 ± 0.06 | 0.1890 ± 0.0095 | 20 | 0.05 ± 0.03[7] | 305.25 ± 33.92 | 7.16 ± 0.78 | 42.6 ± 6.6 (SAR) |
| HK13464 | WLL954 | 5.72 ± 0.50 | 5.43 ± 0.29 | 5.92 ± 0.41 | 24.20 ± 0.29 | 2.23 ± 0.05 | 0.1691 ± 0.0085 | 24 | 0.07 ± 0.03[7] | 6.48 ± 0.47 | 5.87 ± 0.68 | 1.1 ± 0.2 (MA[8]) |
| HK13465 | WLL955 | 5.13 ± 0.48 | 4.51 ± 0.27 | 4.01 ± 0.36 | 30.49 ± 0.33 | 2.68 ± 0.06 | 0.1458 ± 0.0073 | 16 | 0.06 ± 0.04 | 130.0 ± 17.3 | 6.75 ± 0.96 | 19.3 ± 3.8 (MA[8]) |
| HK13466 | WLL956 | 4.74 ± 0.34 | 4.29 ± 0.20 | 4.16 ± 0.26 | 20.01 ± 0.21 | 2.16 ± 0.04 | 0.1601 ± 0.0080 | 14 | 0.07 ± 0.03[7] | 5.01 ± 0.55 | 5.60 ± 0.57 | 0.9 ± 0.1 (MA[8]) |
| HK13467 | WLL957 | 4.80 ± 0.40 | 5.07 ± 0.24 | 5.54 ± 0.33 | 39.30 ± 0.39 | 2.50 ± 0.05 | 0.1407 ± 0.0070 | 19 | 0.06 ± 0.01 | 136.8 ± 15.2 | 7.37 ± 0.46 | 18.6 ± 2.4 (MA[8]) |
| HK13468 | WLL958 | 4.90 ± 0.45 | 5.08 ± 0.27 | 5.56 ± 0.37 | 25.16 ± 0.28 | 1.78 ± 0.04 | 0.1978 ± 0.0099 | 13 | 0.07 ± 0.03[7] | 9.3 ± 0.6 | 6.12 ± 0.70 | 1.5 ± 0.2 (MA[8]) |
| HK13469 | WLL959 | 6.52 ± 0.59 | 5.75 ± 0.33 | 6.37 ± 0.45 | 42.98 ± 0.45 | 2.72 ± 0.06 | 0.1769 ± 0.0088 | 16 | 0.05 ± 0.03[7] | 227.66 ± 18.85 | 8.08 ± 0.94 | 28.2 ± 4.0 (SAR) |
| | | | | | | | | | | | | |
| *Mui Wo* | | | | | | | | | | | | |
| HK13824 | WLL1099 | 7.83 ± 0.66 | 7.69 ± 0.41 | 7.33 ± 0.50 | 45.31 ± 0.49 | 2.70 ± 0.06 | 0.1733 ± 0.0087 | 0.261 | 0.07 ± 0.01 | 125.92 ± 4.79 | 8.79 ± 0.65 | 14.3 ± 1.2 (MA[8]) |
| HK13825 | WLL1100 | 7.50 ± 0.66 | 8.31 ± 0.42 | 8.37 ± 0.55 | 37.56 ± 0.43 | 2.37 ± 0.06 | 0.1794 ± 0.0090 | 0.197 | 0.05 ± 0.01 | 52.97 ± 1.86 | 7.88 ± 0.51 | 6.7 ± 0.5 (MA[8]) |
| HK13826 | WLL1101 | 6.48 ± 0.62 | 6.47 ± 0.36 | 5.63 ± 0.46 | 32.99 ± 0.39 | 2.39 ± 0.06 | 0.1733 ± 0.0087 | 0.23 | 0.07 ± 0.01 | 39.32 ± 2.93 | 7.27 ± 0.49 | 5.4 ± 0.5 (MA[8]) |
| HK13827 | WLL1102 | 5.74 ± 0.54 | 5.35 ± 0.32 | 4.87 ± 0.41 | 29.66 ± 0.35 | 2.88 ± 0.06 | 0.1964 ± 0.0098 | 0.222 | 0.07 ± 0.01 | 9.20 ± 0.96 | 7.09 ± 0.47 | 1.3 ± 0.2 (MA[8]) |
| | | | | | | | | | | | | |
| *Sheung Yeung* | | | | | | | | | | | | |
| HK13728 | WLL1028 | 7.43 ± 0.61 | 6.41 ± 0.35 | 5.68 ± 0.44 | 42.10 ± 0.45 | 1.67 ± 0.04 | 0.1745 ± 0.0087 | 31.2 | 0.07 ± 0.02[7] | 108.39 ± 27.33 | 6.84 ± 0.72 | 15.9 ± 4.3 (SAR[9]) |
| HK13729 | WLL1029 | 9.75 ± 0.71 | 10.06 ± 0.44 | 8.60 ± 0.53 | 39.98 ± 0.43 | 1.34 ± 0.04 | 0.1794 ± 0.0090 | 30.5 | 0.07 ± 0.02 | 62.31 ± 8.09 | 7.53 ± 0.82 | 8.3 ± 1.4 (MA[8]) |
| HK13730 | WLL1030 | 8.59 ± 0.65 | 8.53 ± 0.40 | 7.68 ± 0.49 | 30.23 ± 0.35 | 1.36 ± 0.04 | 0.1745 ± 0.0087 | 32 | 0.08 ± 0.01 | 48.44 ± 5.14 | 6.43 ± 0.51 | 7.5 ± 1.0 (MA[8]) |
| HK13731 | WLL1031 | 10.49 ± 0.75 | 8.34 ± 0.45 | 6.39 ± 0.50 | 36.57 ± 0.41 | 1.67 ± 0.04 | 0.1979 ± 0.0099 | 40.2 | 0.06 ± 0.01 | 181.07 ± 21.24 | 6.19 ± 0.29 | 29.2 ± 3.7 (MA[8]) |
| HK13732 | WLL1032 | 8.12 ± 0.65 | 8.62 ± 0.40 | 7.83 ± 0.49 | 39.50 ± 0.43 | 1.46 ± 0.04 | 0.1721 ± 0.0086 | 36.9 | 0.07 ± 0.02[7] | 114.83 ± 15.46 | 6.76 ± 0.74 | 17.0 ± 2.9 (SAR) |
| | | | | | | | | | | | | |
| *Tai Wan Tau Rd* | | | | | | | | | | | | |
| HK13855 | WLL1129 | 7.35 ± 0.52 | 7.71 ± 0.33 | 6.14 ± 0.38 | 34.69 ± 0.36 | 1.64 ± 0.04 | 0.1889 ± 0.0094 | 0.264 | 0.08 ± 0.02 | 69.45 ± 12.93 | 7.26 ± 0.73 | 9.6 ± 2.0 (MA[8]) |
| HK13856 | WLL1130 | 8.55 ± 0.47 | 8.48 ± 0.30 | 8.07 ± 0.36 | 38.93 ± 0.37 | 2.31 ± 0.05 | 0.1855 ± 0.0093 | 0.206 | 0.09 ± 0.01 | 58.28 ± 6.59 | 9.27 ± 0.57 | 6.3 ± 0.8 (MA[8]) |
| HK13857 | WLL1131 | 7.28 ± 0.43 | 7.35 ± 0.28 | 6.83 ± 0.34 | 29.18 ± 0.29 | 1.91 ± 0.04 | 0.1726 ± 0.0086 | 0.134 | 0.08 ± 0.02 | 15.20 ± 2.56 | 7.78 ± 0.64 | 2.0 ± 0.4 (MA[8]) |

## Table 4.3 Radiocarbon[1] and Optically Stimulated Luminescence Data for the Analysed Samples (Sheet 2 of 2)

| Sample No. | Lab. Code[2] | U (µg g$^{-1}$)[3] | U (µg g$^{-1}$)[4] | U (µg g$^{-1}$)[5] | Th (µg g$^{-1}$)[6] | K% | d$D_e$/dt (Gy ka$^{-1}$) | Water % | *a*-value | $D_e$ (Gy) | d$D$/dt (Gy ka$^{-1}$) | OSL age (ka) |
|---|---|---|---|---|---|---|---|---|---|---|---|---|
| *Razor Hill* | | | | | | | | | | | | |
| HK13354 | RDL | 9.94 ± 0.51 | 7.80 ± 1.50 | 11.26 ± 3.28 | 42.17 ± 2.53 | 1.32 ± 0.06 | 0.1462 ± 0.0073 | 24 | 0.06 ± 0.01[7] | 84.90 ± 3.80 | 8.31 ± 0.41 | 10.2 ± 0.7 (SAR) |
| HK13355 | RDL | 8.08 ± 0.69 | 5.30 ± 0.70 | 10.02 ± 2.90 | 35.21 ± 2.10 | 1.20 ± 0.04 | 0.1455 ± 0.0073 | 23 | 0.06 ± 0.01[7] | 194.3 ± 8.6 | 6.85 ± 0.36 | 28.4 ± 1.9 (SAR) |
| HK13873 | WLL1147 | 8.12 ± 0.53 | 7.66 ± 0.32 | 6.80 ± 0.39 | 36.46 ± 0.37 | 1.10 ± 0.03 | 0.1654 ± 0.0083 | 32 | 0.08 ± 0.02 | 128.19 ± 9.10 | 6.63 ± 0.71 | 19.3 ± 2.5 (MA[8]) |
| HK13874 | WLL1148 | 7.30 ± 0.41 | 7.15 ± 0.26 | 7.29 ± 0.33 | 37.58 ± 0.36 | 1.18 ± 0.02 | 0.1447 ± 0.0072 | 32 | 0.03 ± 0.01[7] | 265.00 ± 7.39 | 5.25 ± 0.44 | 50.5 ± 4.4 (SAR) |
| HK13875 | WLL1149 | 6.98 ± 0.40 | 6.66 ± 0.25 | 5.87 ± 0.29 | 30.37 ± 0.29 | 3.41 ± 0.07 | 0.1711 ± 0.0086 | 25 | 0.03 ± 0.01[7] | 603.87 ± 14.00 | 6.79 ± 0.44 | 88.9 ± 6.1 (SAR) |
| HK13876 | WLL1150 | 10.64 ± 0.53 | 10.50 ± 0.35 | 9.93 ± 0.42 | 27.57 ± 0.27 | 2.95 ± 0.06 | 0.1436 ± 0.0072 | 19 | 0.03 ± 0.01[7] | 608.31 ± 11.42 | 7.59 ± 0.49 | 80.1 ± 5.4 (SAR) |
| HK13877 | WLL1151 | 7.57 ± 0.43 | 7.08 ± 0.27 | 6.97 ± 0.33 | 43.46 ± 0.41 | 0.79 ± 0.02 | 0.1593 ± 0.0082 | 37 | 0.03 ± 0.01[7] | 323.02 ± 9.25 | 5.14 ± 0.46 | 62.8 ± 5.9 (SAR[9]) |
| | | | | | | | | | | | | |
| *Tai Mong Tsai Rd* | | | | | | | | | | | | |
| HK13868 | WLL1142 | 9.59 ± 0.66 | 8.78 ± 0.36 | 8.46 ± 0.50 | 29.62 ± 0.34 | 1.66 ± 0.04 | 0.1242 ± 0.0062 | 15.6 | 0.03 ± 0.01 | 344.78 ± 23.88 | 6.34 ± 0.41 | 54.4 ± 5.2 (MA[8]) |
| HK13869 | WLL1143 | 9.38 ± 0.62 | 8.67 ± 0.37 | 8.17 ± 0.46 | 32.69 ± 0.35 | 1.66 ± 0.04 | 0.0907 ± 0.0045 | 19.2 | 0.03 ± 0.01[7] | 368.38 ± 13.55 | 6.29 ± 0.44 | 58.6 ± 4.7 (SAR) |
| HK13870 | WLL1144 | 8.80 ± 0.53 | 8.10 ± 0.30 | 7.82 ± 0.40 | 32.00 ± 0.33 | 1.36 ± 0.03 | 0.0847 ± 0.0042 | 19.9 | 0.03 ± 0.01 | 337.78 ± 54.17 | 5.78 ± 0.41 | 58.5 ± 10.3 (MA[8]) |
| HK13871 | WLL1145 | 8.84 ± 0.56 | 7.45 ± 0.33 | 6.25 ± 0.37 | 46.05 ± 0.45 | 1.55 ± 0.03 | 0.1775 ± 0.0089 | 14.9 | 0.07 ± 0.01 | 77.55 ± 2.07 | 8.79 ± 0.41 | 8.8 ± 0.5 (MA[9]) |
| HK13872 | WLL1146 | 8.68 ± 0.60 | 7.89 ± 0.36 | 6.64 ± 0.42 | 48.29 ± 0.48 | 1.99 ± 0.04 | 0.1800 ± 0.0090 | 21.1 | 0.07 ± 0.01 | 112.28 ± 14.92 | 8.97 ± 0.57 | 12.5 ± 1.8 (MA[8]) |

Notes:

1 Radiocarbon ages on duplicate samples: HK13834: 7940 ± 40 yr BP (8990-8360 cal. Yr BP), HK13827: 240 ± 30 yr BP (300-270 cal. yr BP), HK13466: 330 ± 30 yr BP (490-300 cal. yr BP). The probability method has been used for calibrating the radiocarbon ages using the 'Oxcal' programme and the InCal98 calibration curve. The age range shown is for the 95% confidence level.

2 Samples with codes WLL measured at Luminescence Dating Laboratory, Victoria University, Wellington, NZ (Analyst: N. Wang), all other samples measured at Radiation Dosimetry Laboratory (RDL), OSU, Stillwater, USA (Analyst: R. DeWitt).

3 U (µg/g) from $^{234}$Th.

4 U (µg/g) from $^{226}$Ra, $^{214}$Pb, $^{214}$Bi.

5 U (µg/g) from $^{210}$Pb.

6 Th (µg/g) from $^{208}$Tl, $^{212}$Pb, $^{228}$Ac.

7 a-value estimated, as alpha-irradiated subsample was saturated. MA = Multi-Aliquot; SAR = Single Aliquot Regenerative.

8 4-11µm multimineral sample, infrared stimulation, 410 nm 'blue' optical OSL filter.

9 4-11µm multimineral sample, infrared stimulation, broadband BG39+L40 filters (400-600 nm).

# 5 Geomorphological Assessment, Dating Results and Interpretation

## 5.1 Lantau Island

### 5.1.1 Keung Shan

Detailed geomorphological assessment has identified a complex landscape located on a broad, upper to middle valley side slope with a significant variety of colluvial deposits distributed within several geomorphological terrain units based on API, detailed field mapping, and ground investigation works (AFJV, 2012). Samples were collected for OSL and $^{14}C$ dating from two trial trenches excavated within landslide debris overlying alluvial deposits in TT1, and basal colluvium in TT2. The two trenches were excavated at similar elevations in adjacent drainage catchments overlooking Keung Shan Road (Figure 3.2a). Landslide debris was mapped within the Middle Terrain unit, and is considered to be relatively younger material deposited as a result of landslide processes, but without an identifiable source location.

The basal colluvium is considered to be one of the oldest colluvium overlying weathered rock in the Middle Terrain unit.

#### 5.1.1.1 Results

Trial Trench TT1, excavated to a depth of about 2.7 m, exposed a 2.6-m thick sequence of colluvium and alluvium overlying moderately decomposed coarse ash tuff. Four distinct layers were identified, including: an upper 1-m thick unit of soft to firm, light grey mottled brown, slightly clayey sandy silt; an upper middle 0.1-0.35-m thick unit of soft to firm, black to blackish grey, sandy clayey silt; a lower middle 0.4-0.6-m thick unit of loose, bluish grey, slightly clayey silty sand, with lenses of well sorted sand and clay; and, a lower 0.2-0.7-m thick unit of dense, orangish brown, gravel and cobbles with a matrix of slightly clayey sandy silt.

The volume of the landslide debris represented by the upper unit in TT1, based on the mapped area, is estimated to be up to approximately 1,500 $m^3$.

The upper middle unit contained woody organic material suggestive of a buried soil horizon, whereas the loose sand, with lenses of well sorted sand and clay, of the lower middle unit probably represents buried alluvium. The matrix-supported character of the upper unit is indicative of a debris flow deposit, whereas the clast-supported character of the lower unit suggests a debris flood deposit.

Two samples from different faces were sampled from the upper unit for OSL dating, one sample was taken from the upper middle unit for both OSL and $^{14}C$ dating, while one sample was taken from the lower unit for OSL dating.

The upper unit yielded an MAAD age of 1.1±0.2 ka and an SAR age of 42.6±6.6 ka, respectively.

The upper middle unit yielded an MAAD age of 0.9±0.1 ka and a radiocarbon age of 330±30 BP (Cal yr BP 490-300).

The lower unit yielded an MAAD age of 19.3±3.8 ka.

Trial Trench TT2, exposed a minimum thickness of colluvium excavated to a depth of about 3.0 m. The colluvium could be divided into three main units, including: an upper 0.6-1.0-m thick layer of firm to stiff, yellowish brown slightly sandy silt; a middle layer, up to 1.9 m thick, of firm to stiff, orangish brown, slightly sandy silt; and, a lower layer (i.e. basal colluvium) at the base of the trench of grey mottled orange and yellow slightly sandy silty clay. The upper two layers of landslide debris were interpreted as debris flow deposits.

The volume of the landslide debris represented by the upper unit in TT2, based on the mapped area, is estimated to be approximately 4,000 $m^3$.

One sample collected for OSL dating from the upper debris flow deposit yielded an MAAD age of 1.1±0.2 ka, whereas two samples collected from different faces from the lower debris flow deposit yielded a MAAD age of 18.6±2.4 ka and an SAR age of 28.2±4.1 ka, respectively.

#### 5.1.1.2 Interpretation

The MAAD ages from the upper unit of both trial trenches overlap within error with an average age of about 1,000 years (1.0±0.1 ka, $\chi^2/\upsilon = 1.25$). The considerably older SAR age (42.6±6.6 ka) for the upper unit in TT1 is considered anomalous possibly due to incomplete bleaching of the sediment grains. However, there is no indication from the laboratory report to suggest that the luminescence signal has been compromised.

The OSL and $^{14}C$ ages from the upper middle unit of TT1 are largely consistent with the age for the upper unit and corroborates the preliminary interpretation that this unit is likely to represent a buried soil horizon. Depositional events in adjacent drainage catchments therefore appear to have occurred concurrently approximately 1,000 years ago.

The OSL ages from the lower unit in both trial trenches are considerably older than those of the upper unit. The two MAAD ages are in agreement within error with an average age of 19.0±0.5 ka ($\chi^2/\upsilon = 0.03$) indicating that depositional events took place approximately 19,000 years ago. The older SAR age of 28.2±4.1 ka from the lower unit in TT2 suggests that some grains may have been incompletely bleached during deposition, although there is no indication of this possibility in the laboratory report.

In summary, the dating of superficial deposits at Keung Shan suggest depositional events at about 19,000 years and 1,000 years ago.

### 5.1.2 Mui Wo

A detailed geomorphological assessment identified several types of superficial deposits along lower valley side slopes immediately above the valley floor in Wang Tong, Mui Wo (Fugro, 2015). Superficial deposits are divided into colluvium (undifferentiated superficial deposits), landslide debris (superficial deposits ascribed to specific landslide sources) and debris fan deposits (fan shaped features at the distal ends of drainage catchments, and comprising both landslide debris together with debris flood and alluvial deposits). Samples from four trial pits excavated within superficial deposits were collected for OSL and $^{14}C$ dating. Trial pits TP3 and

TP4 were excavated at the upper and lower parts of the same debris fan. In the adjacent catchment, trial pits TP5 and TP6 were excavated at the lower and upper parts, respectively, of debris fan deposits (Figure 3.2b). TP6 was excavated on a debris lobe at the top of the fan.

#### 5.1.2.1 Results

Trial Pits TP3 and TP4 were excavated to depths of 3 m and 1.8 m, respectively. TP3 exposed a single 2.0-m thick layer of colluvium overlying completed to highly decomposed granite, and capped by a 0.15-m thick layer of top soil. The colluvium comprised stiff, reddish brown sandy clayey silt. TP4 exposed two layers of colluvium; an upper 1.2-m thick unit of stiff, reddish brown sandy clayey silt, and a lower 0.6-m thick unit of dense, reddish brown, cobbles and boulders, overlying moderately decomposed granite.

One sample each from the upper units in TP3 and TP4 were sampled for OSL dating, whereas one sample from the upper unit in TP4 was also collected for $^{14}C$ dating.

The upper unit in TP3 yielded an MAAD age of 14.3±1.2 ka. The upper unit in TP4 yielded an MAAD age of 6.7±0.5 ka and a radiocarbon age of 7950±40 yr BP (Cal yr BP 8990-8630).

Trial Pits TP5 and TP6 were excavated to 2.8 m and 3.0 m, respectively. TP5 revealed two main layers of colluvium: an upper 2.0-m thick unit of firm to stiff, yellowish brown to reddish brown sandy clayey silt, and a lower approximately 1-m thick unit of dense, pale brown boulders, with some stiff, reddish brown sandy clayey silt matrix. TP6 exposed a single colluvial unit with a minimum thickness of 3.0 m and comprising firm, yellowish brown sandy clayey silt.

One sample each from the upper unit in TP5 and TP6 were sampled for OSL dating, whereas the same sample from TP6 was also subjected to $^{14}C$ dating.

The upper unit in TP5 yielded an MAAD age of 5.4±0.5 ka, whereas the upper unit in TP6 yielded an MAAD age of 1.3±0.2 ka and a radiocarbon age of 240±30 yr BP (Cal yr BP 300-270).

#### 5.1.2.2 Interpretation

The MAAD ages from the upper units of TP3 and TP4 indicate separate events at approximately 14,000 years and 7,000 years ago, respectively. The radiocarbon age from TP4 is within error of the OSL age, confirming an event of approximately 7,000 years ago.

The MAAD ages from the upper units of TP5 and TP6 indicate separate events at approximately 5,000 years and 1,000 years, respectively. Although the radiocarbon age from TP4 is slightly younger than the OSL age, it is consistent with a relatively young age for the unit.

In summary, the dating of superficial deposits at Mui Wo suggests separate depositional events at 14,000, 7,000, 5,000 and 1,000 years ago. The ages confirm the division of debris fan deposits based on API into layers of relatively young landslide debris overlying older colluvium.

## 5.2 Eastern New Territories

### 5.2.1 Tai Wan Tau Road

Four varieties of superficial deposits were identified across upper slopes, mid-slopes and foot slopes during the geomorphological assessment (Fugro, 2012a). The superficial deposits consist of coarse, thick, reworked and thin colluvial units. Samples from three trial pits were collected for dating (Figure 5.1a). Trial pit TP3 was located in the upper slopes covered with thin colluvium. Trial Pit TP6 was located in mid-slope coarse colluvium whilst trial pit TP10 was located in thicker colluvial foot slope fan deposits.

#### 5.2.1.1 Results

TP3 was excavated to a depth of approximately 0.8 m and revealed a 0.5-m thick unit of colluvium overlying highly decomposed fine ash tuff, and capped by a 0.2-m thick layer of top soil. One sample comprising firm to stiff, yellowish brown, slightly sandy clayey silt was collected for OSL dating from a depth of 0.5 m, and yielded a MAAD age of 9.6±2.0 ka and a SAR age of 7.5±0.9 ka, respectively.

TP6 was excavated to a depth of 1.1 m and revealed a single 0.9-m thick unit of firm to stiff, brown to yellowish brown, sandy clayey silt overlying highly decomposed fine ash tuff, and capped by a 0.2-m thick layer of topsoil. One sample was collected for OSL dating at a depth of 0.6 m and yielded a MAAD age of 6.3±0.8 ka.

TP10 was excavated to a depth of 1.7 m and also revealed a single 1-m thick unit of colluvium overlying highly decomposed fine ash tuff, and capped by a 0.15-m thick layer of topsoil. One sample comprising firm to stiff, brown to yellowish brown, sandy clayey silt was collected for OSL dating from the base of the colluvium at a depth of 1.1 m and yielded a MAAD age of 2.0±0.4 ka.

#### 5.2.1.2 Interpretation

The two OSL ages obtained from colluvial deposits in TP3 are in agreement within error (8.6±1.5 ka, $\chi^2/\upsilon$ = 1.64) and suggest a depositional event at approximately 8,000 to 10,000 years ago. The slightly younger age for colluvium from TP6 suggests an event at approximately 6,000 years ago, while an appreciably younger age for colluvium from TP10 suggest an event at approximately 2,000 years ago. The ages indicate younger deposits in a down slope direction through the study area, confirming the geomorphological model which suggested the mass wasting processes were older in the upper slopes.

### 5.2.2 Sheung Yeung

Geomorphological assessment has identified four terrain features and eight varieties of superficial deposits from the Sheung Yeung study area (Fugro, 2012b). From the highest to the lowest elevation, the terrain features comprise ridges and spurlines, open hillslopes and foot slopes with incised valleys (recorded as 'mid-slope' terrain) extending from below the ridges

and through the foot slopes. The superficial deposits are sub-divided into talus, thick colluvium, bouldery colluvium, valley colluvium, thin colluvium, ancient landslide debris, lobes and levees, reworked colluvium and debris fan materials. Samples from four trial pits were collected for dating. Trial pits TP8, TP11 and TP15 were excavated in separate catchments. Trial pits TP11 and TP15 were excavated in the valleys incised through foot slope areas, whereas TP8 was excavated above the valley in the foot slope area. In contrast, TP4 was excavated on a spurline near the head of the catchment above TP11 (Figure 5.1b).

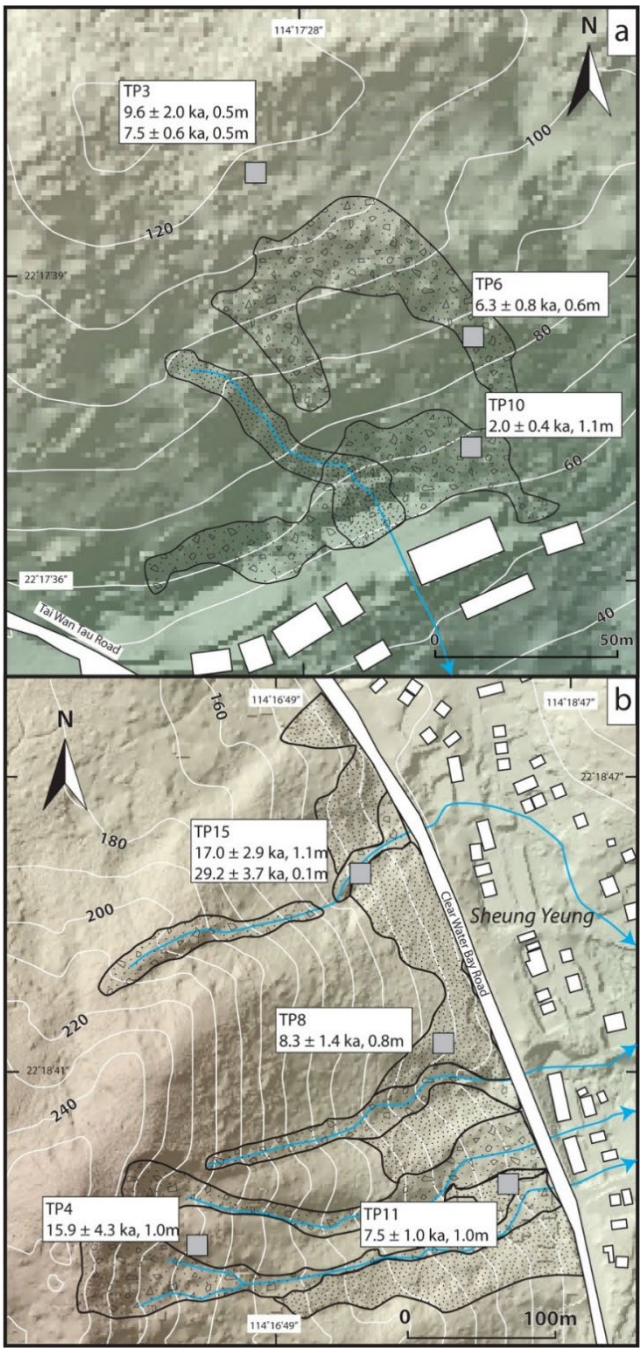


**Figure 5.1 Dated Hillside Catchments at (a) Tai Wan Tau Road, and (b) Sheung Yeung, Eastern New Territories. Legend as for Figure 3.2**

#### 5.2.2.1 Results

TP4 was excavated to a depth of 3.2 m and revealed a single 0.7-m thick layer of colluvium overlying completely decomposed fine ash tuff, and overlain by a 0.3-m thick layer of topsoil. One sample, comprising firm to stiff, pinkish brown to greyish brown, slightly sandy clayey silt was collected for OSL dating from the base of the colluvium at a depth of 1.0 m. This sample yielded a SAR age of 15.9±4.3 ka.

TP8 was excavated to a depth of 2.2 m and revealed a single 0.5-m thick layer of colluvium overlying completely decomposed fine ash tuff, and capped by a 0.2-m thick layer of topsoil. The main colluvial unit comprised firm to stiff, orangish brown, slightly sandy clayey silt. One sample was collected for OSL dating at a depth of 0.8 m and yielded a MAAD age of 8.3±1.4 ka.

TP11 was excavated to a depth of about 1.4 m and exposed two layers of colluvium overlying highly decomposed fine ash tuff. The upper unit comprised a 0.45-m thick layer of firm, dark brown, slightly clayey sandy silt, whereas the lower, ~1-m thick unit comprised firm to stiff, pinkish brown, slightly sandy clayey silt. One sample from the lower unit was collected for OSL dating at a depth of 1.2 m and yielded a MAAD age of 7.5±1.0 ka.

TP15 was excavated to a depth of 3.2 m and revealed two main layers of colluvium overlying completely decomposed fine ash tuff, and capped by a 0.1-m thick layer of top soil. The upper 0.6-m thick colluvium comprised firm, pinkish brown to greyish brown, slightly sandy clayey silt, whereas the lower 1.2-2.2-m thick colluvium comprised firm, pinkish brown to reddish brown, slightly sandy clayey silt. One sample from each layer was collected for OSL dating at depths of 0.1 m and 1.1 m, respectively. The sample from the upper unit yielded a MAAD age of 29.2±3.7 ka, whereas the sample from the lower unit yielded a SAR age of 17.0±2.9 ka.

#### 5.2.2.2 Interpretation

The ages of the main units dated from TP8 and TP11 are in agreement within error, (7.9±0.6 ka, $\chi^2/\upsilon = 1$) suggesting that deposition occurred at approximately 8,000 years ago. Similarly, the lower unit from TP15 and main unit from TP4 are in agreement within error (16.5±0.8 ka, $\chi^2/\upsilon = 0.05$), and suggest depositional events occurred approximately 16,000 years ago. The appreciably older age (29.2±3.7 ka) obtained for the upper unit from TP15 may suggest that this sample was incompletely bleached during emplacement although there is no indication of this possibility in the laboratory report.

In summary, the ages of superficial deposits from Sheung Yeung debris fans suggest two main periods of accumulation at 16,000 years and 8,000 years ago. The 8000-year accumulation event is consistent with the ages of debris fans near Tai Wan Tau Road.

### 5.2.3 Razor Hill

Detailed geomorphological assessments for two study areas on Razor Hill are provided by Fugro (2014) and OAP (2014). The lower east-facing slopes overlooking Clear Water Bay

Road (east sub-area) comprise coalescing debris lobes which have been incised by younger drainage lines infilled with more recent colluvium (Figure 5.2a). The colluvium has been divided into four types, namely lower spurline colluvium, valley colluvium, footslope colluvium and landslide debris. Boulder-filled depressions, talus and taluvium were also recorded (OAP, 2014). Samples for dating were collected from two drillholes, BDH2 and BDH4 in foot slope areas of the study area, with BDH4 located on a colluvium covered spurline, while BDH2 was located within a lower debris fan complex.

The northeastern-facing slopes overlooking Clear Water Bay Road (northeast sub-area) comprise relict colluvium/taluvium across the upper slopes, and more recent colluvium infilling a prominent gully and a minor gully identified as topographic depressions TD2 and TD1, respectively, in the lower slopes (Fugro, 2014). Samples were collected from three trial pits at different elevations (Figure 5.2a). TP11 was excavated at the highest elevation on a spurline covered with thick, relict colluvium and located between the two gullies, whereas TP8 was excavated in the floor of the prominent gully in the lower foot slope area below and to the northeast of TP11. TP6 was excavated just above the gully floor in the topographic depression below and to the north of TP11.

#### 5.2.3.1 Results

BDH2 revealed 3.1-m thick colluvium overlying completely decomposed fine ash tuff. Three main layers of colluvium were identified: an upper, 1.0-m thick, greyish orangish brown, slightly sandy clayey silt; a middle, 1.2-m thick, reddish brown slightly sandy clay/silt; and, a lower, 1.1-m thick colluvium. The lower colluvium layer was sampled and logged in detail and comprised another three separate units. One sample for OSL dating was collected from a depth of 2.4 m from the middle 0.3-m thick unit of the lower colluvium layer and yielded a SAR age of 10.2±0.7 ka.

BDH4 revealed a 7.6-m thickness of colluvium overlying completely decomposed fine ash tuff. Three different types of colluvium were identified from an examination of three intact samples recovered from depths of 2-3 m, 4.7-5.7 m and 6.9-7.6 m. The upper unit comprised > 0.9-m thick firm, yellowish brown, slightly sandy clayey silt, the middle unit comprised > 0.9-m thick dense, light yellowish brown, very sandy, silty fine to medium gravel, and the lower unit comprised > 0.5-m thick, firm, light yellowish brown, sandy clayey silt. Minimum thicknesses are due to incomplete Mazier records. One sample for OSL dating was collected from a depth of 2.5 m in the upper unit, and yielded a SAR age of 28.4±1.9 ka.

On the northeastern flank of Razor Hill, trail pit TP8 was excavated to a depth of 3.2 m in the base of the prominent gully in the lower part of the largest and most degraded topographic depression (TD2). Two layers of colluvium were recorded. The upper layer (1.2 m thick) comprised firm, brown slightly clayey silt with some subangular to subrounded fine to coarse gravel, whereas the lower layer (1.3 m thick) comprised firm, brown, slightly clayey sandy silt with some subangular fine to coarse gravel. Two samples for OSL dating were obtained from depths of 1.3 m and 2.5 m, and yielded SAR ages of 88.9±6.1 ka and 80.1±5.4 ka, respectively.

TP6 was excavated to a depth of 3.2 m above the minor gully floor of the smaller topographic depression (TD1). Two layers of colluvium were recorded. The upper layer (0.9 m thick) comprised firm, light brown, slightly sandy silt with some subangular to

subrounded fine to coarse gravel, whereas the lower layer (minimum thickness 1.1 m) comprised firm to stiff, light brown, slightly sandy slightly clayey silt with some subangular to subrounded fine to coarse gravel. Two samples for OSL dating were obtained from depths of 1.5 m and 2.5 m. The upper colluvium returned a MAAD age of 19.3±2.5 ka, whereas the lower colluvium yielded an SAR age of 50.5±4.4 ka.

TP11 was excavated to a depth of 2.7 m on the spurline between the two gullies (in TD1 and TD2). One layer of colluvium (0.3-2.1 m thick) was recorded and comprised firm, light brown very clayey silt with some subangular to subrounded fine to coarse gravel. One sample for OSL dating was obtained from a depth of 1.8 m and yielded an SAR age of 62.8±5.9 ka.

#### 5.2.3.2 Interpretation

In the east sub-area, the age of colluvium from BDH2 is in general agreement with the age obtained from the upper terrain unit at Tai Wan Tau Road (8,000-10,000 years). The older SAR age from BDH4 has no known equivalent. Nonetheless, the ages confirm the geomorphological model which suggested the presence of older foot slope colluvium which has been incised along several drainage lines with younger debris lobes subsequently deposited.

In the northeast sub-area, the two ages of colluvium from TP8 are within analytical error with an average age of 84.5±6.22 ka ($\chi^2/v$ = 1.18); the upper layer being slightly older than the lower layer. The descriptions of the colluvial layers are very similar, with the only difference being in the roundness and sorting of the included fragments. Therefore, the two layers probably record the same depositional event. The ages of colluvium from the base of the prominent gully in TD2 are the oldest so far dated by OSL methods in Hong Kong.

The two ages of colluvium from TP6 indicate two separate events, one at approximately 20,000 years ago and one approximately 50,000 years ago. Both ages coincide with similar ages dated from other landslide sites approximately Hong Kong and show that the deposits exposed above the minor gully in TD1 are younger than those exposed in the gully floor in TD2, with possible reactivation of processes in the TD1 catchment at approximately 20,000 years ago. It is postulated that the erosion in TD2 has exposed deeper and older colluvium underlying the study area foot slopes, whereas the gully in TD1, which is less well developed than in TD2, has not yet entrenched deep enough to expose the older deposits.

### 5.2.4 Tai Mong Tsai Road

The geomorphological assessment (Jacobs, 2014) identified a number of landslide scars and gullies incising into planar valley side slopes between a ridgeline and steep coastal slopes, together with four main types of superficial deposits, namely taluvium, colluvium, landslide debris and alluvium, at the Tai Mong Tsai Road study area. Debris from one prominent large relict landslide in the mid- to lower slopes was dated using samples from one drillhole and one trial pit (Figure 5.2b).

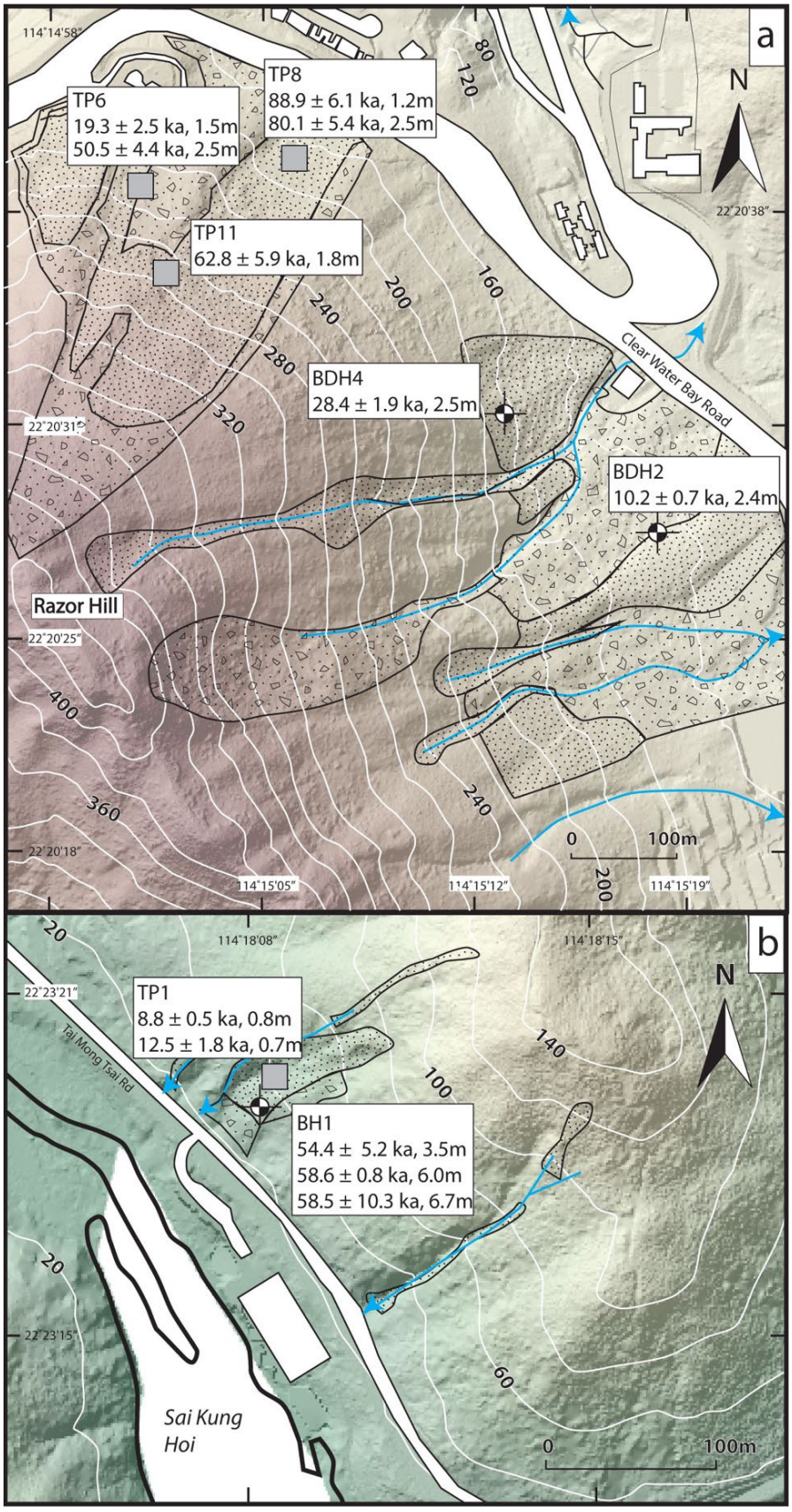


**Figure 5.2 Dated Hillside Catchments at (a) Razor Hill, and (b) Tai Mong Tsai Road, Eastern New Territories. Legend as for Figure 3.2**

#### 5.2.4.1 Results

Trial Pit TP1 was located in the centre of a large debris lobe and excavated to a depth of 1.5 m. One single 1.4-m thick colluvial unit comprising stiff, yellowish brown, clayey sandy silt was exposed overlying dense bouldery colluvium, and capped by a 0.2-m thick layer of topsoil. Two samples for OSL dating were obtained from depths of 0.7 m and 0.8 m, and yielded MAAD ages of 12.5±1.8 ka and 8.8±0.5 ka, respectively.

BH1 was located at a slightly lower elevation in the same large debris lobe as TP1. This drillhole revealed 7.4-m thick colluvium overlying completely decomposed siltstone. The colluvium comprised two main units: an upper 3.7-m thick unit of clast-supported cobbles and boulders with an interstitial matrix of firm to stiff, brown, slightly sandy clayey silt, and a lower 3.7-m thick layer of similar clast-supported cobbles and boulders within a matrix of orangish brown, slightly sandy clayey silt. Three samples for OSL dating were obtained from depths of 3.5 m, 6.0 m, and 6.7 m and yielded MAAD ages of 54.4±5.2 ka, 58.6±0.8 ka, and 58.5±10.3 ka, respectively.

#### 5.2.4.2 Interpretation

Although the two ages obtained from TP1 came from the same colluvial unit at slightly different depths (Table 4.1), their OSL–MAAD ages do not overlap. According to the laboratory report, the younger sample had very low blue luminescence under infrared stimulation. Therefore, broad band luminescence (400-660 nm) was detected using BG39+L40 filters in order to increase the signal intensity. In all other samples, luminescence was detected focusing on the blue emission band of potassium feldspars (410 nm). Thus, the reliability of the younger age may be questionable. We therefore consider that the older age from TP1 more likely reflects the true depositional age of the unit suggesting an event approximately 12,500 years ago.

The age of the upper unit in BH1 is slightly younger than the two ages obtained from the lower unit, which overlap within error yielding an average age of 58.6±0.1 ka ($\chi^2/\upsilon = 0.01$). Together, these ages suggest two significantly older periods of accumulation at approximately 58,000 years and 54,000 years ago. The materials are from a large, relict debris lobe complex, and the ages are similar to that previously obtained for large, deep-seated landslides in Hong Kong (Sewell et al, 2006).

## 6 Discussion

A summary of the dating results for colluvium from the six catchments investigated is presented in Figure 6.1. If some SAR ages are excluded due to possible incomplete bleaching, then hillside catchments from Lantau Island reveal pulses of accumulation at 19,000, 14,000, 7,500, and 5,000 years ago.

Considerably older ages of colluvium are revealed from two sites in eastern New Territories (Razor Hill and Tai Mong Tsai Road) indicating accumulation events at approximately 85,000 years ago and between 60,000 and 45,000 years ago. Pulses of accumulation in eastern New Territories are also recorded at 28,000, 19,000, 12,500, 10,000 - 8,000, 6,000 and 2,000 years ago.

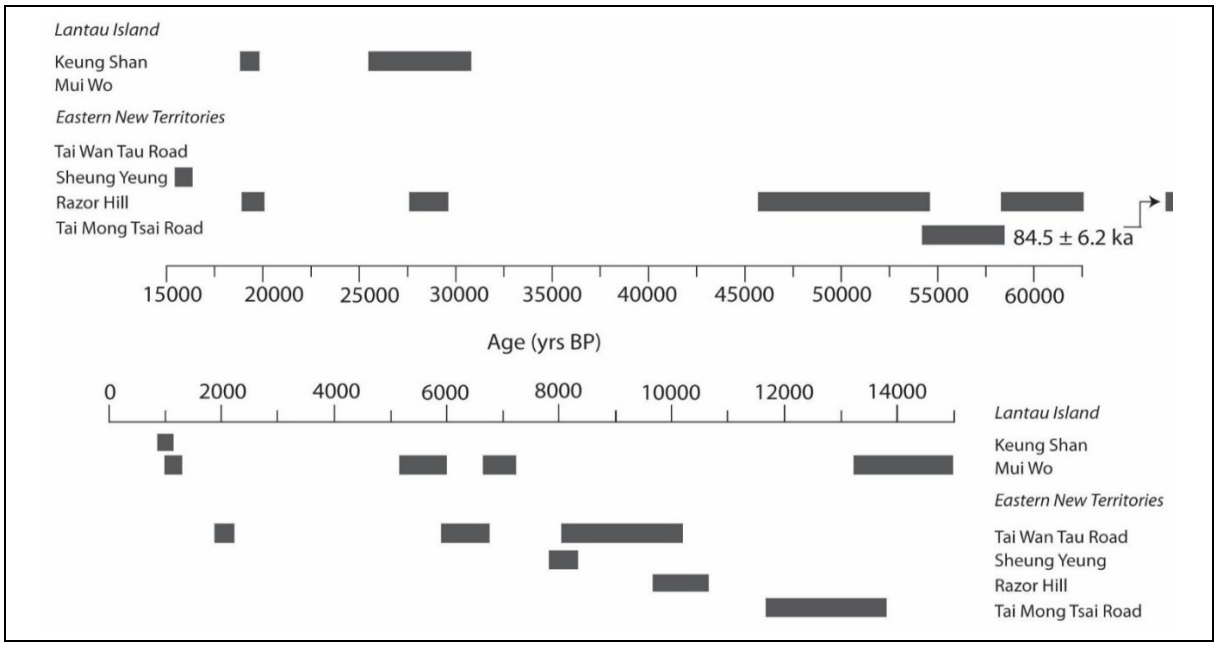


**Figure 6.1 Summary of Ages of Colluvium from Six Hillside Catchments on Lantau Island and Eastern New Territories**

Pulses of debris accumulation have previously been reported from Lantau Island coastal fan complexes for the periods of 28,000-20,000 ka, 14,500-10,500 ka, 5,800-5,000 ka, 4,370-4,230 ka, 3,560-3,320 ka, and 1,350-1,050 (Sewell et al, 2015). Pulses of deep-seated landslide activity from inland areas of Hong Kong have also been reported for the periods 65,000-45,000, 32,000, 14,500-10,500, 8,500-5,500 ka, and 3,800-2,900 ka (Sewell et al, 2006). The new age data from hillside catchments on Lantau Island and Eastern New Territories are therefore largely consistent with the earlier reported findings.

## 7 Conclusion

Dating of colluvium from hillside catchments on Lantau Island and Eastern New Territories has contributed thirty-one new ages to the relict landslide age dataset for Hong Kong. The new data are largely consistent with the results from earlier dating studies and reveal that the relict colluvium in hillside catchments is 1,000s (with some 10,000s) rather than 100s of years old. Clusters of large, deep-seated landslides occur between 65,000-45,000 years and at approximately 32,000 years ago. More frequent pulses of landslide activity are recorded during the early to mid-Holocene probably in association with climatic amelioration and rising sea levels.

## 8 References

Arup Fugro Joint Venture (AFJV), 2012. *Natural Terrain Hazard Study Report. Study Area No. 13NW-B/SA2 (Hillside Catchment Nos. 13NW-B/DF4, 13NW-B/DF4a, 13NW-B/DF4b, 13NW-B/DF4c, 13NW-B/DFd, 13NW-B/DF4e, 13NW-B/DF4f, 13NW-B/DF4g and 13NW-B/DFh) Hillside Above Keung Shan Road East, West Lantau*. 331 p.

Fugro (Hong Kong) Limited (Fugro), 2015. *Stage 2(H) Report. Study Area 10SW-A/SA1 (Hillside Catchment Nos. 10SW-A/DF2, 10SW-A/DF6, 10SW-A/DF6a, 10SW-A/DF6b, 10SW-A/DF7, 10SW-A/DF9, 10SW-A/DF10, 10SW-A/DF11 and 10SW-A/OH27 Mui Wo.* 75 p.

Fugro (Hong Kong) Limited (Fugro), 2014. *Stage 2(H) Report. Study Area No. 11NE B/SA3 at Razor Hill, Clear Water Bay Road*. 276 p.

Fugro (Hong Kong) Limited (Fugro), 2012a. *Natural Terrain Hazard Study Report. Study Area No. 12SW-A/SA1 Above Tai Wan Tau Road, Sai Kung.* 115 p.

Fugro (Hong Kong) Limited (Fugro), 2012b. *Natural Terrain Hazard Study Report. Study Area No. 12NW-C/SA2 (Hillside Catchment Nos. 12NW-C/DF4; 12NW-C/OH16; 12NW-C/DF9 and 12NW-C/DF9a) Above Clear Water Bay Road in Sheung Yeung, Sai Kung.* 284 p.

Geotechnical Engineering Office (GEO) 2000. *Geological Map of Hong Kong. Hong Kong Geological Survey, 1:100,000 Series HGM100.* Hong Kong Government.

IPCC, 2013. Climate Change 2013: *The Physical Science Basis. Contribution of Working Group 1 to the Fifth Assessment Panel Report of the Intergovernmental Panel on Climate Change (IPCC)*. Cambridge University Press.

Jacobs China Limited (Jacobs), 2014. *Stage 2(H) Report. Study Area 8SW-B/SA3 Tai Mong Tsai Road, Sai Kung*. 284 p.

Ove Arup & Partners Limited (OAP), 2014. *Natural Terrain Hazard Study for Study Area Overlooking HKUST Staff Quarters.* 202 p.

Sewell, R.J., Barrows, T.T., Campbell, S.D.G. & Fifield, L.K. (2006). Exposure Dating ($^{10}$Be, $^{26}$Al) of Natural Terrain Landslides in Hong Kong, China. In Siame, L.L., Bourles, D.L. and Brown, E.T. (eds). *In Situ-produced Cosmogenic Nuclides and Quantification of Geological Processes: Geological Society of America Special Paper* 415, 131–146.

Sewell, R.J. & Campbell, S.D.G. (2005). *Report on the Dating of Natural Terrain Landslides in Hong Kong*. GEO Report No. 170, Geotechnical Engineering Office, Civil Engineering and Development Department, The Government of the Hong Kong Special Administrative Region, 151 p.

Sewell, R.J., Campbell, S.D.G., Fletcher, C.J.N., Lai, K.W. & Kirk, P.A. (2000). *The Pre-Quaternary Geology of Hong Kong*. Geotechnical Engineering Office, Civil Engineering Department, The Government of the Hong Kong Special Administrative Region, 181 p.

Sewell, R.J., Parry, S., Millis, S.W., Wang, N., Rieser, U. & DeWitt, R. (2015). Dating of debris flow fan complexes from Lantau Island, Hong Kong, China: The potential relationship between landslide activity and climate change. *Geomorphology* 248, 205-227

Sewell, R.J. & Tang, D.L.K. (2015). *The Potential Evidence for Neotectonic Fault Movement and Correlation with Natural Terrain Landslides in Hong Kong*. GEO Report No. 307, Geotechnical Engineering Office, Civil Engineering and Development Department, The Government of the Hong Kong SAR, 33 p.

Tang, D.L.K., Ding, Y.Z., Lee, C.W., Wong, J.C.F. & Sewell, R.J. (2009). *Study of The Potential Evidence For Neotectonic Fault Movement and Correlation with Natural Terrain Landslides in Hong Kong (Part 1: Ho Lek Pui Area)*. Geological Report GR 1/2009. Geotechnical Engineering Office, Civil Engineering and Development Department, The Government of the Hong Kong Special Administrative Region, 44 p.

Tang, D.L.K., Sewell, R.J., Wong, J.C.F. & Ding, Y.Z. (2010). *Study of The Potential Evidence For Neotectonic Fault Movement and Correlation with Natural Terrain Landslides in Hong Kong (Part 3: Tung Chung East)*. Geological Report GR 3/2010. Geotechnical Engineering Office, Civil Engineering and Development Department, The Government of the Hong Kong Special Administrative Region, 30 p.

Wong, J.C.F. & Ding, Y.Z. (2010). *Study of The Potential Evidence For Neotectonic Fault Movement and Correlation with Natural Terrain Landslides in Hong Kong (Part 2: Wong Chuk Yeung Area)*. Geological Report GR 1/2010. Geotechnical Engineering Office, Civil Engineering and Development Department, The Government of the Hong Kong Special Administrative Region, 39 p.

Wong, J.C.F., Tang, D.L.K., Sewell, R.J. & Lee, C.W. (2010). *Study of The Potential Evidence For Neotectonic Fault Movement and Correlation with Natural Terrain Landslides in Hong Kong (Part 4: Nam Shan and Pui O Areas)*. Geological Report GR 4/2010. Geotechnical Engineering Office, Civil Engineering and Development Department, The Government of the Hong Kong Special Administrative Region, 36 p.

# Appendix A

## Laboratory Dating Test Reports

# Report to Geotechnical Engineering Office Civil Engineering Department on Age Determination of Natural Terrain Landslides By Luminescence Dating LPMitP Phase I

by

Dr. Regina DeWitt

Oklahoma State University
Department of Physics
Radiation Dosimetry Laboratory
Venture I Suite 201
1110 S. Innovation Way Drive
Stillwater, OK 74074, USA
e-mail: regina.kalchgruber@okstate.edu
ph: 405-744-1013
fax: 405-744-1112

Technical Report

5th April 2011

CONTENTS

# OSL results for Batch 1, 20 samples

April 5, 2011
by Regina DeWitt

Oklahoma State University, Department of Physics, Radiation Dosimetry Laboratory,
Venture1 Suite 201, 1110 S. Innovation Way Drive, Stillwater, OK 74074

## Summary

Batch 1 included 20 samples from 5 different locations. The samples contained predominantly fine grained material. Coarser grains (90-212μm) have been dated for 2 samples and the ages were compared with the results for fine grains (4-11μm). In both cases the larger grains resulted in higher ages. One possible reason is that coarser grains were bleached to a lesser extent during transport by the landslide. All samples have been dated therefore by extracting fine grained quartz and using a SAR procedure. Some samples were contaminated with feldspar after the extraction procedure. Those samples were measured with a post-IR blue SAR procedure to eliminate contributions from feldspar to the signal.
All samples showed a radioactive disequilibrium in the uranium decay chain.

## 1. General Principles of Luminescence Dating

Ionizing radiation from natural radioactive isotopes and from cosmic rays liberates charge carriers within silicate mineral grains like quartz and feldspar over geologic time. Charge carriers become localized at crystal defects and lead to the accumulation of a "trapped" charge population. Exposure to solar radiation releases the charges from the trap sites and thereby resets the "luminescence clock." If the mineral grains are then shielded from further solar radiation by burial, the trapped charge population begins to reaccumulate. When the sample is collected at a later time the trapped charge population is representative of the time elapsed since the mineral grains were last exposed to solar radiation, i.e., the time since burial. As the samples are heated or illuminated in the laboratory, the thermal or optical stimulation results in the release of trapped charge, which subsequently undergoes recombination with charge of the opposite sign. The light emitted during this process is called TL (Thermally Stimulated Luminescence) or OSL (Optically Stimulated Luminescence). The intensity of this "natural" luminescence signal is proportional to the radiation dose (in units of Gray, 1 Gy = 1 J/kg) absorbed in the time since burial. The natural equivalent dose is determined by comparing the natural luminescence signal with that obtained after known radiation exposures administered in the laboratory, the dose response. With the dose rate, the rate of natural irradiation of the minerals, the age of the sample (i.e., the burial time) is derived from

$$Age\left[a\right] = \frac{\text{Equivalent Dose}\left[\text{Gy}\right]}{\text{Dose Rate}\left[\text{Gy/a}\right]}.$$

Detailed discussions of luminescence dating methods including equivalent dose and dose rate determination can be found in publications by Aitken (1985, 1998) and by Wintle (1997).

## 2. Natural Dose-rate

The rate at which the trapped charge population accumulates is proportional to the rate at which energy from ionising radiation is absorbed by the crystal. The ionising radiation originates mainly from the radioactive decays of $^{232}$Th, $^{235}$U, $^{238}$U (and their daughter nuclides), $^{40}$K and $^{87}$Rb, and to a lesser extent from cosmic radiation. As the energy release of each decay and the half-life of the nuclides are well known, the dose rate (unit: Gy/a) can be determined from the concentration of the nuclides in the soil. The concentration of $^{232}$Th, natural uranium, and $^{40}$K is measured by means of gamma spectrometry and the dose rate is calculated using the conversion factors given by Adamiec and Aitken (1998).

Water in the pores of the sediment absorbs part of the radiation that would otherwise reach the crystals. Therefore the dose-rate in wet sediment is less than in the same sediment when it is dry. The water content of the sample as found can be measured. Taking into account the type of sediment, its environment, and its pore-structure, assumptions about the average wetness over the burial time span have to be made. Usually the water content *w* is calculated from the mass of the sample before ($m_w$) and after ($m_d$) drying: $w = (m_w - m_d)/m_d$.

An effect that also influences the dose rate is the different penetrating power of alpha, beta, and gamma radiation. Gamma-radiation has a range of about 30 cm in sediments, so that the sample taken for the gamma spectrometry must be representative for the whole 30 cm sphere of influence. Beta radiation, with a range of 2-3 mm, does not uniformly penetrate the grains but is attenuated. The beta dose-rate therefore depends on the diameter of the grains, and the effect has to be allowed for by using the attenuation factors calculated by Mejdahl (1979). Alpha radiation only penetrates the outer 10 μm of a grain.

Disequilibria: In most of the samples a disequilibrium in the uranium decay chain has been detected. No information about the possible development of the equilibrium was available. The dose rate was therefore calculated using the average value of two extreme scenarios: (1) equilibrium as indicated by the nuclides of $^{214}$Bi and $^{214}$Pb for the lower limit and (2) measured concentration of each separate nuclide in the decay chain for the upper limit. As uncertainty we used the difference between the average and the limts.

With the concentrations Th ($^{232}$Th in ppm; 1 ppm = 1 μg/g), U (natural uranium in ppm) and K (natural element potassium in %), the beta and gamma contribution of the dose rate of the dry sediment can be calculated. Taking into account the water content *w*, the effective dose-rate is determined from the following equation:

$$\dot{D} = \frac{\dot{D}_{\alpha,dry}}{1+1.50\times w} + \frac{\dot{D}_{\beta,dry}}{1+1.25\times w} + \frac{\dot{D}_{\gamma,dry}}{1+1.14\times w} + \dot{D}_{\text{cosm}} = \dot{D}_{\alpha,eff} + \dot{D}_{\beta,eff} + \dot{D}_{\gamma,eff} + \dot{D}_{\text{cosm}} .$$

For coarse grains the outer shell affected by alpha radiation is removed through etching. For those samples the contribution by alpha radiation to the total dose rate is not included.

The fraction of the dose rate caused by cosmic radiation depends on the geographical location of the site and can be calculated as described by Barbouti and Rastin (1983) and Prescott and Stephan (1982).

## 3. Sample preparation

All samples had a small fraction of coarse grained material (90-212μm), but were predominantly fine grained. In environments where a complete resetting of samples by sunlight is questionable, coarse grains offer the possibility to use small aliquots and thereby detect incomplete bleaching. We initially chose the 2 samples with the largest fraction of coarser material (HK13348, HK13349), and we prepared both coarse grains and fine grain material to compare the results. Quartz bleaches faster than feldspar and is not affected by anomalous fading. For colluvial samples quartz is therefore preferable to feldspar.

Coarse grain preparation (90-150 μm): After sieving, the grains were treated with HCl (concentration 3.75 %) and $H_2O_2$ to remove carbonates and organic components, respectively. Subsequent treatment with 40 % HF for 50 min etched away the outer surface of the grains (10-20 μm), which had been affected by alpha-radiation, and also removed most feldspar contaminations. Finally the samples were treated with HCl again to remove fluoride precipitates that may have formed during the etching process, rinsed with deionised water, and dried. Density separation was carried out with sodium polytungstate. In a first step, heavy minerals with a density greater than 2.75 g/cm$^3$ were separated from quartz and feldspar. In a second step quartz with a density greater than 2.62 g/cm$^3$ was separated from feldspar.

Small aliquots (subsamples) were prepared by fixing the grains on steel cups with silicone spray. We used the grain size fraction with the most material.

Fine grain preparation: After sieving the grains smaller than 63 μm were treated with HCl (concentration 3.75 %) and $H_2O_2$ to remove carbonates and organic components, respectively. Between each treatment the samples were rinsed three times with deionized water. Grains were allowed to settle for at least 4 hours and the supernatant fluid was carefully decanted. Subsequently grains >11μm were removed with the Stokes method by allowing a suspension of the samples to settle for 20 min. Grains between 4 and 11 μm were subsequently separated with a centrifuge. Finally, quartz separates were prepared by etching for 3 days with Hexafluorosilicic acid. We used a suspension of quartz in water and prepared aliquots by pipetting the suspension on Al disks.

All dosimetry samples were dried at 55 °C, and the wet and dry weight was measured to obtain the water content of the samples. The dry samples were filled in air-tight containers and stored for 4 weeks. The thorium, uranium and potassium concentrations were measured with low level gamma spectrometry.

## 4. Measurements

*Instrumentation:*

Measurements were conducted using a Risø TL/OSL-DA-15 reader, Risø National Laboratory, with a bialkali PM tube (Thorn EMI 9635Q B) and Hoya U-340 filters (290-370 nm). The built-in $^{90}Sr/^{90}Y$ beta source gives a dose rate of 100 mGy/s (error 4.1 %). Optical stimulation was carried out with blue LEDs (470 nm), delivering 31 mW/cm$^2$ to the sample; IR stimulation was from an IR LED array at 875 ± 80 nm with 36 mW/cm$^2$ power at the sample. The heating rate used was 5 °C/s.

*Measurement procedure:*

The measurement procedure was based on the single aliquot regenerative-dose (SAR) procedure described by Murray and Wintle (2000) and Wintle and Murray (2006):

1. **Give dose $D_i$**
2. **Preheat at T for 10 s to remove unstable signals**
3. **Stimulate with blue LEDs for 100 s at 125 °C, measure OSL signal $L_i$**
4. **Give test dose, 15-20% of expected dose**
5. **Preheat at T-20°C for 10 s to remove unstable signals**
6. **Stimulate with blue LEDs for 100 s at 125 °C, measure OSL signal $T_i$**
7. **Return to 1**

The doses $D_i$ change in each cycle. For the natural signal $D_0 = 0$ Gy and no dose is administered. The regeneration doses $D_1$ to $D_6$ are increasing doses. The repeat doses $D_7$ (expected equivalent dose) and $D_8$ (equal to $D_1$) are administered to check the precision with which a known dose can be recovered with the method. $D_9 = 0$ Gy to check for an unwanted recuperation of the OSL (zero dose signal). A possible contamination of the samples by feldspar inclusions is examined in the last cycle with two equal doses $D_{10} = D_3$. In cycles 0 through 9 all steps are carried out as listed above. In cycle 10 the aliquot is stimulated with IR (60°C for 100 s) between steps 1 and 2 to test for an IR depletion of the OSL signal.
For younger samples only 4 regeneration doses were used.

*Determination of the preheat temperature T:*
The preheat temperature T was determined with a plateau test for 4 samples from different locations (HK13348, HK13349, HK13354, HK13361). All tests resulted in a preheat temperature of 200°C. This value was therefore used for all samples.

*Determination of the equivalent dose for one aliquot:*
We determined the luminescence signals $L_i$ and $T_i$ by integrating over the first 0.8 seconds of an OSL decay curve and subtracting an average of the next 4 seconds as background (early background). The signal uncertainty followed from counting statistics. The sensitivity corrected signal is given by $C_i = L_i/T_i$. The dose response of every aliquot was determined by fitting a saturating exponential to the luminescence signals $C_1$ to $C_6$ and including the origin. For smaller doses the signals $C_1$ to $C_4$ were fitted with a linear fit. The dose $D_0$, corresponding to the natural sensitivity-corrected luminescence signal $C_0$, was calculated with the fitting parameters A and B of the exponential or linear fit. All uncertainties were calculated using the Gaussian law of error propagation and Poisson statistics.

*Selection of reliable aliquots:*
Only aliquots that passed the following criteria were deemed "reliable" and were used to calculate the equivalent dose:

1. Dose recovery of known dose $D_7$ better than 10%
2. Recycling ratio: $0.9 < C_8/C_1 < 1.1$
3. Recuperation: $C_9/C_0 < 5\%$
4. IR depletion: $C_{10}/C_3 > 0.9$

Only few aliquots had to be discarded for not passing tests 1-3. Several samples however showed a large feldspar contamination. For these samples a post-IR blue sequence was used to measure the equivalent dose. This post-IR blue sequence was similar to the SAR procedure

listed above. Before each OSL measurement (steps 3 and 6) another step was added to deplete the feldspar signal:

Stimulate with IR LEDs for 300 s at 60 °C

*Total equivalent dose:*

The equivalent dose $D_e$ was determined with the common age model (Galbraith et al., 1999). The weights were the statistical errors. The full uncertainty also includes 4.1% error for the source calibration.

## 5. Results

A detailed report for each of the 20 samples is provided below. A summary is given in the following table.

| HK Rock No. | Location | GI Station | Age (ka) | Error (ka) |
|---|---|---|---|---|
| HK13345 | Queen's Mary Hospital | DH7 | 10.79 | 0.60 |
| HK13346 | Queen's Mary Hospital | DH7 | 15.26 | 0.88 |
| HK13347 | Sham Wat | SW-TP1 | 5.59 | 0.30 |
| HK13348 | Sham Wat | SW-TP2 | 4.31 | 0.32 |
| HK13349 | Sham Wat | SW-TP5 | 3.14 | 0.17 |
| HK13350 | Sham Wat | SW-TP6 | 2.69 | 0.14 |
| HK13351 | Sham Wat | SW-TP10 | 4.93 | 0.26 |
| HK13352 | Sham Wat | SW-TP14 | 3.43 | 0.18 |
| HK13353 | Sham Wat | SW-TP15 | 3.39 | 0.18 |
| HK13354 | HKUST Staff Quarters (GIU51687) | BDH2 | 10.22 | 0.69 |
| HK13355 | HKUST Staff Quarters (GIU51688) | BDH4 | 28.40 | 1.90 |
| HK13356 | Nam Chung | NC-TP1 | 22.70 | 1.41 |
| HK13357 | Nam Chung | NC-TP13 | 10.44 | 0.60 |
| HK13358 | Nam Chung | NC-TP19 | 1.34 | 0.07 |
| HK13359 | Nam Chung | NC-TP26 | 1.02 | 0.07 |
| HK13360 | Nam Chung | NC-TP32 | 2.30 | 0.14 |
| HK13361 | Nam Chung | NC-TP34 | 4.26 | 0.26 |
| HK13362 | Nam Chung | NC-TP34 | 6.97 | 0.40 |
| HK13363 | Nam Chung | NC-TP37 | 2.73 | 0.15 |
| HK13364 | Tai O East | TOE-TP2 | 18.27 | 1.12 |

## 6. Discussion and Conclusions

Complete solar resetting of grains in colluvia is often questionable. Coarser grains separated from two samples resulted in larger ages than the fine grain fraction. A radial plot indicated overdispersion, which can be indicative of incomplete bleaching during transport. An attempt to apply the minimum age model (Galbraith et al., 1999) was not successful and simply resulted in the dose value of the aliquot with the lowest dose. Even using this value the calculated age was still larger than the one obtained with fine grains. We therefore used fine grain quartz for all samples. Only one sample (HK13356) showed clear overdispersion in a radial plot of the data, indicating an incomplete resetting of this sample.

All samples also showed radioactive disequilibria in the uranium decay chain.

Measurement of a considerably larger number of small coarse-grain aliquots (> 50 reliable aliquots) would be necessary to clearly detect or exclude incomplete bleaching of the samples. This is however not possible in the tight timeframe of 3 months for 20 samples, particularly given the long irradiation times and the necessity of post-IR blue measurements. For this purpose a minimum of 6 months would be necessary. Another possibility are single-grain measurements (currently not possible at OSU).

**References:**


Adamiec, G. and Aitken M.J. 1998. Dose-rate conversion factors: update. *Ancient TL* **16**, 37-50.

Aitken, M. J. 1985. *Thermoluminescence Dating.* Academic Press, London.

Aitken, M. J. 1998. *Optical Dating.* Academic Press, London.

Barbouti, A. und B. Rastin (1983). A Study of the Absolute Intensity of Muons at Sea Level and under Various Thicknesses of Absorber. *J. Pys. G: Nucl. Phys.* **9**, 1577–1595.

Galbraith, R.F., Roberts, R.G., Laslett, G.M., Yoshida, H. and Olley, J.M. (1999). Optical dating of single and multiple grains of quartz from Jinmium Rockshelter, Northern Australia: Part I, Experimental design and statistical models. *Archaeometry* **41**, 339-364.

Mejdahl, V. 1979.Thermoluminescence dating: Beta-dose attenuation in quartz grains. *Archaeomtery* **21**, 61-72.

Murray, A. S. and A.G. Wintle 2000.Luminescence dating of quartz using an improved single-aliquot regenerative-dose protocol. *Radiation Measurements* **32**, 57-73.

Prescott, J. R. and L. G. Stephan (1982). The Contribution of Cosmic Radiation to the Environmental Dose for Thermoluminescence Dating. *PACT* **6**, 17–25.

Wintle, A. G. 19 97. Luminescence dating: Laboratory procedures and protocols. *Radiat. Meas.* **27**, 769–817.

Wintle, A.G., Murray, A.S. (2006). A review of quartz optically stimulated luminescence characteristics and their relevance in single-aliquot regeneration dating protocols. *Radiation Measurements* **41**, 369-391.

# HK13345

DH7, Queen's Mary Hospital

| Sample type | latitude | longitude | altitude | depth | Depositional type |
|---|---|---|---|---|---|
| Core | 22.25260172 | 113.5801317 | 183.19 | 5.10-5.25 | Colluvial |

| | | Error | Error (%) |
|---|---|---|---|
| **Equivalent Dose (Gy)** | **152.7** | **6.2** | **4.1** |
| **Total Dose rate (Gy/ka)** | **14.16** | **0.53** | **3.8** |
| **Age (ka)** | **10.79** | **0.60** | **5.5** |

## Equivalent dose measurement:

| | |
|---|---|
| Grain size (μm) | fine, 4-11 |
| Aliquots measured | 19 |
| Reliable aliquots | 17 |
| Regeneration doses (Gy) | 10, 20, 40, 70, 120, 230 |

Observations: feldspar contamination; post-IR blue sequence

## Dose rate measurement:

Observations: Disequilibrium in Uranium decay chain

| | | Error |
|---|---|---|
| water content | 0.01 | 0.01 |
| | | |
| Th (ppm) | 47.57 | 2.83 |
| K (%) | 3.72 | 0.12 |
| U (ppm): | | |
| weighted mean (all) | 7.38 | 0.52 |
| Th234 | 11.45 | 1.02 |
| Ra226 | 7.89 | 2.45 |
| Pb214 and Bi214 | 7.10 | 0.50 |
| Pb210 | 12.00 | 3.73 |

Concentrations of Thorium, Potassium and Uranium

| | Effective DR (Gy/ka) | Error |
|---|---|---|
| alpha | 4.72 | 0.45 |
| beta | 5.37 | 0.25 |
| gamma | 3.94 | 0.15 |
| cosmic | 0.1223 | 0.0061 |

Effective dose rates

# HK13346

DH7, Queen's Mary Hospital

Observations: Core consisted mostly of one solid rock, only 10% of the material consisted of sediment

| Sample type | latitude | longitude | altitude | depth | Depositional type |
|---|---|---|---|---|---|
| Core | 22.25260172 | 113.5801317 | 183.19 | 5.70-5.90 | Colluvial |

| | | Error | Error (%) |
|---|---|---|---|
| **Equivalent Dose (Gy)** | **169.4** | **7.6** | **4.5** |
| **Total Dose rate (Gy/ka)** | **11.10** | **0.40** | **3.6** |
| **Age (ka)** | **15.26** | **0.88** | **5.7** |

## Equivalent dose measurement:

| | |
|---|---|
| Grain size (μm) | fine, 4-11 |
| Aliquots measured | 40 |
| Reliable aliquots | 26 |
| Regeneration doses (Gy) | 10, 20, 50, 90 150, 250 |

Observations: feldspar contamination; post-IR blue sequence

## Dose rate measurement:

Observations: Disequilibrium in Uranium decay chain

| | | Error |
|---|---|---|
| water content | 0.01 | 0.01 |
| | | |
| Th (ppm) | 36.16 | 2.16 |
| K (%) | 3.06 | 0.10 |
| U (ppm): | | |
| weighted mean (all) | 5.81 | 0.41 |
| Th234 | 8.25 | 0.73 |
| Ra226 | 6.17 | 1.92 |
| Pb214 and Bi214 | 5.62 | 0.40 |
| Pb210 | 9.97 | 3.10 |

Concentrations of Thorium, Potassium and Uranium

| | Effective DR (Gy/ka) | Error |
|---|---|---|
| alpha | 3.62 | 0.34 |
| beta | 4.29 | 0.18 |
| gamma | 3.07 | 0.11 |
| cosmic | 0.1176 | 0.0059 |

Effective dose rates

# HK13347

SW-TP-1, Sham Wat

Observations: Core consisted mostly of one solid rock, only 10% of the material consisted of sediment

| Sample type | latitude | longitude | altitude | depth | Depositional type |
|---|---|---|---|---|---|
| U-100 Sample, horizontal | 22.16052879 | 113.531931 | 17 | 0.8 | Colluvial |

| | | Error | Error (%) |
|---|---|---|---|
| **Equivalent Dose (Gy)** | **51.6** | **2.1** | **4.1** |
| **Total Dose rate (Gy/ka)** | **9.23** | **0.34** | **3.6** |
| **Age (ka)** | **5.59** | **0.30** | **5.5** |

## Equivalent dose measurement:

| | |
|---|---|
| Grain size (μm) | fine, 4-11 |
| Aliquots measured | 16 |
| Reliable aliquots | 16 |
| Regeneration doses (Gy) | 5, 10, 20, 35 60, 90 |

## Dose rate measurement:

Observations: Equilibrium in Uranium decay chain

| | | Error |
|---|---|---|
| water content | 0.15 | 0.03 |
| | | |
| Th (ppm) | 35.69 | 2.13 |
| K (%) | 3.07 | 0.10 |
| U (ppm): | | |
| weighted mean (all) | 5.54 | 0.39 |
| Th234 | 8.07 | 0.71 |
| Ra226 | 5.52 | 1.72 |
| Pb214 and Bi214 | 5.40 | 0.38 |
| Pb210 | 5.12 | 1.60 |

Concentrations of Thorium, Potassium and Uranium

| | Effective DR (Gy/ka) | Error |
|---|---|---|
| alpha | 2.89 | 0.27 |
| beta | 3.57 | 0.16 |
| gamma | 2.61 | 0.12 |
| cosmic | 0.1606 | 0.00803 |

Effective dose rates

# HK13348

SW-TP-2, Sham Wat

| Sample type | latitude | longitude | altitude | depth | Depositional type |
|---|---|---|---|---|---|
| U-100 Sample, horizontal | 22.16074219 | 113.5319258 | 26.56 | 0.5 | Colluvial |

| | | Error | Error (%) |
|---|---|---|---|
| **Equivalent Dose (Gy)** | **43.4** | **2.7** | **6.2** |
| **Total Dose rate (Gy/ka)** | **10.08** | **0.40** | **4.0** |
| **Age (ka)** | **4.31** | **0.32** | **7.4** |

## Equivalent dose measurement:

| | |
|---|---|
| Grain size (μm) | fine, 4-11 |
| Aliquots measured | 24 |
| Reliable aliquots | 16 |
| Regeneration doses (Gy) | 5, 10, 15, 20, 35, 60 |

## Dose rate measurement:

Observations: Disequilibrium in Uranium decay chain

| | | Error |
|---|---|---|
| water content | 0.15 | 0.03 |
| | | |
| Th (ppm) | 43.51 | 2.59 |
| K (%) | 3.37 | 0.11 |
| U (ppm): | | |
| weighted mean (all) | 4.63 | 0.33 |
| Th234 | 8.79 | 0.78 |
| Ra226 | 4.70 | 1.48 |
| Pb214 and Bi214 | 4.40 | 0.31 |
| Pb210 | 3.97 | 1.25 |

Concentrations of Thorium, Potassium and Uranium

| | Effective DR (Gy/ka) | Error |
|---|---|---|
| alpha | 3.15 | 0.32 |
| beta | 3.87 | 0.19 |
| gamma | 2.90 | 0.14 |
| cosmic | 0.1643 | 0.008215 |

Effective dose rates

**Coarse grain fraction:**

For this sample we also measured quartz grains 90-150 µm. An average dose value and minimum dose value were calculated. **The results are listed below for the sake of completeness, but were not used for age calculation of the sample**.

| | |
|---|---|
| Grain size (µm) | 90-150 |
| Aliquots measured | 24 |
| Reliable aliquots | 22 |
| Regeneration doses (Gy) | 5, 10, 20, 40 70, 120 |

| | Effective DR (Gy/ka) | Error |
|---|---|---|
| alpha | N.A. | |
| beta | 3.55 | 0.23 |
| gamma | 2.90 | 0.14 |
| cosmic | 0.1643 | 0.008215 |

| | | Error | Error (%) |
|---|---|---|---|
| **Equivalent Dose (Gy) (Average value)** | **43.4** | **2.7** | **6.2** |
| **Total Dose rate (Gy/ka)** | **6.62** | **0.27** | **4.0** |
| **Age (ka)** | **6.56** | **0.49** | **7.4** |

| | | Error | Error (%) |
|---|---|---|---|
| **Equivalent Dose (Gy) (Minimum value)** | **30.9** | **0.96** | **3.1** |
| **Total Dose rate (Gy/ka)** | **6.62** | **0.27** | **4.0** |
| **Age (ka)** | **4.67** | **0.24** | **5.1** |

# HK13349

SW-TP-5, Sham Wat

| Sample type | latitude | longitude | altitude | depth | Depositional type |
|---|---|---|---|---|---|
| U-100 Sample, horizontal | 22.16107922 | 113.5318031 | 17.44 | 1.5 | Colluvial |

| | | Error | Error (%) |
|---|---|---|---|
| **Equivalent Dose (Gy)** | **25.7** | **1.1** | **4.3** |
| **Total Dose rate (Gy/ka)** | **8.19** | **0.29** | **3.5** |
| **Age (ka)** | **3.14** | **0.17** | **5.5** |

## Equivalent dose measurement:

| | |
|---|---|
| Grain size (μm) | fine, 4-11 |
| Aliquots measured | 23 |
| Reliable aliquots | 21 |
| Regeneration doses (Gy) | 5, 10, 15, 20, 35, 60 |

## Dose rate measurement:

Observations: Disequilibrium in Uranium decay chain

| | | Error |
|---|---|---|
| water content | 0.12 | 0.024 |
| | | |
| Th (ppm) | 29.57 | 1.77 |
| K (%) | 2.98 | 0.10 |
| U (ppm): | | |
| weighted mean (all) | 4.19 | 0.29 |
| Th234 | 6.35 | 0.56 |
| Ra226 | 4.07 | 1.25 |
| Pb214 and Bi214 | 4.08 | 0.29 |
| Pb210 | 5.30 | 1.63 |

Concentrations of Thorium, Potassium and Uranium

| | Effective DR (Gy/ka) | Error |
|---|---|---|
| alpha | 2.43 | 0.23 |
| beta | 3.33 | 0.14 |
| gamma | 2.28 | 0.10 |
| cosmic | 0.153 | 0.00765 |

Effective dose rates

**Coarse grain fraction:**

For this sample we also measured quartz grains 90-150 µm. **The results are listed below for the sake of completeness, but were not used for age calculation of the sample**.

| | |
|---|---|
| Grain size (µm) | 90-150 |
| Aliquots measured | 35 |
| Reliable aliquots | 23 |
| Regeneration doses (Gy) | 5, 10, 20, 40 70, 120 |

| | Effective DR (Gy/ka) | Error |
|---|---|---|
| alpha | N.A. | |
| beta | 3.08 | 0.18 |
| gamma | 2.28 | 0.10 |
| cosmic | 0.153 | 0.00765 |

| | | Error | Error (%) |
|---|---|---|---|
| **Equivalent Dose (Gy)** | **25.6** | **1.1** | **4.3** |
| **Total Dose rate (Gy/ka)** | **5.51** | **0.20** | **3.7** |
| **Age (ka)** | **4.64** | **0.26** | **5.6** |

# HK13350

SW-TP-6, Sham Wat

| Sample type | latitude | longitude | altitude | depth | Depositional type |
|---|---|---|---|---|---|
| U-100 Sample, horizontal | 22.16137012 | 113.5319449 | 50.56 | 0.8 | Colluvial |

| | | Error | Error (%) |
|---|---|---|---|
| **Equivalent Dose (Gy)** | **18.94** | **0.8** | **4.2** |
| **Total Dose rate (Gy/ka)** | **7.04** | **0.23** | **3.2** |
| **Age (ka)** | **2.69** | **0.14** | **5.3** |

## Equivalent dose measurement:

| | |
|---|---|
| Grain size (μm) | fine, 4-11 |
| Aliquots measured | 25 |
| Reliable aliquots | 15 |
| Regeneration doses (Gy) | 12, 15, 19, 22 |

## Dose rate measurement:

Observations: Disequilibrium in Uranium decay chain

| | | Error |
|---|---|---|
| water content | 0.08 | 0.016 |
| | | |
| Th (ppm) | 23.12 | 1.39 |
| K (%) | 2.45 | 0.08 |
| U (ppm): | | |
| weighted mean (all) | 3.77 | 0.27 |
| Th234 | 5.32 | 0.48 |
| Ra226 | 3.84 | 1.21 |
| Pb214 and Bi214 | 3.64 | 0.26 |
| Pb210 | 4.51 | 1.42 |

Concentrations of Thorium, Potassium and Uranium

| | Effective DR (Gy/ka) | Error |
|---|---|---|
| alpha | 2.09 | 0.19 |
| beta | 2.86 | 0.11 |
| gamma | 1.93 | 0.07 |
| cosmic | 0.1615 | 0.008075 |

Effective dose rates

# HK13351

SW-TP-10, Sham Wat

| Sample type | latitude | longitude | altitude | depth | Depositional type |
|---|---|---|---|---|---|
| U-100 Sample, horizontal | 22.1620508 | 113.5320679 | 47.2 | 0.7 | Colluvial |

| | | Error | Error (%) |
|---|---|---|---|
| **Equivalent Dose (Gy)** | **18.11** | **0.74** | **4.1** |
| **Total Dose rate (Gy/ka)** | **3.67** | **0.12** | **3.4** |
| **Age (ka)** | **4.93** | **0.26** | **5.3** |

## Equivalent dose measurement:

| | |
|---|---|
| Grain size (μm) | fine, 4-11 |
| Aliquots measured | 20 |
| Reliable aliquots | 19 |
| Regeneration doses (Gy) | 14, 16, 20, 22 |

## Dose rate measurement:

Observations: Disequilibrium in Uranium decay chain

| | | Error |
|---|---|---|
| water content | 0.094 | 0.0188 |
| | | |
| Th (ppm) | 11.54 | 0.69 |
| K (%) | 1.42 | 0.05 |
| U (ppm): | | |
| weighted mean (all) | 1.71 | 0.12 |
| Th234 | 2.93 | 0.27 |
| Ra226 | 1.75 | 0.58 |
| Pb214 and Bi214 | 1.62 | 0.12 |
| Pb210 | 2.11 | 0.70 |

Concentrations of Thorium, Potassium and Uranium

| | Effective DR (Gy/ka) | Error |
|---|---|---|
| alpha | 1.00 | 0.10 |
| beta | 1.54 | 0.07 |
| gamma | 0.97 | 0.04 |
| cosmic | 0.1625 | 0.008125 |

Effective dose rates

# HK13352

SW-TP-14, Sham Wat

| Sample type | latitude | longitude | altitude | depth | Depositional type |
|---|---|---|---|---|---|
| U-100 Sample, horizontal | 22.16232972 | 113.5324815 | 60.01 | 0.7 | Colluvial |

| | | Error | Error (%) |
|---|---|---|---|
| **Equivalent Dose (Gy)** | **13.81** | **0.56** | **4.1** |
| **Total Dose rate (Gy/ka)** | **4.03** | **0.13** | **3.2** |
| **Age (ka)** | **3.43** | **0.18** | **5.2** |

## Equivalent dose measurement:

| | |
|---|---|
| Grain size (μm) | fine, 4-11 |
| Aliquots measured | 21 |
| Reliable aliquots | 17 |
| Regeneration doses (Gy) | 10, 13, 17, 20 |

## Dose rate measurement:

Observations: Disequilibrium in Uranium decay chain

| | | Error |
|---|---|---|
| water content | 0.11 | 0.022 |
| | | |
| Th (ppm) | 14.21 | 0.85 |
| K (%) | 1.34 | 0.04 |
| U (ppm): | | |
| weighted mean (all) | 2.18 | 0.15 |
| Th234 | 3.14 | 0.28 |
| Ra226 | 2.11 | 0.67 |
| Pb214 and Bi214 | 2.14 | 0.15 |
| Pb210 | 1.70 | 0.54 |

Concentrations of Thorium, Potassium and Uranium

| | Effective DR (Gy/ka) | Error |
|---|---|---|
| alpha | 1.20 | 0.11 |
| beta | 1.56 | 0.06 |
| gamma | 1.11 | 0.05 |
| cosmic | 0.1629 | 0.008145 |

Effective dose rates

# HK13353

SW-TP-15, Sham Wat

| Sample type | latitude | longitude | altitude | depth | Depositional type |
|---|---|---|---|---|---|
| U-100 Sample, horizontal | 22.16255674 | 113.5323633 | 40.95 | 0.8 | Colluvial |

| | | Error | Error (%) |
|---|---|---|---|
| **Equivalent Dose (Gy)** | **20.15** | **0.83** | **4.1** |
| **Total Dose rate (Gy/ka)** | **5.94** | **0.20** | **3.4** |
| **Age (ka)** | **3.39** | **0.18** | **5.4** |

## Equivalent dose measurement:

| | |
|---|---|
| Grain size (μm) | fine, 4-11 |
| Aliquots measured | 17 |
| Reliable aliquots | 17 |
| Regeneration doses (Gy) | 16, 18, 22, 24 |

## Dose rate measurement:

Observations: Disequilibrium in Uranium decay chain

| | | Error |
|---|---|---|
| water content | 0.17 | 0.034 |
| | | |
| Th (ppm) | 17.63 | 1.06 |
| K (%) | 2.81 | 0.09 |
| U (ppm): | | |
| weighted mean (all) | 3.41 | 0.24 |
| Th234 | 4.81 | 0.43 |
| Ra226 | 3.64 | 1.15 |
| Pb214 and Bi214 | 3.29 | 0.23 |
| Pb210 | 3.85 | 1.22 |

Concentrations of Thorium, Potassium and Uranium

| | Effective DR (Gy/ka) | Error |
|---|---|---|
| alpha | 1.52 | 0.14 |
| beta | 2.67 | 0.12 |
| gamma | 1.59 | 0.07 |
| cosmic | 0.1612 | 0.00806 |

Effective dose rates

# HK13354

HKUST Staff Quarters (GIU51687), BDH2

| Sample type | latitude | longitude | altitude | depth | Depositional type |
|---|---|---|---|---|---|
| Mazier | 22.32252551 | 114.0227887 | 141.25 | 2.38-2.52 | Colluvial |

| | | Error | Error (%) |
|---|---|---|---|
| **Equivalent Dose (Gy)** | **84.9** | **3.8** | **4.5** |
| **Total Dose rate (Gy/ka)** | **8.31** | **0.41** | **5.0** |
| **Age (ka)** | **10.22** | **0.69** | **6.7** |

## Equivalent dose measurement:

Observations: feldspar contamination, post-IR blue sequence

| | |
|---|---|
| Grain size (μm) | fine, 4-11 |
| Aliquots measured | 21 |
| Reliable aliquots | 16 |
| Regeneration doses (Gy) | 10, 20, 50, 80 120, 200 |

## Dose rate measurement:

Observations: Disequilibrium in Uranium decay chain

| | | Error |
|---|---|---|
| water content | 0.24 | 0.048 |
| | | |
| Th (ppm) | 42.17 | 2.53 |
| K (%) | 1.32 | 0.06 |
| U (ppm): | | |
| weighted mean (all) | 7.23 | 0.51 |
| Th234 | 9.94 | 0.87 |
| Ra226 | 8.84 | 2.58 |
| Pb214 and Bi214 | 6.75 | 0.48 |
| Pb210 | 11.26 | 3.28 |

Concentrations of Thorium, Potassium and Uranium

| | Effective DR (Gy/ka) | Error |
|---|---|---|
| alpha | 3.20 | 0.34 |
| beta | 2.53 | 0.19 |
| gamma | 2.43 | 0.14 |
| cosmic | 0.1462 | 0.00731 |

Effective dose rates

# HK13355

HKUST Staff Quarters (GIU51688), BDH4

| Sample type | latitude | longitude | altitude | depth | Depositional type |
|---|---|---|---|---|---|
| Mazier | 22.32223622 | 114.02318 | 167.13 | 2.5-2.63 | Colluvial |

| | | Error | Error (%) |
|---|---|---|---|
| **Equivalent Dose (Gy)** | **194.3** | **8.6** | **4.4** |
| **Total Dose rate (Gy/ka)** | **6.85** | **0.36** | **5.2** |
| **Age (ka)** | **28.35** | **1.94** | **6.8** |

## Equivalent dose measurement:

Observations: feldspar contamination, post-IR blue sequence

| | |
|---|---|
| Grain size (μm) | fine, 4-11 |
| Aliquots measured | 20 |
| Reliable aliquots | 20 |
| Regeneration doses (Gy) | 10, 20, 50, 90 150, 250 |

## Dose rate measurement:

Observations: Disequilibrium in Uranium decay chain

| | | Error |
|---|---|---|
| water content | 0.23 | 0.046 |
| | | |
| Th (ppm) | 35.21 | 2.10 |
| K (%) | 1.20 | 0.04 |
| U (ppm): | | |
| weighted mean (all) | 5.08 | 0.36 |
| Th234 | 8.08 | 0.69 |
| Ra226 | 5.78 | 1.67 |
| Pb214 and Bi214 | 4.80 | 0.34 |
| Pb210 | 10.02 | 2.90 |

Concentrations of Thorium, Potassium and Uranium

| | Effective DR (Gy/ka) | Error |
|---|---|---|
| alpha | 2.59 | 0.29 |
| beta | 2.13 | 0.17 |
| gamma | 1.99 | 0.12 |
| cosmic | 0.1455 | 0.007275 |

Effective dose rates

# HK13356

Nam Chung, NC-TP1

| Sample type | latitude | longitude | altitude | depth | Depositional type |
|---|---|---|---|---|---|
| U-100 Sample, horizontal | 22.14479311 | 113.5159052 | 79.85 | 2 | Colluvial |

| | | Error | Error (%) |
|---|---|---|---|
| **Equivalent Dose (Gy)** | **191.8** | **8.9** | **4.6** |
| **Total Dose rate (Gy/ka)** | **8.45** | **0.35** | **4.1** |
| **Age (ka)** | **22.70** | **1.41** | **6.2** |

## Equivalent dose measurement:

Observations: feldspar contamination, post-IR blue sequence

**Overdispersion, sample possibly not fully bleached**

| | |
|---|---|
| Grain size (μm) | fine, 4-11 |
| Aliquots measured | 30 |
| Reliable aliquots | 20 |
| Regeneration doses (Gy) | 10, 20, 50, 90 150, 250 |

## Dose rate measurement:

Observations: Disequilibrium in Uranium decay chain

| | | Error |
|---|---|---|
| water content | 0.15 | 0.03 |
| | | |
| Th (ppm) | 37.91 | 2.26 |
| K (%) | 2.83 | 0.09 |
| U (ppm): | | |
| weighted mean (all) | 3.36 | 0.24 |
| Th234 | 6.78 | 0.60 |
| Ra226 | 3.47 | 1.07 |
| Pb214 and Bi214 | 3.14 | 0.22 |
| Pb210 | 4.42 | 1.36 |

Concentrations of Thorium, Potassium and Uranium

| | Effective DR (Gy/ka) | Error |
|---|---|---|
| alpha | 2.64 | 0.28 |
| beta | 3.23 | 0.17 |
| gamma | 2.44 | 0.12 |
| cosmic | 0.1492 | 0.00746 |

Effective dose rates

# HK13357

Nam Chung, NC-TP13

| Sample type | latitude | longitude | altitude | depth | Depositional type |
|---|---|---|---|---|---|
| U-100 Sample, horizontal | 22.14413037 | 113.5152338 | 130.23 | 1.1 | Colluvial |

| | | Error | Error (%) |
|---|---|---|---|
| **Equivalent Dose (Gy)** | **50.9** | **2.3** | **4.5** |
| **Total Dose rate (Gy/ka)** | **4.88** | **0.17** | **3.6** |
| **Age (ka)** | **10.44** | **0.60** | **5.8** |

## Equivalent dose measurement:

| | |
|---|---|
| Grain size (μm) | fine, 4-11 |
| Aliquots measured | 20 |
| Reliable aliquots | 16 |
| Regeneration doses (Gy) | 5, 10, 20, 40, 70 |

## Dose rate measurement:

Observations: Equilibrium in Uranium decay chain

| | | Error |
|---|---|---|
| water content | 0.11 | 0.022 |
| | | |
| Th (ppm) | 14.77 | 0.89 |
| K (%) | 1.14 | 0.04 |
| U (ppm): | | |
| weighted mean (all) | 4.54 | 0.32 |
| Th234 | 4.91 | 0.44 |
| Ra226 | 4.72 | 1.45 |
| Pb214 and Bi214 | 4.49 | 0.32 |
| Pb210 | 6.07 | 1.87 |

Concentrations of Thorium, Potassium and Uranium

| | Effective DR (Gy/ka) | Error |
|---|---|---|
| alpha | 1.67 | 0.15 |
| beta | 1.73 | 0.07 |
| gamma | 1.33 | 0.06 |
| cosmic | 0.1601 | 0.008005 |

Effective dose rates

# HK13358

Nam Chung, NC-TP19

| Sample type | latitude | longitude | altitude | depth | Depositional type |
|---|---|---|---|---|---|
| U-100 Sample, horizontal | 22.14389816 | 113.5135091 | 34.12 | 1.5 | Colluvial |

| | | Error | Error (%) |
|---|---|---|---|
| **Equivalent Dose (Gy)** | **14.04** | **0.58** | **4.1** |
| **Total Dose rate (Gy/ka)** | **10.48** | **0.39** | **3.7** |
| **Age (ka)** | **1.34** | **0.07** | **5.6** |

## Equivalent dose measurement:

| | |
|---|---|
| Grain size (μm) | fine, 4-11 |
| Aliquots measured | 21 |
| Reliable aliquots | 21 |
| Regeneration doses (Gy) | 12, 15, 19, 22 |

## Dose rate measurement:

Observations: Disequilibrium in Uranium decay chain

| | | Error |
|---|---|---|
| water content | 0.11 | 0.022 |
| | | |
| Th (ppm) | 24.36 | 1.46 |
| K (%) | 2.51 | 0.08 |
| U (ppm): | | |
| weighted mean (all) | 12.29 | 0.86 |
| Th234 | 7.62 | 0.67 |
| Ra226 | 11.03 | 3.33 |
| Pb214 and Bi214 | 12.85 | 0.90 |
| Pb210 | 14.83 | 4.48 |

Concentrations of Thorium, Potassium and Uranium

| | Effective DR (Gy/ka) | Error |
|---|---|---|
| alpha | 3.62 | 0.33 |
| beta | 3.85 | 0.18 |
| gamma | 2.86 | 0.11 |
| cosmic | 0.1534 | 0.00767 |

Effective dose rates

# HK13359

Nam Chung, NC-TP26

| Sample type | latitude | longitude | altitude | depth | Depositional type |
|---|---|---|---|---|---|
| U-100 Sample, horizontal | 22.14517251 | 113.5158579 | 24.52 | 1.2 | Colluvial |

| | | Error | Error (%) |
|---|---|---|---|
| **Equivalent Dose (Gy)** | **9.05** | **0.37** | **4.1** |
| **Total Dose rate (Gy/ka)** | **7.52** | **0.28** | **3.8** |
| **Age (ka)** | **1.20** | **0.07** | **5.6** |

## Equivalent dose measurement:

| | |
|---|---|
| Grain size (μm) | fine, 4-11 |
| Aliquots measured | 30 |
| Reliable aliquots | 19 |
| Regeneration doses (Gy) | 5, 7, 11, 13 |

## Dose rate measurement:

Observations: Disequilibrium in Uranium decay chain

| | | Error |
|---|---|---|
| water content | 0.125 | 0.025 |
| | | |
| Th (ppm) | 28.58 | 1.71 |
| K (%) | 2.20 | 0.07 |
| U (ppm): | | |
| weighted mean (all) | 4.65 | 0.33 |
| Th234 | 6.76 | 0.60 |
| Ra226 | 4.87 | 1.51 |
| Pb214 and Bi214 | 4.49 | 0.32 |
| Pb210 | 6.58 | 2.04 |

Concentrations of Thorium, Potassium and Uranium

| | Effective DR (Gy/ka) | Error |
|---|---|---|
| alpha | 2.45 | 0.23 |
| beta | 2.81 | 0.13 |
| gamma | 2.11 | 0.09 |
| cosmic | 0.1564 | 0.00782 |

Effective dose rates

# HK13360

Nam Chung, NC-TP32

| Sample type | latitude | longitude | altitude | depth | Depositional type |
|---|---|---|---|---|---|
| U-100 Sample, horizontal | 22.14453842 | 113.514365 | 30.83 | 0.9 | Colluvial |

| | | Error | Error (%) |
|---|---|---|---|
| **Equivalent Dose (Gy)** | **27.8** | **1.2** | **4.3** |
| **Total Dose rate (Gy/ka)** | **12.09** | **0.52** | **4.3** |
| **Age (ka)** | **2.30** | **0.14** | **6.1** |

## Equivalent dose measurement:

| | |
|---|---|
| Grain size (μm) | fine, 4-11 |
| Aliquots measured | 16 |
| Reliable aliquots | 16 |
| Regeneration doses (Gy) | 5, 10, 20, 35 50 |

## Dose rate measurement:

Observations: Disequilibrium in Uranium decay chain

| | | Error |
|---|---|---|
| water content | 0.07 | 0.014 |
| | | |
| Th (ppm) | 24.66 | 1.48 |
| K (%) | 2.10 | 0.08 |
| U (ppm): | | |
| weighted mean (all) | 16.27 | 1.14 |
| Th234 | 11.76 | 1.05 |
| Ra226 | 16.21 | 5.07 |
| Pb214 and Bi214 | 16.62 | 1.17 |
| Pb210 | 9.55 | 2.99 |

Concentrations of Thorium, Potassium and Uranium

| | Effective DR (Gy/ka) | Error |
|---|---|---|
| alpha | 4.51 | 0.43 |
| beta | 4.12 | 0.27 |
| gamma | 3.29 | 0.12 |
| cosmic | 0.1598 | 0.00799 |

Effective dose rates

# HK13361

Nam Chung, NC-TP34

| Sample type | latitude | longitude | altitude | depth | Depositional type |
|---|---|---|---|---|---|
| U-100 Sample, horizontal | 22.14416302 | 113.5134085 | 13.38 | 0.8 | Colluvial |

| | | Error | Error (%) |
|---|---|---|---|
| **Equivalent Dose (Gy)** | **38.8** | **1.7** | **4.4** |
| **Total Dose rate (Gy/ka)** | **9.11** | **0.39** | **4.2** |
| **Age (ka)** | **4.26** | **0.26** | **6.1** |

## Equivalent dose measurement:

| | |
|---|---|
| Grain size (μm) | fine, 4-11 |
| Aliquots measured | 23 |
| Reliable aliquots | 20 |
| Regeneration doses (Gy) | 5, 10, 20, 35 60, 90 |

## Dose rate measurement:

Observations: Disequilibrium in Uranium decay chain

| | | Error |
|---|---|---|
| water content | 0.1 | 0.02 |
| | | |
| Th (ppm) | 35.25 | 2.10 |
| K (%) | 1.28 | 0.05 |
| U (ppm): | | |
| weighted mean (all) | 8.06 | 0.56 |
| Th234 | 10.12 | 0.88 |
| Ra226 | 10.21 | 3.05 |
| Pb214 and Bi214 | 7.62 | 0.54 |
| Pb210 | 12.39 | 3.70 |

Concentrations of Thorium, Potassium and Uranium

| | Effective DR (Gy/ka) | Error |
|---|---|---|
| alpha | 3.56 | 0.33 |
| beta | 2.83 | 0.16 |
| gamma | 2.56 | 0.11 |
| cosmic | 0.1605 | 0.008025 |

Effective dose rates

# HK13362

Nam Chung, NC-TP34

| Sample type | latitude | longitude | altitude | depth | Depositional type |
|---|---|---|---|---|---|
| U-100 Sample, horizontal | 22.14416302 | 113.5134085 | 13.38 | 0.8 | Colluvial |

| | | Error | Error (%) |
|---|---|---|---|
| **Equivalent Dose (Gy)** | **58.8** | **2.5** | **4.3** |
| **Total Dose rate (Gy/ka)** | **8.43** | **0.33** | **4.0** |
| **Age (ka)** | **6.97** | **0.40** | **5.8** |

## Equivalent dose measurement:

| | |
|---|---|
| Grain size (μm) | fine, 4-11 |
| Aliquots measured | 20 |
| Reliable aliquots | 20 |
| Regeneration doses (Gy) | 5, 10, 20, 35 50, 90 |

## Dose rate measurement:

Observations: Disequilibrium in Uranium decay chain

| | | Error |
|---|---|---|
| water content | 0.1 | 0.02 |
| | | |
| Th (ppm) | 30.31 | 1.81 |
| K (%) | 2.52 | 0.08 |
| U (ppm): | | |
| weighted mean (all) | 5.00 | 0.35 |
| Th234 | 7.25 | 0.64 |
| Ra226 | 5.60 | 1.70 |
| Pb214 and Bi214 | 4.77 | 0.34 |
| Pb210 | 9.86 | 2.99 |

Concentrations of Thorium, Potassium and Uranium

| | Effective DR (Gy/ka) | Error |
|---|---|---|
| alpha | 2.72 | 0.27 |
| beta | 3.23 | 0.17 |
| gamma | 2.33 | 0.10 |
| cosmic | 0.1497 | 0.007485 |

Effective dose rates

# HK13363

Nam Chung, NC-TP37

| Sample type | latitude | longitude | altitude | depth | Depositional type |
|---|---|---|---|---|---|
| U-100 Sample, horizontal | 22.14408773 | 113.5144942 | 77.72 | 1.3 | Colluvial |

| | | Error | Error (%) |
|---|---|---|---|
| **Equivalent Dose (Gy)** | **23.48** | **0.97** | **4.1** |
| **Total Dose rate (Gy/ka)** | **8.60** | **0.29** | **3.4** |
| **Age (ka)** | **2.73** | **0.15** | **5.4** |

## Equivalent dose measurement:

| | |
|---|---|
| Grain size (μm) | fine, 4-11 |
| Aliquots measured | 19 |
| Reliable aliquots | 18 |
| Regeneration doses (Gy) | 18, 21, 25, 28 |

## Dose rate measurement:

Observations: Disequilibrium in Uranium decay chain

| | | Error |
|---|---|---|
| water content | 0.1 | 0.02 |
| | | |
| Th (ppm) | 26.89 | 1.61 |
| K (%) | 2.37 | 0.08 |
| U (ppm): | | |
| weighted mean (all) | 7.05 | 0.49 |
| Th234 | 6.72 | 0.60 |
| Ra226 | 7.43 | 2.30 |
| Pb214 and Bi214 | 7.01 | 0.49 |
| Pb210 | 9.34 | 2.90 |

Concentrations of Thorium, Potassium and Uranium

| | Effective DR (Gy/ka) | Error |
|---|---|---|
| alpha | 2.84 | 0.25 |
| beta | 3.23 | 0.12 |
| gamma | 2.38 | 0.10 |
| cosmic | 0.1566 | 0.00783 |

Effective dose rates

# HK13364

Tai O East, TOE-TP2

| Sample type | latitude | longitude | altitude | depth | Depositional type |
|---|---|---|---|---|---|
| U-100 Sample, horizontal | 22.15222095 | 113.5135359 | 51.89 | 1.4 | Colluvial |

| | | Error | Error (%) |
|---|---|---|---|
| **Equivalent Dose (Gy)** | **128.1** | **5.1** | **4.0** |
| **Total Dose rate (Gy/ka)** | **7.01** | **0.33** | **4.7** |
| **Age (ka)** | **18.27** | **1.12** | **6.1** |

## Equivalent dose measurement:

Observations: feldspar contamination; post-IR blue sequence

| | |
|---|---|
| Grain size (μm) | fine, 4-11 |
| Aliquots measured | 17 |
| Reliable aliquots | 16 |
| Regeneration doses (Gy) | 10, 20, 40, 70 120, 200 |

## Dose rate measurement:

Observations: Disequilibrium in Uranium decay chain

| | | Error |
|---|---|---|
| water content | 0.145 | 0.029 |
| | | |
| Th (ppm) | 32.43 | 1.94 |
| K (%) | 0.97 | 0.04 |
| U (ppm): | | |
| weighted mean (all) | 5.29 | 0.37 |
| Th234 | 7.54 | 0.67 |
| Ra226 | 5.74 | 1.73 |
| Pb214 and Bi214 | 5.07 | 0.36 |
| Pb210 | 9.65 | 2.91 |

Concentrations of Thorium, Potassium and Uranium

| | Effective DR (Gy/ka) | Error |
|---|---|---|
| alpha | 2.73 | 0.27 |
| beta | 2.11 | 0.15 |
| gamma | 2.02 | 0.10 |
| cosmic | 0.1549 | 0.007745 |

Effective dose rates

BETA ANALYTIC INC.
DR. M.A. TAMERS and MR. D.G. HOOD
4985 S.W. 74 COURT
MIAMI, FLORIDA, USA 33155
PH: 305-667-5167 FAX:305-663-0964
beta@radiocarbon.com

# REPORT OF RADIOCARBON DATING ANALYSES

Ms. Denise Lai Kwan Tang

Report Date: 9/22/2011

CEDD

Material Received: 9/8/2011

| Sample Data | Measured Radiocarbon Age | 13C/12C Ratio | Conventional Radiocarbon Age(*) |
|---|---|---|---|
| Beta - 305530 | 400 +/- 30 BP | -29.1 o/oo | 330 +/- 30 BP |

SAMPLE : HK13466(A)
ANALYSIS : AMS-Standard delivery
MATERIAL/PRETREATMENT : (charred material): acid/alkali/acid
2 SIGMA CALIBRATION : Cal AD 1460 to 1650 (Cal BP 490 to 300)

Dates are reported as RCYBP (radiocarbon years before present, "present" = AD 1950). By international convention, the modern reference standard was 95% the 14C activity of the National Institute of Standards and Technology (NIST) Oxalic Acid (SRM 4990C) and calculated using the Libby 14C half-life (5568 years). Quoted errors represent 1 relative standard deviation statistics (68% probability) counting errors based on the combined measurements of the sample, background, and modern reference standards. Measured 13C/12C ratios (delta 13C) were calculated relative to the PDB-1 standard.

The Conventional Radiocarbon Age represents the Measured Radiocarbon Age corrected for isotopic fractionation, calculated using the delta 13C. On rare occasion where the Conventional Radiocarbon Age was calculated using an assumed delta 13C, the ratio and the Conventional Radiocarbon Age will be followed by "*". The Conventional Radiocarbon Age is not calendar calibrated. When available, the Calendar Calibrated result is calculated from the Conventional Radiocarbon Age and is listed as the "Two Sigma Calibrated Result" for each sample.

# CALIBRATION OF RADIOCARBON AGE TO CALENDAR YEARS

(Variables: C13/C12=-29.1:lab. mult=1)

**Laboratory number:** **Beta-305530**

**Conventional radiocarbon age:** **330±30 BP**

**2 Sigma calibrated result: (95% probability)** **Cal AD 1460 to 1650 (Cal BP 490 to 300)**

Intercept data

Intercepts of radiocarbon age with calibration curve: Cal AD 1520 (Cal BP 430) and
Cal AD 1580 (Cal BP 370) and
Cal AD 1630 (Cal BP 320)

1 Sigma calibrated result: (68% probability) Cal AD 1490 to 1640 (Cal BP 460 to 310)

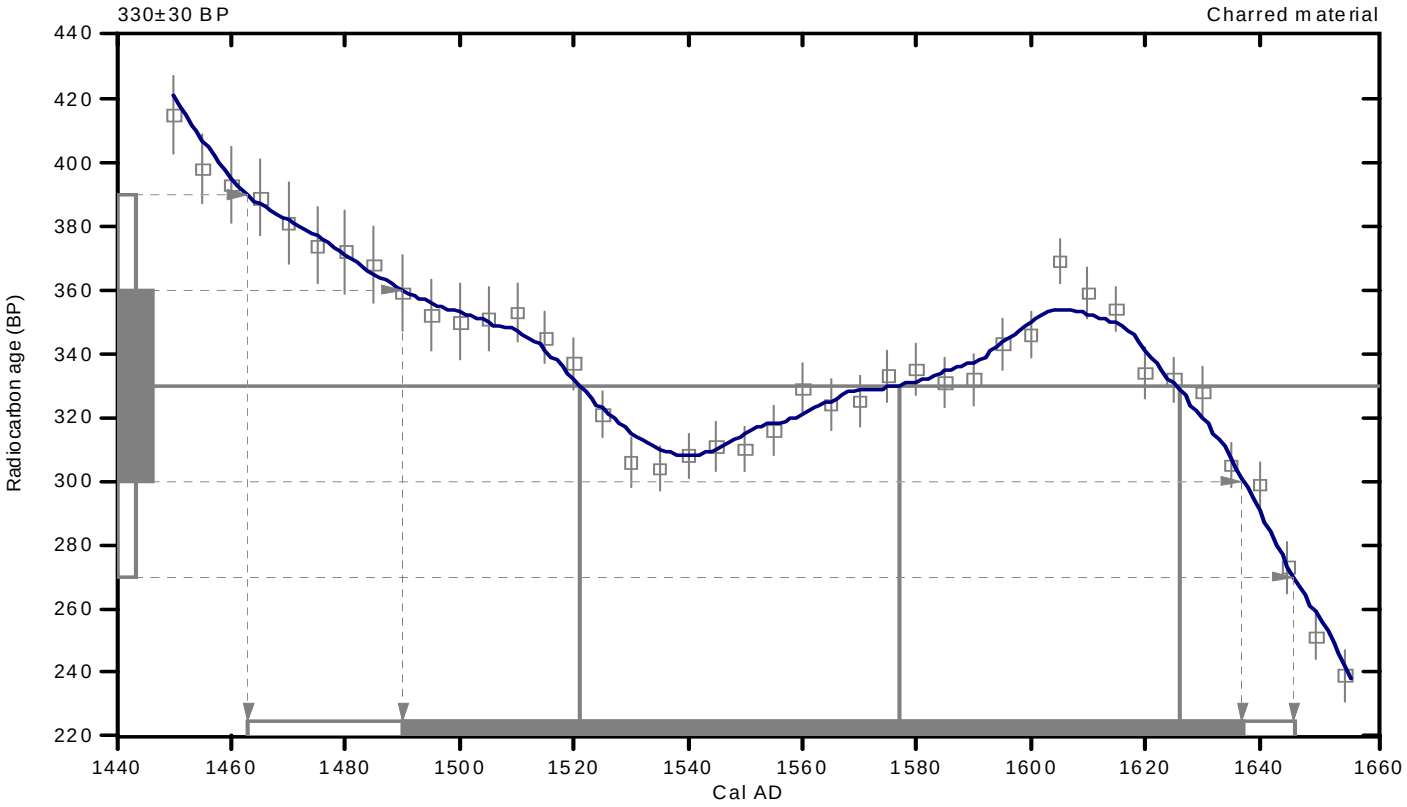


References:

***Database used***

*INTCAL04*

***Calibration Database***

***INTCAL04 Radiocarbon Age Calibration***

*IntCal04: Calibration Issue of Radiocarbon (Volume 46, nr 3, 2004).*

***Mathematics***

***A Simplified Approach to Calibrating C14 Dates***

*Talma, A. S., Vogel, J. C., 1993, Radiocarbon 35(2), p317-322*

**Beta Analytic Radiocarbon Dating Laboratory**

*4985 S.W. 74th Court, Miami, Florida 33155 • Tel: (305)667-5167 • Fax: (305)663-0964 • E-Mail: beta@radiocarbon.com*

**Report No. 1/12**

# Luminescence Dating Technical Report

**Luminescence Dating Laboratory**
**School of Geography, Environment and Earth Sciences**
**Victoria University of Wellington**
**Wellington**
**New Zealand**

Reported by: Ms. Ningsheng Wang (MSc)
Date of Issue: 24-01-2012
Contact: Room 414
Cotton Building
Victoria University of Wellington
Ph: (04) 463 6127

**CONTENTS**

# 1. INTRODUCTION

Eleven samples (laboratory code WLL949-959) were submitted for Luminescence Dating by the Geotechnical Engineering Office, Civil Engineering and Development Department, Hong Kong SAR Government.

The deposition ages have been determined for these samples using the silt fraction (4-11μm). Dependent on the relative luminescence intensities of feldspars, the palaeodose, i.e. the radiation dose accumulated in the sample after the last light exposure (assumed at deposition), was determined by measuring the broadband luminescence output during infrared optical stimulation of the feldspar fraction.

The dose rate was estimated on the basis of a low level gamma spectrometry measurement.

All measurements were done in the Luminescence Dating Laboratory, School of Geography, Environment and Earth Sciences, Victoria University of Wellington.

# 2. EXPERIMENTAL WORK

## 2.1 Sample Preparation

The samples contained a considerable amount of silt, and we decided to apply a so-called fine grain technique, i.e. use the grain size 4-11 μm for dating.

Sample preparation was done under extremely subdued safe orange light in a darkroom. Outer surfaces, which may have seen light during sampling, were removed and discarded. The actual water content and the saturation content were measured using 'fresh' inside material.

The samples were treated with 10%HCl to remove carbonates until the reaction stopped, then carefully rinsed with distilled water. Thereafter, all organic matter was destroyed with 10%$H_2O_2$ until the reaction stopped, then carefully rinsed with distilled water. By treatment with a solution of sodium citrate, sodium bicarbonate and sodium dithionate iron oxide coatings were removed from the mineral grains and then the sample was carefully rinsed again.

The grain size 4-11μm was extracted from the samples in a water-filled (with added dispersing agent to deflocculate clay) measuring cylinder using Stokes' Law. The other fractions were discarded. The samples then are brought into suspension in pure acetone and deposited evenly in a thin layer on up to 50 aluminum discs (1cm diameter).

Luminescence measurements were done using a standard Riso TL-DA15 measurement system, equipped with
• Schott BG39 + L40 optical filters to select the board luminescence band of feldspars. Stimulation was done cw at about 40mW/cm$^2$ with infrared diodes at 880Δ80nm.

β-irradiations were done by the built in $^{90}Sr,^{90}Y$ β-irradiator, calibrated against the Riso National Laboratory to about 3% accuracy. α-irradiations were done on a $^{241}Am$ irradiator supplied and calibrated by ELSEC, Littlemore, UK.

## 2.2 Luminescence Measurements

### *Multiple Aliquot Additive Method (MAAD)*

For sample WLL949-952 and WLL954-WLL958, the Paleodose was estimated by use of the multiple aliquot additive-dose method (with late-light subtraction). After an initial test-measurement, 30 aliquots were β-irradiated in six groups up to five times of the dose result taken from the test. 9 aliquots were α-irradiated in three groups up to three times of the dose result taken from the test. These 39 disks were stored in the dark for four weeks to relax the crystal lattice after irradiation.

After storage, these 39 disks and 9 unirradiated disks were preheated for 5mins at $220^0C$ to remove unstable signal components, and then measured for 100 seconds under IR stimulation, resulting in 48 shinedown curves. These curves were then normalized for their luminescence response, using 0.1s shortshine measurements taken before irradiation from all aliquots.

The luminescence growth curve (β-induced luminescence intensity vs added dose) is then constructed by using the initial 10 seconds of the shine down curves and subtracting the average of the last 20 seconds, the so called late light which is thought to be a mixture of background and hardly bleachable components. The shine plateau was checked to be flat after this manipulation. Extrapolation of this growth curve to the dose-axis gives the equivalent dose $D_e$, which is used as an estimate of the Paleodose.

A similar plot for the alpha-irradiated disks allows an estimate of the α-efficiency, the a-value (Luminescence/dose generated by the α-source divided by the luminescence/dose generated by the β-source).

### *Single Aliquot Regenerative Method (SAR)*

Palaeodoses for samples WLL953 and WLL959 were estimated by use of the Single Aliquot Regenerative Method (SAR; see Murray and Wintle, 2000) under IR stimulation as the growth curves of the two samples are near saturation, using SAR method can improve curves' positions.

In the SAR method a number of aliquots are subjected to a repetitive cycle of irradiation, preheat and measurement. In the first cycle the natural luminescence output is measured, in all following cycles an artificial dose is applied. Usually four or five of these dose points are used to build the luminescence growth curve (β-induced luminescence intensity vs added dose) and bracket the natural luminescence output. This allows interpolation of the equivalent dose (the β-dose equivalent to the palaeodose). In order to correct for potential sensitivity changes from cycle to cycle, a test dose is applied between the cycles, preheated ('cut heat') and measured.

For the samples reported here 10 aliquots were measured, preheat and cutheat temperature was $260^0$C for 20s, and measurement time 100s (IR stimulation), which resets the luminescence signal to a negligible residual. All feldspar measurements at room temperature.

The measurement of 10 aliquots resulted in 10 equivalent doses ($D_e$s). The $D_e$s were accepted within 10% recycling ratio, which spread over the so called dose distribution. The arithmetic mean of this distribution was interpreted as the best estimate for the equivalent dose, and subsequently used for age calculation. A dose recovery test and a zero dose were checked no anomalies.

### 2.3 Gamma Spectrometry

The dry, ground and homogenised soil samples were encapsuled in airtight perspex containers and stored for at least 4 weeks. This procedure minimizes the loss of the short-lived noble gas $^{222}$Rn and allows $^{226}$Ra to reach equilibrium with its daughters $^{214}$Pb and $^{214}$Bi.

The samples were counted using high resolution gamma spectrometry with a CANBERRA broad energy Ge detector for a minimum time of 24h. The spectra were analysed using GENIE2000 software. The doserate calculation is based on the activity concentration of the nuclides $^{40}$K, $^{208}$Tl, $^{212}$Pb, $^{228}$Ac, $^{214}$Bi, $^{214}$Pb, $^{226}$Ra.

## 3. RESULTS

The radionuclide contents were calculated from the raw gammaspectrometry data. The Uranium and Thorium contents of most samples were quite high, similar to what we've measured in the previous phases of this project reported earlier. Table 2 gives a summary of the radiometric data.

The high radionuclide contents cause high doserates for most samples, compared to 2…3 Gy/ka for what would be an 'average' sample. Owing to the high doserates, some samples showed the onset of saturation of the electron traps, despite being relatively young for the OSL dating technique.

Table 1 gives sample summaries and calculated cosmic doserates, whereas Table 3 gives a summary of all equivalent doses, doserates and ages.

All errors in this report are stated as 1 sigma errors. A radioactive disequilibrium was considered as significant, if the equivalent Uranium contents do not overlap in a 2 sigma interval.

## 4. REFERENCES

Adamiec G. and Aitken M. (1998) Dose-rate conversion factors: update. *Ancient TL* 16, 37-50.

Murray A.S. and Wintle A.G. (2000) Luminescence dating of quartz using an improved single-aliquot regenerative-dose protocol. *Radiation Measurements* 32, 57-73.

Prescott & Hutton (1994), *Radiation Measurements*, Vol. 23.

# LIST OF TABLES

**Table 1 - Doserate contribution of cosmic radiation**

| Sample no. | depth below surface (m) | $dD_c/dt$ (Gy/ka)[1] | Field code |
|---|---|---|---|
| WLL949 | 1.7 | 0.1579±0.0079 | HK13459 |
| WLL950 | 3.3 | 0.1279±0.0064 | HK13460 |
| WLL951 | 0.9 | 0.1795±0.0090 | HK13461 |
| WLL952 | 2.2 | 0.1504±0.0075 | HK13462 |
| WLL953 | 0.4 | 0.1890±0.0095 | HK13463 |
| WLL954 | 1.2 | 0.1691±0.0085 | HK13464 |
| WLL955 | 2.3 | 0.1458±0.0073 | HK13465 |
| WLL956 | 1.6 | 0.1601±0.0080 | HK13466 |
| WLL957 | 2.7 | 0.1407±0.0070 | HK13467 |
| WLL958 | 0.2 | 0.1978±0.0099 | HK13468 |
| WLL959 | 1 | 0.1769±0.0088 | HK13469 |

[1] Contribution of cosmic radiation to the total doserate, calculated as proposed by Prescott & Hutton (1994), Radiation Measurements, Vol. 23.

**Table 2 - Radionuclide and water contents**

| Sample no. | Water content (%)δ[1] | U (μg/g) from $^{234}$Th | U (μg/g)[2] from $^{226}$Ra, $^{214}$Pb, $^{214}$Bi | U (μg/g) from $^{210}$Pb | Th (μg/g)[2] from $^{208}$Tl, $^{212}$Pb, $^{228}$Ac | K (%) | Field code |
|---|---|---|---|---|---|---|---|
| WLL949 | 11.3 | 4.11±0.45 | 4.60±0.27 | 4.24±0.35 | 37.28±0.39 | 2.51±0.05 | HK13459 |
| WLL950 | 18.5 | 4.70±0.49 | 5.30±0.30 | 6.41±0.42 | 37.37±0.39 | 2.59±0.06 | HK13460 |
| WLL951 | 10.1 | 5.10±0.44 | 5.80±0.27 | 5.21±0.34 | 49.14±0.47 | 2.62±0.05 | HK13461 |
| WLL952 | 14.0 | 5.57±0.55 | 5.36±0.32 | 4.88±0.41 | 43.07±0.45 | 2.47±0.05 | HK13462 |
| WLL953 | 20.4 | 4.80±0.56 | 4.54±0.32 | 4.76±0.43 | 38.76±0.42 | 2.88±0.06 | HK13463 |
| WLL954 | 23.5 | 5.72±0.50 | 5.43±0.29 | 5.92±0.41 | 24.20±0.29 | 2.23±0.05 | HK13464 |
| WLL955 | 16.2 | 5.13±0.48 | 4.51±0.27 | 4.01±0.36 | 30.49±0.33 | 2.68±0.06 | HK13465 |
| WLL956 | 13.5 | 4.74±0.34 | 4.29±0.20 | 4.16±0.26 | 20.01±0.21 | 2.16±0.04 | HK13466 |
| WLL957 | 18.9 | 4.80±0.40 | 5.07±0.24 | 5.54±0.33 | 39.30±0.39 | 2.50±0.05 | HK13467 |
| WLL958 | 13.0 | 4.90±0.45 | 5.08±0.27 | 5.56±0.37 | 25.16±0.28 | 1.78±0.04 | HK13468 |
| WLL959 | 15.9 | 6.52±0.59 | 5.75±0.33 | 6.37±0.45 | 42.98±0.45 | 2.72±0.06 | HK13469 |

[1] Errors assumed 25% of (δ).
[2] U and Th-content are calculated from the error weighted mean of the isotope equivalent contents.

**Table3: a-value and equivalent dose, doserate and luminescence age**

| Sample no. | Method | a-value | $D_e$ (Gy) | dD/dt (Gy/ka)[#] | **OSL-age (ka)** | Field code |
|---|---|---|---|---|---|---|
| WLL949 | MAAD | 0.07±0.03* | 9.96±2.74 | 7.93±0.89 | **1.3±0.4** | HK13459 |
| WLL950 | MAAD | 0.07±0.01 | 43.11±5.48 | 7.63±0.30 | **5.6±0.8** | HK13460 |
| WLL951 | MAAD | 0.06±0.01 | 126.49±19.46 | 9.46±0.49 | **13.4±2.2** | HK13461 |
| WLL952 | MAAD | 0.07±0.03* | 25.81±3.71 | 8.50±1.01 | **3.0±0.6** | HK13462 |
| WLL953 | SAR | 0.05±0.03* | 305.25±33.92 | 7.16±0.78 | **42.6±6.6** | HK13463 |
| WLL954 | MAAD | 0.07±0.03* | 6.48±0.47 | 5.87±0.68 | **1.1±0.2** | HK13464 |
| WLL955 | MAAD | 0.06±0.04 | 130.0±17.3 | 6.75±0.96 | **19.3±3.8** | HK13465 |
| WLL956 | MAAD | 0.07±0.03* | 5.01±0.55 | 5.60±0.57 | **0.9±0.1** | HK13466 |
| WLL957 | MAAD | 0.06±0.01 | 136.8±15.2 | 7.37±0.46 | **18.6±2.4** | HK13467 |
| WLL958 | MAAD | 0.07±0.03* | 9.3±0.6 | 6.12±0.70 | **1.5±0.2** | HK13468 |
| WLL959 | SAR | 0.05±0.03* | 227.66±18.85 | 8.08±0.94 | **28.2±4.0** | HK13469 |

[#] The doserate dD/dt was calculated using the conversion factors of Adamiec and Aitken (1998)
[*] The a-values were estimated
MAAD Multiple Aliquot Additive Method
SAR Single Aliquot Regenerative Method

**Some comments**

- Our standard method is 'MAAD', i.e. a multiple aliquot approach focusing on the blue emission band of potassium feldspars (410nm). However, all samples had very low blue luminescence under infrared stimulation. Thus, we decided to detect broad band luminescence (400-660nm) by using BG39+L40 filters, to increase signal intensity.

- Samples WLL949, WLL954 and WLL958 contained traces of artificial $^{137}Cs$ , which likely results from atmospheric atomic bomb tests in the 1960s.

**Report No. 13/12**

# Luminescence Dating Technical Report

**Luminescence Dating Laboratory**
**School of Geography, Environment and Earth Sciences**
**Victoria University of Wellington**
**Wellington**
**New Zealand**

Reported by: Ms. Ningsheng Wang (MSc)
Date of Issue: 18-10-2012
Contact: Room 414
Cotton Building
Victoria University of Wellington
Ph: (04) 463 6127

**CONTENTS**

# 1. INTRODUCTION

Nine samples (Field code: HK13547,HK13548, HK13551 and HK13728-HK13733) were submitted to Luminescence Dating by the Geotechnical Engineering Office, Civil Engineering and Development Department, Hong Kong SAR Government. The laboratory codes of the samples are WLL1025_WLL1033 respectively.

The deposition ages have been determined for these samples using the silt fraction (4-11μm). Dependent on the relative luminescence intensities of feldspars in the samples, the palaeodose, i.e. the radiation dose accumulated in the sample after the last light exposure (assumed at deposition), was determined either by:

• measuring the blue or broadband luminescence output from feldspar fraction during infrared optical stimulation.

The dose rate was estimated on the basis of a low level gamma spectrometry measurement.

All measurements were done in the Luminescence Dating Laboratory, School of Geography, Environment and Earth Sciences, Victoria University of Wellington.

# 2. EXPERIMENTAL WORK

## 2.1 Sample Preparation

The samples contained a considerable amount of silt, and we decided to apply a so-called fine grain technique, i.e. use the grain size 4-11 μm for dating.

Sample preparation was done under extremely subdued safe orange light in a darkroom. Outer surfaces, which may have seen light during sampling, were removed and discarded. The actual water content and the saturation content were measured using 'fresh' inside material.

The samples were treated with 10%HCl to remove carbonates until the reaction stopped, then carefully rinsed with distilled water. Thereafter, all organic matter was destroyed with 10%$H_2O_2$ until the reaction stopped, then carefully rinsed with distilled water. By treatment with a solution of sodium citrate, sodium bicarbonate and sodium dithionate iron oxide coatings were removed from the mineral grains and then the sample was carefully rinsed again.

The grain size 4-11μm was extracted from the samples in a water-filled (with added dispersing agent to deflocculate clay) measuring cylinder using Stokes' Law. The other fractions were discarded. The samples then are brought into suspension in pure acetone and deposited evenly in a thin layer on up to 50 aluminum discs (1cm diameter).

## 2.2 Luminescence Measurements

Luminescence measurements were done using a standard Riso TL-DA15 measurement system, equipped with:

• Schott BG39+5-58+L40 optical filters to select the blue luminescence of feldspars.
• Schott BG39 + L40 optical filters to select the broad band luminescence of feldspars.
Stimulation was done cw at about 40mW/cm$^2$ with infrared diodes at 880Δ80nm.
β-irradiations were done by the built in $^{90}$Sr,$^{90}$Y β-irradiator, calibrated against the Riso National Laboratory to about 3% accuracy. α-irradiations were done on a $^{241}$Am irradiator supplied and calibrated by ELSEC, Littlemore, UK.

### *Multiple Aliquot Additive Method (MAAD)*

For samples WLL1025-WLL1027, WLL1029-WLL1031 and WLL1033, the Paleodose was estimated by use of the multiple aliquot additive-dose method (with late-light subtraction) by measuring the blue luminescence under IR Stimulation. After an initial test-measurement, 30 aliquots were β-irradiated in six groups up to five times of the dose result taken from the test. 9 aliquots were α-irradiated in three groups up to three times of the dose result taken from the test. These 39 disks were stored in the dark for four weeks to relax the crystal lattice after irradiation.

After storage, these 39 disks and 9 unirradiated disks were preheated for 5mins at 220$^0$C to remove unstable signal components, and then measured for 100 seconds under IR stimulation, resulting in 48 shinedown curves. These curves were then normalized for their luminescence response, using 0.1s shortshine measurements taken before irradiation from all aliquots.

The luminescence growth curve (β-induced luminescence intensity vs added dose) is then constructed by using the initial 10 seconds of the shine down curves and subtracting the average of the last 20 seconds, the so called late light which is thought to be a mixture of background and hardly bleachable components. The shine plateau was checked to be flat after this manipulation. Extrapolation of this growth curve to the dose-axis gives the equivalent dose $D_e$, which is used as an estimate of the Paleodose.

A similar plot for the alpha-irradiated disks allows an estimate of the α-efficiency, the a-value (Luminescence/dose generated by the α-source divided by the luminescence/dose generated by the β-source).

### *Single Aliquot Regenerative Method (SAR)*

Palaeodoses of the samples WLL1028 and WLL1032 were estimated by the use of the Single Aliquot Regenerative Method (SAR; see Murray and Wintle, 2000). The two types of luminescence were measured for the following two groups.

- Broadband luminescence of WLL1028 was measured under IR stimulation as the sample had no blue luminescence under IR stimulation.

- Blue luminescence of WLL1032 was measured under IR stimulation as the three.

In the SAR method a number of aliquots are subjected to a repetitive cycle of irradiation, preheat and measurement. In the first cycle the natural luminescence output is measured, in all following cycles an artificial dose is applied. Usually four or five of these dose points are used to build the luminescence growth curve (β-induced luminescence intensity vs added dose) and bracket the natural luminescence output. This allows interpolation of the equivalent dose (the β-dose equivalent to the palaeodose). In order to correct for potential sensitivity changes from cycle to cycle, a test dose is applied between the cycles, preheated ('cut heat') and measured.

For the samples reported here, 12-16 aliquots were measured. For IR stimulation, preheat and cutheat temperature was $260^0$C for 20s, and measurement time was 100s at the room temperature for all feldspar, which resets the luminescence signal to a negligible residual.

The measurement of 12-16 aliquots resulted in 12-16 equivalent doses ($D_e$s). The $D_e$s were accepted within 10% recycling ratio, which spread over the so called dose distribution. The arithmetic mean of this distribution was interpreted as the best estimate for the equivalent dose, and subsequently used for age calculation. A dose recovery test and a zero dose were checked no anomalies.

### 2.3 Gamma Spectrometry

The dry, ground and homogenised soil samples were encapsuled in airtight perspex containers and stored for at least 4 weeks. This procedure minimizes the loss of the short-lived noble gas $^{222}$Rn and allows $^{226}$Ra to reach equilibrium with its daughters $^{214}$Pb and $^{214}$Bi.

The samples were counted using high resolution gamma spectrometry with a CANBERRA broad energy Ge detector for a minimum time of 24h. The spectra were analysed using GENIE2000 software. The doserate calculation is based on the activity concentration of the nuclides $^{40}$K, $^{208}$Tl, $^{212}$Pb, $^{228}$Ac, $^{214}$Bi, $^{214}$Pb, $^{226}$Ra.

## 3. RESULTS

The radionuclide contents were calculated from the raw gammaspectrometry data. The Uranium and Thorium contents of most samples were quite high, similar to what we've measured in the previous phases of Hong Kong project reported earlier. Table 2 gives a summary of the radiometric data.

The high radionuclide contents cause high doserates for all samples, compared to 2-3 Gy/ka for what would be an 'average' sample. Owing to the high doserates, some samples showed the onset of saturation of the electron traps, despite being relatively young for the OSL dating technique.

Table 1 gives sample summaries and calculated cosmic doserates, whereas Table 3 gives a summary of all equivalent doses, doserates and ages.

All errors in this report are stated as 1 sigma errors. A radioactive disequilibrium was considered as significant, if the equivalent Uranium contents do not overlap in a 2 sigma interval.

## 4. REFERENCES

Guérin, G., Mercier, N., Adamiec, G. 2011: Dose- rate conversion factors: update. *Ancient TL*, Vol.29, No.1, 5-8.

Murray A.S. and Wintle A.G. (2000) Luminescence dating of quartz using an improved single-aliquot regenerative-dose protocol. *Radiation Measurements* 32, 57-73.

Prescott & Hutton (1994), *Radiation Measurements*, Vol. 23.

**LIST OF TABLES**

**Table 1 - Doserate contribution of cosmic radiation**

| Laboratory Code | Depth Below the Surface(m) | Cosmic Dose Rate (Gy/ka) | Field Code |
|---|---|---|---|
| WLL1025 | 1.95 | 0.1533±0.0077 | HK13547 |
| WLL1026 | 0.60 | 0.1845±0.0092 | HK13548 |
| WLL1027 | 2.10 | 0.1503±0.0075 | HK13551 |
| WLL1028 | 1.00 | 0.1745±0.0087 | HK13728 |
| WLL1029 | 0.80 | 0.1794±0.0090 | HK13729 |
| WLL1030 | 1.00 | 0.1745±0.0087 | HK13730 |
| WLL1031 | 0.10 | 0.1979±0.0099 | HK13731 |
| WLL1032 | 1.10 | 0.1721±0.0086 | HK13732 |
| WLL1033 | 2.60 | 0.1407±0.0070 | HK13733 |

[1] Contribution of cosmic radiation to the total doserate, calculated as proposed by Prescott & Hutton (1994), Radiation Measurements, Vol. 23

**Table 2 - Radionuclide and water contents**

| Laboratory Code | Water content (%)[1] | U(ppm) from $^{234}$Th | U(ppm)[2] from $^{226}$Ra, $^{214}$Pb, $^{214}$Bi | U(ppm) from $^{210}$Pb | Th(ppm)[2] From $^{208}$Tl $^{212}$Pb $^{228}$Ac | K(%) | Field Code |
|---|---|---|---|---|---|---|---|
| WLL1025 | 17.3 | 13.87±0.92 | 12.84±0.55 | 10.51±0.64 | 79.56±0.78 | 2.33±0.05 | HK13547 |
| WLL1026 | 13.4 | 11.41±0.61 | 11.11±0.39 | 10.49±0.47 | 62.78±0.58 | 2.61±0.05 | HK13548 |
| WLL1027 | 19.8 | 5.90±0.66 | 7.27±0.40 | 7.71±0.53 | 63.03±0.63 | 1.82±0.05 | HK13551 |
| WLL1028 | 31.2 | 7.43±0.61 | 6.41±0.35 | 5.68±0.44 | 42.10±0.45 | 1.67±0.04 | HK13728 |
| WLL1029 | 30.5 | 9.75±0.71 | 10.06±0.44 | 8.60±0.53 | 39.98±0.43 | 1.34±0.04 | HK13729 |
| WLL1030 | 32.0 | 8.59±0.65 | 8.53±0.40 | 7.68±0.49 | 30.23±0.35 | 1.36±0.04 | HK13730 |
| WLL1031* | 40.2 | 10.49±0.75 | 8.34±0.45 | 6.39±0.50 | 36.57±0.41 | 1.67±0.04 | HK13731 |
| WLL1032 | 36.9 | 8.12±0.65 | 8.62±0.40 | 7.83±0.49 | 39.50±0.43 | 1.46±0.04 | HK13732 |
| WLL1033 | 32.6 | 8.93±0.64 | 8.23±0.39 | 8.08±0.49 | 32.46±0.36 | 1.90±0.05 | HK13733 |

[1] Errors assumed 25% of (δ).
[2] U and Th-content are calculated from the error weighted mean of the isotope equivalent contents.
*WLL 1031 was observed disequilibrium of U decay chains.

**Table3: a-value and equivalent dose, dose rate and luminescence age**

| Laboratory Code | Method | a-value | $D_e$(Gy) | Dose Rate(Gy/ka) | **Luminescence Age(ka)** | Field Code |
|---|---|---|---|---|---|---|
| WLL1025 | MAAD | 0.09±0.01 | 200.70±8.69 | 15.33±0.90 | **13.1±1.0** | HK13547 |
| WLL1026 | MAAD | 0.08±0.01 | 268.69±11.36 | 13.22±0.69 | **20.3±1.4** | HK13548 |
| WLL1027 | MAAD | 0.06±0.02 | 195.78±26.29 | 9.54±0.96 | **20.5±3.5** | HK13551 |
| WLL1028 | SARbroadband | *0.07±0.02 | 108.39±27.33 | 6.84±0.72 | **15.9±4.3** | HK13728 |
| WLL1029 | MAAD | 0.07±0.02 | 62.31±8.09 | 7.53±0.82 | **8.3±1.4** | HK13729 |
| WLL1030 | MAAD | 0.08±0.01 | 48.44±5.14 | 6.43±0.51 | **7.5±1.0** | HK13730 |
| WLL1031 | MAAD | 0.06±0.01 | 181.07±21.24 | 6.19±0.29 | **29.2±3.7** | HK13731 |
| WLL1032 | SAR | *0.07±0.02 | 114.83±15.46 | 6.76±0.74 | **17.0±2.9** | HK13732 |
| WLL1033 | MAAD | 0.09±0.01 | 42.16±5.58 | 7.12±0.55 | **5.9±0.9** | HK13733 |

[*] The a-values of samples WLL1028 and WLL1032 were estimated.

**Some comments**

- Our standard method is 'MAAD', i.e. a multiple aliquot approach focusing on the blue emission band of potassium feldspars (410nm). However, one sample WLL1028 had very low blue luminescence under infrared stimulation. Thus, we decided to detect broad band luminescence (400-660nm) by using BG39+L40 filters, to increase signal intensity.

- From Table 2, WLL1031 displays disequilibrium in the uranium chains. This is probably the result of radionuclide mobility during their burial time. An adjustment of uranium content slightly affects the age, however if uncertainty of the age is taken into account, the effect is negligible.

- In Table 3, the ages of WLL1028 and WLL1032 were obtained by the SAR method. The MAAD method gave an inconclusive dataset. At this stage, despite the MAAD yielding more trustful results, the age from the SAR may be only way to represent the age.

BETA ANALYTIC INC.
DR. M.A. TAMERS and MR. D.G. HOOD
4985 S.W. 74 COURT
MIAMI, FLORIDA, USA 33155
PH: 305-667-5167 FAX:305-663-0964
beta@radiocarbon.com

# REPORT OF RADIOCARBON DATING ANALYSES

Dr. Kevin W.F. So

Report Date: 6/17/2013

Civil Engineering and Development Department

Material Received: 6/6/2013

| Sample Data | Measured Radiocarbon Age | 13C/12C Ratio | Conventional Radiocarbon Age(*) |
|---|---|---|---|
| Beta - 350526 | 3120 +/- 30 BP | -25.6 o/oo | 3110 +/- 30 BP |
| SAMPLE : HK13462 (A) | | | |
| ANALYSIS : AMS-Standard delivery | | | |
| MATERIAL/PRETREATMENT : (charred material): acid/alkali/acid | | | |
| 2 SIGMA CALIBRATION : Cal BC 1430 to 1370 (Cal BP 3380 to 3320) AND Cal BC 1360 to 1310 (Cal BP 3310 to 3260) | | | |
| Beta - 350527 | 240 +/- 30 BP | -26.7 o/oo | 210 +/- 30 BP |
| SAMPLE : HK13827 | | | |
| ANALYSIS : AMS-Standard delivery | | | |
| MATERIAL/PRETREATMENT : (charred material): acid/alkali/acid | | | |
| 2 SIGMA CALIBRATION : Cal AD 1650 to 1680 (Cal BP 300 to 270) AND Cal AD 1730 to 1810 (Cal BP 220 to 140) Cal AD 1930 to post 1950 (Cal BP 20 to post 1950) | | | |
| Beta - 350528 | 7950 +/- 40 BP | -25.4 o/oo | 7940 +/- 40 BP |
| SAMPLE : HK13834 | | | |
| ANALYSIS : AMS-Standard delivery | | | |
| MATERIAL/PRETREATMENT : (charred material): acid/alkali/acid | | | |
| 2 SIGMA CALIBRATION : Cal BC 7040 to 6680 (Cal BP 8990 to 8630) AND Cal BC 6660 to 6660 (Cal BP 8610 to 8610) | | | |

Dates are reported as RCYBP (radiocarbon years before present, "present" = AD 1950). By international convention, the modern reference standard was 95% the 14C activity of the National Institute of Standards and Technology (NIST) Oxalic Acid (SRM 4990C) and calculated using the Libby 14C half-life (5568 years). Quoted errors represent 1 relative standard deviation statistics (68% probability) counting errors based on the combined measurements of the sample, background, and modern reference standards. Measured 13C/12C ratios (delta 13C) were calculated relative to the PDB-1 standard.

The Conventional Radiocarbon Age represents the Measured Radiocarbon Age corrected for isotopic fractionation, calculated using the delta 13C. On rare occasion where the Conventional Radiocarbon Age was calculated using an assumed delta 13C, the ratio and the Conventional Radiocarbon Age will be followed by "*". The Conventional Radiocarbon Age is not calendar calibrated. When available, the Calendar Calibrated result is calculated from the Conventional Radiocarbon Age and is listed as the "Two Sigma Calibrated Result" for each sample.

# CALIBRATION OF RADIOCARBON AGE TO CALENDAR YEARS

(Variables: C13/C12=-25.6:lab. mult=1)

**Laboratory number:** **Beta-350526**

**Conventional radiocarbon age:** **3110±30 BP**

**2 Sigma calibrated results: (95% probability)** **Cal BC 1430 to 1370 (Cal BP 3380 to 3320) and Cal BC 1360 to 1310 (Cal BP 3310 to 3260)**

Intercept data

Intercept of radiocarbon age with calibration curve: Cal BC 1410 (Cal BP 3360)

1 Sigma calibrated results: (68% probability) Cal BC 1420 to 1380 (Cal BP 3370 to 3340) and Cal BC 1330 to 1320 (Cal BP 3280 to 3280)

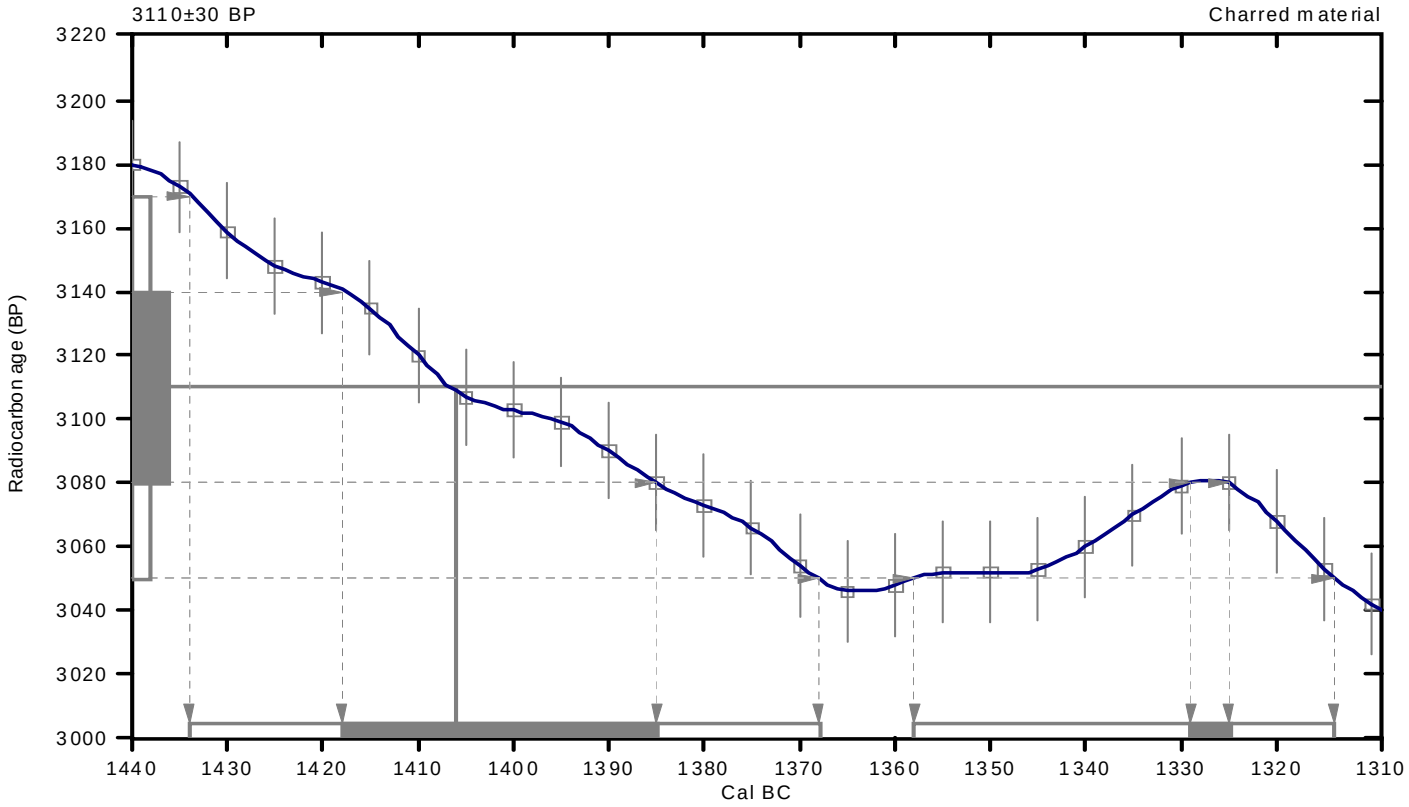


References:

***Database used***

*INTCAL09*

***References to INTCAL09 database***

*Heaton,et.al.,2009, Radiocarbon 51(4):1151-1164, Reimer,et.al, 2009, Radiocarbon 51(4):1111-1150, Stuiver,et.al,1993, Radiocarbon 35(1):137-189, Oeschger,et.al.,1975,Tellus 27:168-192*

***Mathematics used for calibration scenario***

*A Simplified Approach to Calibrating C14 Dates*
*Talma, A. S., Vogel, J. C., 1993, Radiocarbon 35(2):317-322*

**Beta Analytic Radiocarbon Dating Laboratory**

*4985 S.W. 74th Court, Miami, Florida 33155 • Tel: (305)667-5167 • Fax: (305)663-0964 • E-Mail: beta@radiocarbon.com*

# CALIBRATION OF RADIOCARBON AGE TO CALENDAR YEARS

(Variables: C13/C12=-26.7:lab. mult=1)

**Laboratory number:** **Beta-350527**

**Conventional radiocarbon age:** **210±30 BP**

**2 Sigma calibrated results:** **Cal AD 1650 to 1680 (Cal BP 300 to 270) and**
**(95% probability)** **Cal AD 1730 to 1810 (Cal BP 220 to 140) and**
**Cal AD 1930 to post 1950 (Cal BP 20 to post 1950)**

Intercept data

Intercepts of radiocarbon age with calibration curve: Cal AD 1670 (Cal BP 280) and
Cal AD 1780 (Cal BP 170) and
Cal AD 1800 (Cal BP 160) and
Cal AD 1950 (Cal BP 0) and
Cal AD 1950 (Cal BP 0)

1 Sigma calibrated results: Cal AD 1650 to 1670 (Cal BP 300 to 280) and
(68% probability) Cal AD 1780 to 1800 (Cal BP 170 to 150) and
Cal AD 1940 to post 1950 (Cal BP 10 to post 1950)

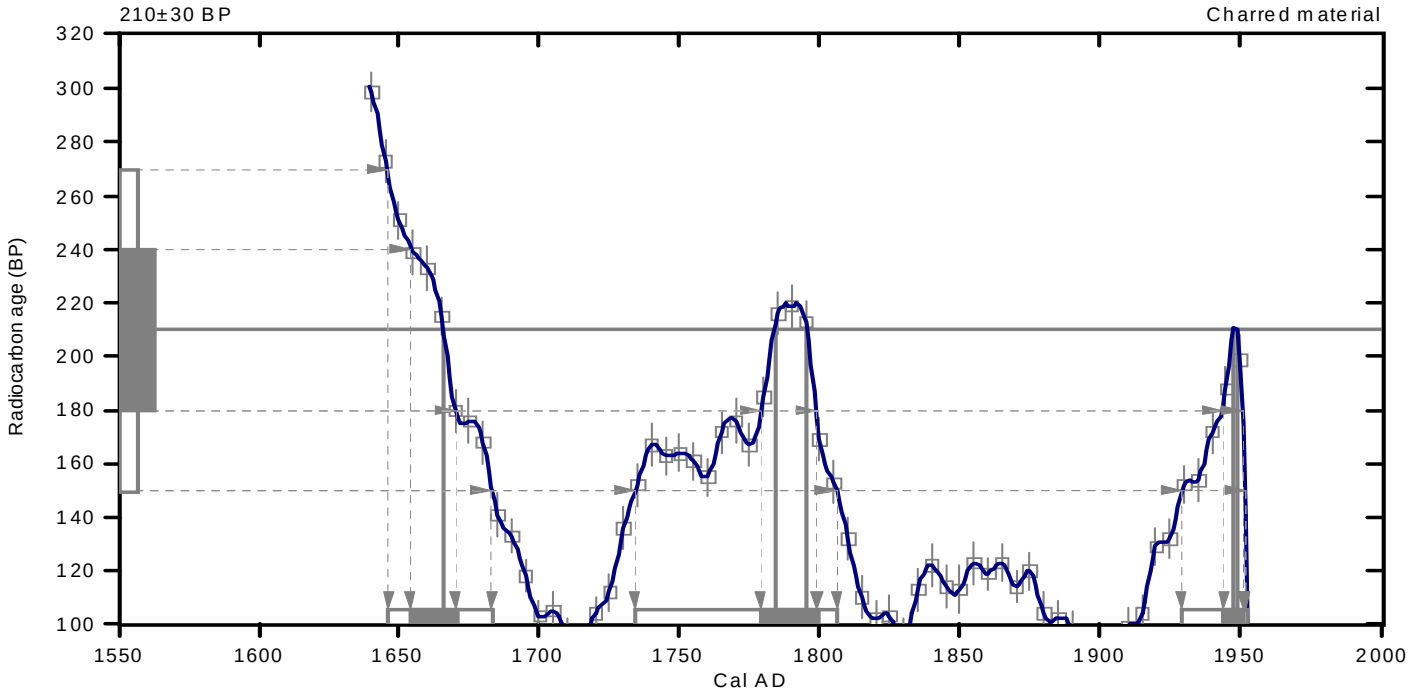


References:

***Database used***

*INTCAL09*

***References to INTCAL09 database***

*Heaton,et.al.,2009, Radiocarbon 51(4):1151-1164, Reimer,et.al, 2009, Radiocarbon 51(4):1111-1150, Stuiver,et.al,1993, Radiocarbon 35(1):1-244, Oeschger,et.al.,1975,Tellus 27:168-192*

***Mathematics used for calibration scenario***

*A Simplified Approach to Calibrating C14 Dates*
*Talma, A. S., Vogel, J. C., 1993, Radiocarbon 35(2):317-322*

**Beta Analytic Radiocarbon Dating Laboratory**

*4985 S.W. 74th Court, Miami, Florida 33155 • Tel: (305)667-5167 • Fax: (305)663-0964 • E-Mail: beta@radiocarbon.com*

# CALIBRATION OF RADIOCARBON AGE TO CALENDAR YEARS

(Variables: C13/C12=-25.4:lab. mult=1)

**Laboratory number:** **Beta-350528**

**Conventional radiocarbon age:** **7940±40 BP**

**2 Sigma calibrated results: (95% probability)** **Cal BC 7040 to 6680 (Cal BP 8990 to 8630) and Cal BC 6660 to 6660 (Cal BP 8610 to 8610)**

Intercept data

Intercept of radiocarbon age with calibration curve: Cal BC 6820 (Cal BP 8770)

1 Sigma calibrated results: (68% probability) Cal BC 7030 to 6960 (Cal BP 8980 to 8910) and Cal BC 6950 to 6930 (Cal BP 8900 to 8880) and Cal BC 6920 to 6880 (Cal BP 8870 to 8830) and Cal BC 6840 to 6700 (Cal BP 8790 to 8650)

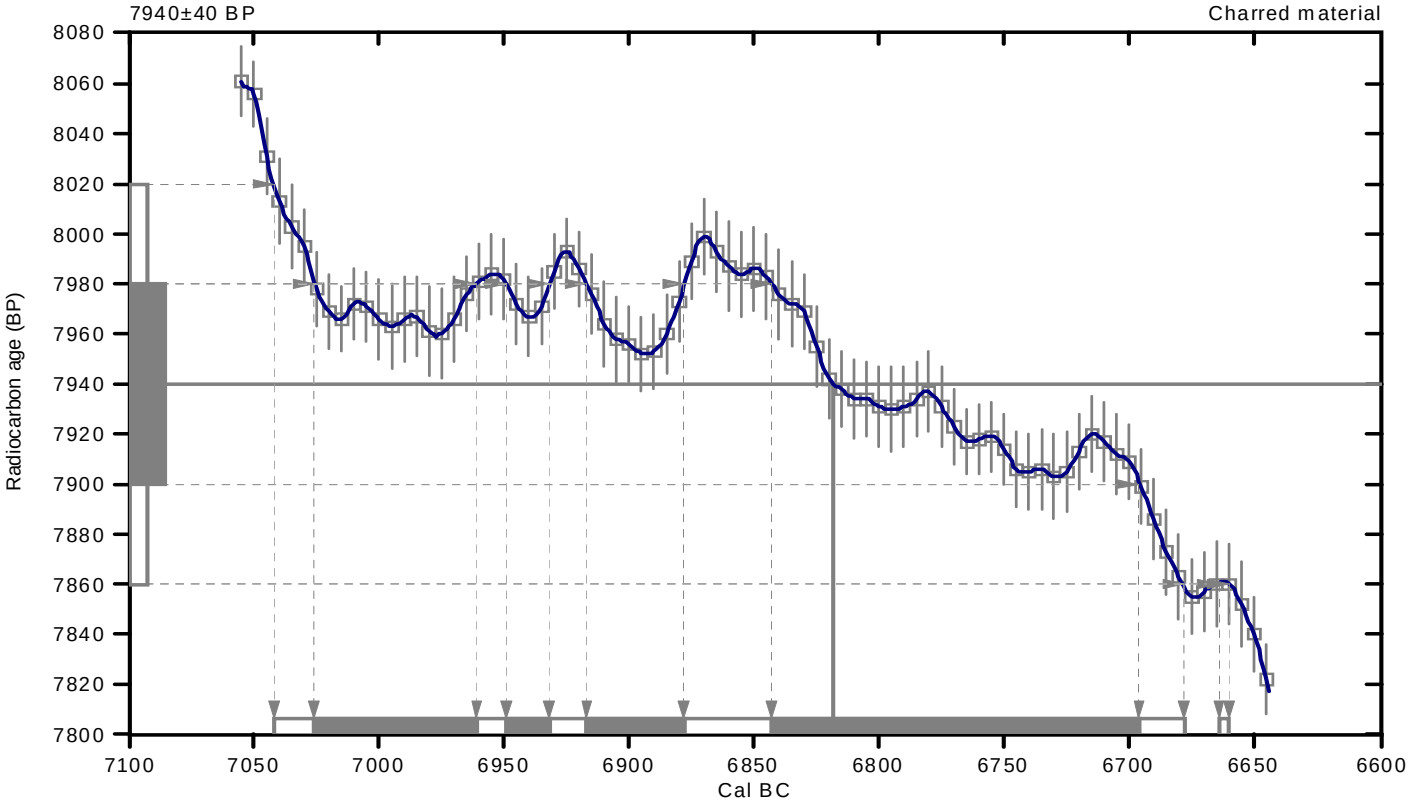


References:

***Database used***

*INTCAL09*

***References to INTCAL09 database***

*Heaton,et.al.,2009, Radiocarbon 51(4):1151-1164, Reimer,et.al, 2009, Radiocarbon 51(4):1111-1150, Stuiver,et.al,1993, Radiocarbon 35(1):137-189, Oeschger,et.al.,1975,Tellus 27:168-192*

***Mathematics used for calibration scenario***

*A Simplified Approach to Calibrating C14 Dates*
*Talma, A. S., Vogel, J. C., 1993, Radiocarbon 35(2):317-322*

**Beta Analytic Radiocarbon Dating Laboratory**

*4985 S.W. 74th Court, Miami, Florida 33155 • Tel: (305)667-5167 • Fax: (305)663-0964 • E-Mail: beta@radiocarbon.com*

**Report No. 16/13**

# Luminescence Dating Technical Report

**Luminescence Dating Laboratory**

**School of Geography, Environment and Earth Sciences**

**Victoria University of Wellington**

**Wellington**

**New Zealand**

Reported by: Ms. Ningsheng Wang (MSc)

Date of Issue: 24-10-2013

Contact: Room 414

Cotton Building

Victoria University of Wellington

Ph: (04) 463 6127

**CONTENTS**

# 1. INTRODUCTION

Ten samples (Field code: HK13824-HK13833) were submitted to Luminescence Dating by the Geotechnical Engineering Office, Civil Engineering and Development Department, Hong Kong SAR Government. The laboratory codes of the samples are WLL1099-WLL1108 respectively.

The deposition ages have been determined for these samples using the silt fraction (4-11μm). Dependent on the relative luminescence intensities of feldspars in the samples, the palaeodose, i.e. the radiation dose accumulated in the sample after the last light exposure (assumed at deposition), was determined by measuring the blue luminescence output from feldspar fraction during infrared optical stimulation.

The dose rate was estimated on the basis of a low level gamma spectrometry measurement.

All measurements were done in the Luminescence Dating Laboratory, School of Geography, Environment and Earth Sciences, Victoria University of Wellington.

# 2. EXPERIMENTAL WORK

## 2.1 Sample Preparation

The samples contained a considerable amount of silt, and we decided to apply a so-called fine grain technique, i.e. use the grain size 4-11 μm for dating.

Sample preparation was done under extremely subdued safe orange light in a darkroom. Outer surfaces, which may have seen light during sampling, were removed and discarded. The actual water content and the saturation content were measured using 'fresh' inside material.

The samples were treated with 10%HCl to remove carbonates until the reaction stopped, then carefully rinsed with distilled water. Thereafter, all organic matter was destroyed with 10%$H_2O_2$ until the reaction stopped, then carefully rinsed with distilled water. By treatment with a solution of sodium citrate, sodium bicarbonate and sodium dithionate iron oxide coatings were removed from the mineral grains and then the sample was carefully rinsed again.

The grain size 4-11μm was extracted from the samples in a water-filled (with added dispersing agent to deflocculate clay) measuring cylinder using Stokes' Law. The other fractions were discarded. The samples then are brought into suspension in pure acetone and deposited evenly in a thin layer on up to 50 aluminum discs (1cm diameter).

## 2.2 Luminescence Measurements

Luminescence measurements were done using a standard Riso TL-DA15 measurement

system, equipped with:

• Schott BG39+5-58+L40 optical filters to select the blue luminescence of feldspars.

Stimulation was done cw at about 40mW/cm$^2$ with infrared diodes at 880Δ80nm. β-irradiations were done by the built in $^{90}$Sr,$^{90}$Y β-irradiator, calibrated against the Riso National Laboratory to about 3% accuracy. α-irradiations were done on a $^{241}$Am irradiator supplied and calibrated by ELSEC, Littlemore, UK.

***Multiple Aliquot Additive Method (MAAD)***

All samples except sample WLL1106, the Paleodose was estimated by use of the multiple aliquot additive-dose method (with late-light subtraction) by measuring the blue luminescence under IR Stimulation. After an initial test-measurement, 30 aliquots were β-irradiated in six groups up to five times of the dose result taken from the test. 9 aliquots were α-irradiated in three groups up to three times of the dose result taken from the test. These 39 disks were stored in the dark for four weeks to relax the crystal lattice after irradiation.

After storage, these 39 disks and 9 unirradiated disks were preheated for 5mins at 220$^0$C to remove unstable signal components, and then measured for 100 seconds under IR stimulation, resulting in 48 shinedown curves. These curves were then normalized for their luminescence response, using 0.1s shortshine measurements taken before irradiation from all aliquots.

The luminescence growth curve (β-induced luminescence intensity vs added dose) is then constructed by using the initial 10 seconds of the shine down curves and subtracting the average of the last 20 seconds, the so called late light which is thought to be a mixture of background and hardly bleachable components. The shine plateau was checked to be flat after this manipulation. Extrapolation of this growth curve to the dose-axis gives the equivalent dose $D_e$, which is used as an estimate of the Paleodose.

A similar plot for the alpha-irradiated disks allows an estimate of the α-efficiency, the a-value (Luminescence/dose generated by the α-source divided by the luminescence/dose generated by the β-source).

***Single Aliquot Regenerative Method (SAR)***

The Palaeodose of the sample WLL1106 was estimated by the use of the Single Aliquot Regenerative Method (SAR; see Murray and Wintle, 2000).by measuring the blue luminescence under infrared situation.

In the SAR method a number of aliquots are subjected to a repetitive cycle of irradiation, preheat and measurement. In the first cycle the natural luminescence output

is measured, in all following cycles an artificial dose is applied. Usually four or five of these dose points are used to build the luminescence growth curve (β-induced luminescence intensity vs added dose) and bracket the natural luminescence output. This allows interpolation of the equivalent dose (the β-dose equivalent to the palaeodose). In order to correct for potential sensitivity changes from cycle to cycle, a test dose is applied between the cycles, preheated ('cut heat') and measured.

For the sample WLL1106, 8 aliquots were measured. For IR stimulation, preheat and cutheat temperature was $260^0$C for 20s, and measurement time was 100s at the room temperature for the feldspar, which resets the luminescence signal to a negligible residual.

The measurement of 8 aliquots resulted in 8 equivalent doses ($D_e$s). The $D_e$s were accepted within 10% recycling ratio, which spread over the so called dose distribution. The arithmetic mean of this distribution was interpreted as the best estimate for the equivalent dose, and subsequently used for age calculation. A dose recovery test and a zero dose were checked no anomalies.

### 2.3 Gamma Spectrometry

The dry, ground and homogenised soil samples were encapsuled in airtight perspex containers and stored for at least 4 weeks. This procedure minimizes the loss of the short-lived noble gas $^{222}$Rn and allows $^{226}$Ra to reach equilibrium with its daughters $^{214}$Pb and $^{214}$Bi.

The samples were counted using high resolution gamma spectrometry with a CANBERRA broad energy Ge detector for a minimum time of 24h. The spectra were analysed using GENIE2000 software. The doserate calculation is based on the activity concentration of the nuclides $^{40}$K, $^{208}$Tl, $^{212}$Pb, $^{228}$Ac, $^{214}$Bi, $^{214}$Pb, $^{226}$Ra.

## 3. RESULTS

The radionuclide contents were calculated from the raw gammaspectrometry data. The Uranium and Thorium contents of most samples were quite high, similar to what we've measured in the previous phases of Hong Kong project reported earlier. Table 2 gives a summary of the radiometric data.

The high radionuclide contents cause high doserates for all samples, compared to 2-3 Gy/ka for what would be an 'average' sample. Owing to the high doserates, some samples showed the onset of saturation of the electron traps, despite being relatively young for the OSL dating technique.

Table 1 gives sample summaries and calculated cosmic doserates, whereas Table 3 gives a summary of all equivalent doses, doserates and ages.

All errors in this report are stated as 1 sigma errors. A radioactive disequilibrium was considered as significant, if the equivalent Uranium contents do not overlap in a 2 sigma interval.

Water content was measured as weight of water divided by dry weight of the sample taking into account a 25% uncertainty.

## 4. REFERENCES

Guérin, G., Mercier, N., Adamiec, G. 2011: Dose- rate conversion factors: update. *Ancient TL*, Vol.29, No.1, 5-8.

Murray A.S. and Wintle A.G. (2000) Luminescence dating of quartz using an improved single-aliquot regenerative-dose protocol. *Radiation Measurements* 32, 57-73.

Prescott & Hutton (1994), *Radiation Measurements*, Vol. 23.

**LIST OF TABLES**

**Table 1 - Doserate contribution of cosmic radiation**

| Laboratory Code | Depth Below the Surface(m) | Cosmic Dose Rate (Gy/ka) [1] | Field Code |
|---|---|---|---|
| WLL1099 | 1.20 | 0.1733±0.0087 | HK13824 |
| WLL1100 | 0.95 | 0.1794±0.0090 | HK13825 |
| WLL1101 | 1.20 | 0.1733±0.0087 | HK13826 |
| WLL1102 | 0.30 | 0.1964±0.0098 | HK13827 |
| WLL1103 | 0.90 | 0.1804±0.0090 | HK13828 |
| WLL1104 | 2.0 | 0.1561±0.0078 | HK13829 |
| WLL1105 | 2.8 | 0.1568±0.0078 | HK13830 |
| WLL1106 | 1.3 | 0.1712±0.0086 | HK13831 |
| WLL1107 | 1.2 | 0.1724±0.0086 | HK13832 |
| WLL1108 | 1.2 | 0.1755±0.0088 | HK13833 |

[1] Contribution of cosmic radiation to the total doserate, calculated as proposed by Prescott & Hutton (1994), Radiation Measurements, Vol. 23

**Table 2 - Radionuclide and water contents**

| Laboratory Code | Water Content (%)[1] | U(ppm) from $^{234}$Th | U(ppm) [2] from $^{226}$Ra, $^{214}$Pb, $^{214}$ Bi | U(ppm) from $^{210}$Pb | Th(ppm) [2] From $^{208}$Tl $^{212}$ Pb $^{228}$ Ac | K(%) | Field Code |
|---|---|---|---|---|---|---|---|
| WLL1099 | 0.261 | 7.83±0.66 | 7.69±0.41 | 7.33±0.50 | 45.31±0.49 | 2.70±0.06 | HK13824 |
| WLL1100 | 0.197 | 7.50±0.66 | 8.31±0.42 | 8.37±0.55 | 37.56±0.43 | 2.37±0.06 | HK13825 |
| WLL1101 | 0.230 | 6.48±0.62 | 6.47±0.36 | 5.63±0.46 | 32.99±0.39 | 2.39±0.06 | HK13826 |
| WLL1102 | 0.222 | 5.74±0.54 | 5.35±0.32 | 4.87±0.41 | 29.66±0.35 | 2.88±0.06 | HK13827 |
| WLL1103 | 0.245 | 6.39±0.58 | 6.03±0.34 | 6.03±0.46 | 35.68±0.40 | 2.74±0.06 | HK13828 |
| WLL1104 | 0.292 | 6.44±0.64 | 5.73±0.39 | 4.86±0.46 | 41.96±0.47 | 1.97±0.05 | HK13829 |
| WLL1105 | 0.267 | 6.29±0.58 | 6.31±0.35 | 6.17±0.46 | 38.85±0.43 | 2.73±0.06 | HK13830 |

| | | | | | | | |
|---|---|---|---|---|---|---|---|
| WLL1106 | 0.279 | 7.49±0.49 | 8.84±0.34 | 8.46±0.42 | 44.29±0.43 | 2.06±0.04 | HK13831 |
| WLL1107 | 0.213 | 7.64±0.57 | 6.67±0.33 | 5.91±0.42 | 28.80±0.33 | 3.32±0.07 | HK13832 |
| WLL1108 | 0.281 | 5.54±0.61 | 5.11±0.35 | 4.71±0.45 | 35.98±0.42 | 1.86±0.05 | HK13833 |

[1] Errors assumed 25% of (δ).
[2] U and Th-content are calculated from the error weighted mean of the isotope equivalent contents.

**Table3 - a-value and equivalent dose, dose rate and luminescence age**

| Laboratory Code | Method | a-value | $D_e$(Gy) | Dose Rate(Gy/ka) | **Luminescence Age(ka)** | Field Code |
|---|---|---|---|---|---|---|
| WLL1099 | MAAD | 0.07±0.01 | 125.92±4.79 | 8.79±0.65 | **14.3±1.2** | HK13824 |
| WLL1100 | MAAD | 0.05±0.01 | 52.97±1.86 | 7.88±0.51 | **6.7±0.5** | HK13825 |
| WLL1101 | MAAD | 0.07±0.01 | 39.32±2.93 | 7.27±0.49 | **5.4±0.5** | HK13826 |
| WLL1102 | MAAD | 0.07±0.01 | 9.20±0.96 | 7.09±0.47 | **1.3±0.2** | HK13827 |
| WLL1103 | MAAD | 0.05±0.003 | 127.42±4.08 | 7.04±0.40 | **18.1±1.2** | HK13828 |
| WLL1104 | MAAD | 0.07±0.003 | 143.36±2.12 | 7.07±0.52 | **20.3±1.5** | HK13829 |
| WLL1105 | MAAD | 0.08±0.01 | 192.09±5.82 | 8.03±0.52 | **23.9±1.7** | HK13830 |
| WLL1106 | SAR | 0.07±0.01 | 322.15±8.26 | 8.39±0.62 | **38.4±3.0** | HK13831 |
| WLL1107 | MAAD | 0.07±0.01 | 115.03±3.23 | 7.85±0.46 | **14.7±1.0** | HK13832 |
| WLL1108 | MAAD | 0.10±0.01 | 181.11±26.50 | 7.09±0.51 | **25.6±4.2** | HK13833 |

# Report to Geotechnical Engineering Office Civil Engineering Department on Age Determination of Natural Terrain Landslides By Luminescence Dating LPMitP Phase 8

by

Ms. Ningsheng Wang (MSc)

Victoria University of Wellington
School of Geography, Environment and Earth Sciences
Luminescence Dating Laboratory
Room 414, Cotton Building
Victoria University of Wellington
Ph: (04) 463-6127

Technical Report

12th Nov 2014

**CONTENTS**

# 1. INTRODUCTION

Ten samples (Field code: HK13868-HK13877) were submitted to Luminescence Dating by the Geotechnical Engineering Office, Civil Engineering and Development Department, Hong Kong SAR Government. The laboratory codes of the samples are WLL1142-WLL1151 respectively.

The deposition ages have been determined for these samples using the silt fraction (4-11μm). Dependent on the relative luminescence intensities of feldspars in the samples, the palaeodose, i.e. the radiation dose accumulated in the sample after the last light exposure (assumed at deposition), was determined either by: measuring the blue or broadband luminescence output from feldspar fraction during infrared optical stimulation.

The dose rate was estimated on the basis of a low level gamma spectrometry measurement.

All measurements were done in the Luminescence Dating Laboratory, School of Geography, Environment and Earth Sciences, Victoria University of Wellington.

# 2. EXPERIMENTAL WORK

## 2.1 Sample Preparation

The samples contained a considerable amount of silt, and we decided to apply a so-called fine grain technique, i.e. use the grain size 4-11 μm for dating.

Sample preparation was done under extremely subdued safe orange light in a darkroom. Outer surfaces, which may have seen light during sampling, were removed and discarded. The actual water content and the saturation content were measured using 'fresh' inside material.

The samples were treated with 10%HCl to remove carbonates until the reaction stopped, then carefully rinsed with distilled water. Thereafter, all organic matter was destroyed with 10%$H_2O_2$ until the reaction stopped, then carefully rinsed with distilled water. By treatment with a solution of sodium citrate, sodium bicarbonate and sodium dithionate iron oxide coatings were removed from the mineral grains and then the sample was carefully rinsed again.

The grain size 4-11μm was extracted from the samples in a water-filled (with added dispersing agent to deflocculate clay) measuring cylinder using Stokes' Law. The other fractions were discarded. The samples then are brought into suspension in pure acetone and deposited evenly in a thin layer on up to 50 aluminum discs (1cm diameter).

## 2.2 Luminescence Measurements

Luminescence measurements were done using a standard Riso TL-DA15 measurement system, equipped with:

- Schott BG39+5-58+L40 optical filters to select the blue luminescence of feldspars.
- Schott BG39 + L40 optical filters to select the broad band luminescence of feldspars.

Stimulation was done cw at about 40mW/cm$^2$ with infrared diodes at 880Δ80nm. β-irradiations were done by the built in $^{90}$Sr,$^{90}$Y β-irradiator, calibrated against the Riso National Laboratory to about 3% accuracy. α-irradiations were done on a $^{241}$Am irradiator supplied and calibrated by ELSEC, Littlemore, UK.

***Multiple Aliquot Additive Method (MAAD)***

Samples WLL1142, WLL1144, WLL1146 and WLL1147, the Paleodoses were estimated by use of the multiple aliquot additive-dose method (with late-light subtraction) by measuring the blue luminescence under IR Stimulation. Sample WLL1145 was measured the broadband luminescence for its paleodose determination. After an initial test-measurement, 30 aliquots were β-irradiated in six groups up to five times of the dose result taken from the test. 9 aliquots were α-irradiated in three groups up to three times of the dose result taken from the test. These 39 disks were stored in the dark for four weeks to relax the crystal lattice after irradiation

After storage, these 39 disks and 9 unirradiated disks were preheated for 5mins at 220$^0$C to remove unstable signal components, and then measured for 100 seconds under IR stimulation, resulting in 48 shinedown curves. These curves were then normalized for their luminescence response, using 0.1s shortshine measurements taken before irradiation from all aliquots.

The luminescence growth curve (β-induced luminescence intensity vs added dose) is then constructed by using the initial 10 seconds of the shine down curves and subtracting the average of the last 20 seconds, the so called late light which is thought to be a mixture of background and hardly bleachable components. The shine plateau was checked to be flat after this manipulation. Extrapolation of this growth curve to the dose-axis gives the equivalent dose $D_e$, which is used as an estimate of the Paleodose.

A similar plot for the alpha-irradiated disks allows an estimate of the α-efficiency, the a-value (Luminescence/dose generated by the α-source divided by the luminescence/dose generated by the β-source).

***Single Aliquot Regenerative Method (SAR)***

The rest of the samples except sample WLL1151 were estimated by the use of the Single Aliquot Regenerative Method (SAR; see Murray and Wintle, 2000) by measuring

the blue luminescence under infrared situation. The sample WLL1151 was measured the broadband luminescence under IR stimulation by SAR method.

In the SAR method a number of aliquots are subjected to a repetitive cycle of irradiation, preheat and measurement. In the first cycle the natural luminescence output is measured, in all following cycles an artificial dose is applied. Usually four or five of these dose points are used to build the luminescence growth curve (β-induced luminescence intensity vs added dose) and bracket the natural luminescence output. This allows interpolation of the equivalent dose (the β-dose equivalent to the palaeodose). In order to correct for potential sensitivity changes from cycle to cycle, a test dose is applied between the cycles, preheated ('cut heat') and measured.

Twelve aliquots of each sample were measured. For IR stimulation, preheat and cutheat temperature was $260^0$C for 20s, and measurement time was 100s at the room temperature for the feldspar, which resets the luminescence signal to a negligible residual.

The measurement of 12 aliquots resulted in 12 equivalent doses ($D_e$s). The $D_e$s were accepted within 10% recycling ratio, which spread over the so called dose distribution. The arithmetic mean of this distribution was interpreted as the best estimate for the equivalent dose, and subsequently used for age calculation. A dose recovery test and a zero dose were checked no anomalies.

### 2.3 Gamma Spectrometry

The dry, ground and homogenised soil samples were encapsuled in airtight perspex containers and stored for at least 4 weeks. This procedure minimizes the loss of the short-lived noble gas $^{222}$Rn and allows $^{226}$Ra to reach equilibrium with its daughters $^{214}$Pb and $^{214}$Bi.

The samples were counted using high resolution gamma spectrometry with a CANBERRA broad energy Ge detector for a minimum time of 24h. The spectra were analysed using GENIE2000 software. The doserate calculation is based on the activity concentration of the nuclides $^{40}$K, $^{208}$Tl, $^{212}$Pb, $^{228}$Ac, $^{214}$Bi, $^{214}$Pb, $^{226}$Ra.

## 3. RESULTS

The radionuclide contents were calculated from the raw gammaspectrometry data. The Uranium and Thorium contents of most samples were quite high, similar to what we've measured in the previous phases of Hong Kong project reported earlier. Table 2 gives a summary of the radiometric data.

Table 1 gives sample summaries and calculated cosmic doserates, whereas Table 3 gives a summary of all equivalent doses, doserates and ages.

All errors in this report are stated as 1 sigma errors. A radioactive disequilibrium was considered as significant, if the equivalent Uranium contents do not overlap in a 2 sigma interval.

Water content was measured as weight of water divided by dry weight of the sample taking into account a 25% uncertainty.

## 4. REFERENCES

Guérin, G., Mercier, N., Adamiec, G. 2011: Dose- rate conversion factors: update. *Ancient TL*, Vol.29, No.1, 5-8.

Murray A.S. and Wintle A.G. (2000) Luminescence dating of quartz using an improved single-aliquot regenerative-dose protocol. *Radiation Measurements* 32, 57-73.

Prescott & Hutton (1994), *Radiation Measurements*, Vol. 23.

**LIST OF TABLES**

**Table 1 - Doserate contribution of cosmic radiation**

| Laboratory Code | Depth Below the Surface(m) | Cosmic Dose Rate (Gy/ka) | Field Code |
|---|---|---|---|
| WLL1142 | 3.43-3.50 | 0.1242±0.0062 | HK13868 |
| WLL1143 | 5.96-6.22 | 0.0907±0.0045 | HK13869 |
| WLL1144 | 6.60-6.79 | 0.0847±0.0042 | HK13870 |
| WLL1145 | 0.80 | 0.1775±0.0089 | HK13871 |
| WLL1146 | 0.70 | 0.1800±0.0090 | HK13872 |
| WLL1147 | 1.50 | 0.1654±0.0083 | HK13873 |
| WLL1148 | 2.50 | 0.1447±0.0072 | HK13874 |
| WLL1149 | 1.20 | 0.1711±0.0086 | HK13875 |
| WLL1150 | 2.50 | 0.1436±0.0072 | HK13876 |
| WLL1151 | 1.80 | 0.1593±0.0082 | HK13877 |

[1] Contribution of cosmic radiation to the total doserate, calculated as proposed by Prescott & Hutton (1994), Radiation Measurements, Vol. 23

**Table 2 - Radionuclide and water contents**

| Laboratory Code | Water Content (%) | U(ppm) from $^{234}$Th | U(ppm) from $^{226}$Ra, $^{214}$Pb, $^{214}$ Bi | U(ppm) from $^{210}$Pb | Th(ppm) From $^{208}$Tl $^{212}$ Pb $^{228}$ Ac | K(%) | Field Code |
|---|---|---|---|---|---|---|---|
| WLL1142 | 15.6 | 9.59±0.66 | 8.78±0.36 | 8.46±0.50 | 29.62±0.34 | 1.66±0.04 | HK13868 |
| WLL1143 | 19.2 | 9.38±0.62 | 8.67±0.37 | 8.17±0.46 | 32.69±0.35 | 1.66±0.04 | HK13869 |
| WLL1144 | 19.9 | 8.80±0.53 | 8.10±0.30 | 7.82±0.40 | 32.00±0.33 | 1.36±0.03 | HK13870 |
| WLL1145 | 14.9 | 8.84±0.56 | 7.45±0.33 | 6.25±0.37 | 46.05±0.45 | 1.55±0.03 | HK13871 |
| WLL1146 | 21.1 | 8.68±0.60 | 7.89±0.36 | 6.64±0.42 | 48.29±0.48 | 1.99±0.04 | HK13872 |
| WLL1147 | 31.7 | 8.12±0.53 | 7.66±0.32 | 6.80±0.39 | 36.46±0.37 | 1.10±0.03 | HK13873 |
| WLL1148 | 31.9 | 7.30±0.41 | 7.15±0.26 | 7.29±0.33 | 37.58±0.36 | 1.18±0.02 | HK13874 |
| WLL1149 | 25.0 | 6.98±0.40 | 6.66±0.25 | 5.87±0.29 | 30.37±0.29 | 3.41±0.07 | HK13875 |
| WLL1150 | 18.5 | 10.64±0.53 | 10.50±0.35 | 9.93±0.42 | 27.57±0.27 | 2.95±0.06 | HK13876 |
| WLL1151 | 36.6 | 7.57±0.43 | 7.08±0.27 | 6.97±0.33 | 43.46±0.41 | 0.79±0.02 | HK13877 |

[1] Errors assumed 25% of (δ).
[2] U and Th-content are calculated from the error weighted mean of the isotope equivalent contents.

**Table3 - a-value and equivalent dose, dose rate and luminescence age**

| Laboratory Code | Method | a-value | $D_e$(Gy) | Dose Rate(Gy/ka) | **Luminescence Age(ka)** | Field Code |
|---|---|---|---|---|---|---|
| WLL1142 | MAAD | 0.03±0.01 | 344.78±23.88 | 6.34±0.41 | **54.4±5.2** | HK13868 |
| WLL1143 | SAR | 0.03±0.01* | 368.38±13.55 | 6.29±0.44 | **58.6±4.7** | HK13869 |
| WLL1144 | MAAD | 0.03±0.01 | 337.78±54.17 | 5.78±0.41 | **58.5±10.3** | HK13870 |
| WLL1145 | MAADbd | 0.07±0.004 | 77.55±2.07 | 8.79±0.41 | **8.8±0.5** | HK13871 |
| WLL1146 | MAAD | 0.07±0.01 | 112.28±14.92 | 8.97±0.57 | **12.5±1.8** | HK13872 |
| WLL1147 | MAAD | 0.08±0.02 | 128.19±9.10 | 6.63±0.71 | **19.3±2.5** | HK13873 |
| WLL1148 | SAR | 0.03±0.01* | 265.00±7.39 | 5.25±0.44 | **50.5±4.4** | HK13874 |
| WLL1149 | SAR | 0.03±0.01* | 603.87±14.00 | 6.79±0.44 | **88.9±6.1** | HK13875 |
| WLL1150 | SAR | 0.03±0.01* | 608.31±11.42 | 7.59±0.49 | **80.1±5.4** | HK13876 |
| WLL1151 | SARbd | 0.03±0.01* | 323.02±9.25 | 5.14±0.46 | **62.8±5.9** | HK13877 |

*a-value was estimated
MAAD Multiple Aliquot Additive
SAR Single Aliquot Regenerative

bd 4-11µm polymineral sample
infrared stimulation (i.e. only feldspars contribute to OSL)
400-660nm "BG39+L40" broadband optical OSL filters

**Some comments**

- Our standard method is „MAAD", i.e. a multiple aliquot approach focusing on the blue emission band of potassium feldspars (410nm). However, the samples of WLL1145and WLL1151 had very low blue luminescence under infrared stimulation. Thus, we decided to detect broad band luminescence (400-660nm) by using BG39+L40 filters, to increase signal intensity.

# GEO PUBLICATIONS AND ORDERING INFORMATION
# 土力工程處刊物及訂購資料

An up-to-date full list of GEO publications can be found at the CEDD Website http://www.cedd.gov.hk on the Internet under "Publications". The following GEO publications can also be downloaded from the CEDD Website:

i. Manuals, Guides and Specifications
ii. GEO technical guidance notes
iii. GEO reports
iv. Geotechnical area studies programme
v. Geological survey memoirs
vi. Geological survey sheet reports

詳盡及最新的土力工程處刊物目錄，已登載於土木工程拓展署的互聯網網頁http://www.cedd.gov.hk 的"刊物"版面之內。以下的土力工程處刊物亦可於該網頁下載：

i. 指南、指引及規格
ii. 土力工程處技術指引
iii. 土力工程處報告
iv. 岩土工程地區研究計劃
v. 地質研究報告
vi. 地質調查圖表報告

**Copies of some GEO publications (except geological maps and other publications which are free of charge) can be purchased either by:**

Writing to
Publications Sales Unit,
Information Services Department,
Room 626, 6th Floor,
North Point Government Offices,
333 Java Road, North Point, Hong Kong.

or

- Calling the Publications Sales Section of Information Services Department (ISD) at (852) 2537 1910
- Visiting the online Government Bookstore at http:// www.bookstore.gov.hk
- Downloading the order form from the ISD website at http://www.isd.gov.hk and submitting the order online or by fax to (852) 2523 7195
- Placing order with ISD by e-mail at puborder@isd.gov.hk

**讀者可採用以下方法購買部分土力工程處刊物(地質圖及免費刊物除外):**

書面訂購
香港北角渣華道333號
北角政府合署6樓626室
政府新聞處
刊物銷售組

或

- 致電政府新聞處刊物銷售小組訂購 (電話：(852) 2537 1910)
- 進入網上「政府書店」選購，網址為 http://www.bookstore.gov.hk
- 透過政府新聞處的網站 (http://www.isd.gov.hk) 於網上遞交訂購表格，或將表格傳真至刊物銷售小組 (傳真：(852) 2523 7195)
- 以電郵方式訂購 (電郵地址：puborder@isd.gov.hk)

**1:100 000, 1:20 000 and 1:5 000 geological maps can be purchased from:**

Map Publications Centre/HK,
Survey & Mapping Office, Lands Department,
23th Floor, North Point Government Offices,
333 Java Road, North Point, Hong Kong.
Tel: (852) 2231 3187
Fax: (852) 2116 0774

**讀者可於下列地點購買1:100 000、1:20 000及1:5 000地質圖：**

香港北角渣華道333號
北角政府合署23樓
地政總署測繪處
電話: (852) 2231 3187
傳真: (852) 2116 0774

**Any enquires on GEO publications should be directed to:**

Chief Geotechnical Engineer/Standards and Testing,
Geotechnical Engineering Office,
Civil Engineering and Development Department,
Civil Engineering and Development Building,
101 Princess Margaret Road,
Homantin, Kowloon, Hong Kong.
Tel: (852) 2762 5351
Fax: (852) 2714 0275
E-mail: ivanli@cedd.gov.hk

**如對本處刊物有任何查詢，請致函：**

香港九龍何文田公主道101號
土木工程拓展署大樓
土木工程拓展署
土力工程處
標準及測試部總土力工程師
電話: (852) 2762 5351
傳真: (852) 2714 0275
電子郵件: ivanli@cedd.gov.hk